Microalgal Biorefinery: Process Optimization and Intensification for Production of Lipids and Other Value-added Products

A
Thesis
Submitted in
Partial Fulfilment of the
Requirements for the degree of

DOCTOR OF PHILOSOPHY

Neha Singh

CENTRE FOR ENERGY
Indian Institute of Technology Guwahati
Guwahati – 781039, Assam, India
March 2021

Dedicated

To

My Parents

INDIAN INSTITUTE OF TECHNOLOGY GUWAHATI

Centre for Energy

STATEMENT

I do hereby declare that the content embodied in this thesis entitled "**Microalgal biorefinery: Process optimization and intensification for production of lipids and other value-added products**" is the result of investigations carried out by me in the Centre for Energy, Indian Institute of Technology Guwahati, Guwahati, India, under the guidance of Prof. Vijayanand S. Moholkar and Prof. Arun Goyal. In keeping with the general practice of reporting scientific observations, due acknowledgements have been made wherever the work described is based on the findings of other investigators.

Date: Neha Singh

(Roll No.-146151015)

INDIAN INSTITUTE OF TECHNOLOGY GUWAHATI

Centre for Energy

CERTIFICATE

It is certified that the work contained in the thesis entitled "**Microalgal biorefinery: Process optimization and intensification for production of lipids and other value-added products**", by **Neha Singh** (Roll No. 146151015), has been carried out under our supervision and that this work has not been submitted elsewhere for degree.

Prof. Vijayanand S. Moholkar **Prof. Arun Goyal**

Date:

ACKNOWLEDGEMENTS

First and foremost, praises and thanks to God, the Almighty, for showers of blessings throughout my Ph.D. tenure and giving strength and confidence to complete the research successfully. I extend my appreciation for the help and support to all the following persons who in one way or another have contributed in making this study and thesis possible.

First and foremost, I express my deepest gratitude and immeasurable appreciation to my supervisors ***Prof. Vijayanand S. Moholkar*** and ***Prof. Arun Goyal*** who have the attitude and the substance of a genius. They have continually and convincingly conveyed a spirit of adventure in regard to research and provided encouragement to make me learn. I am immensely thankful for their valuable suggestions, encouragement, indispensable support and guidance throughout my research work and being a source of constant motivation and knowledge.

I would also like to extend my sincere appreciation and gratitude to all the members of doctoral committee, ***Prof. Animes K. Golder***, ***Prof. T. Punniyamurthy***, and ***Dr. Manish Kumar*** who manifested their distinguished skills and talents of their own field and provided insightful suggestions for the constant improvisation of my thesis.

I am extremely grateful to the faculty and staff members of Centre for Energy for their kind help and support. I am immensely thankful to Central Instruments Facilities (CIF) for providing facilities to carry out my research work. I am also thankful to the Indian Institute of Technology Guwahati for providing me with the infrastructure and facilities for advanced research.

In addition, a heartfelt thanks to my seniors *Dr. Shuchi Singh*, *Dr. Sankar Chakma*, *Dr. Jaykumar B. Bhasarkar*, *Dr. Pritam K. Dixit*, *Dr. Maneesh Poddar*, *Dr. Arup J. Borah*, *Dr. Shyamali Sarma* and research group members, *Dr. Amit*, *Niharika*, *Kuldeep*, *Sushobhan*, *Philip*, *Bhaskar*, *Kajal*, *Udangshree*, *Aradhana*, *Pushpita*, *Kaustabh* and *Karan* for all the worthy support and cooperation. I am highly thankful to my friends, *Rishabh*, *Deepika*, *Swati* and *Naziya* for all the love and support.

I acknowledge with deep sense of reverence, my gratitude towards my brother, *Mr. Asheesh Singh*, sister-in-law, *Mrs. Shikha Gupta*, sisters, *Dr. Shipra Shahi and Miss. Meenakshi Singh* and brother-in-law *Dr. Ashish Shahi* for always loving and supporting me selflessly. At last but not the least, I am highly indebted to my parents, *Mr. Surendra Pratap Singh* and *Mrs. Geeta Singh* for their unconditional love, care, and sacrifices and supporting me morally and spiritually throughout my life. My Ph.D. endeavor would not have been successful without them. I dedicate this to you "*MOM*" and "*DAD*".

ABSTRACT

The speedy depletion of fossil fuels and environmental pollution/climate change demands sustainable and renewable source for production of alternate green biofuels. A potential and promising green liquid fuel is biodiesel, which can be blended with petroleum diesel. Conventional feedstock for biodiesel synthesis is vegetable oil. The new and economic alternate feedstocks for biodiesel include microalgal lipids. Simultaneously, microalgae are promising producers of various other biofuels, such as bioethanol, glycerol and biomaterials like pigments and carotenoids. This thesis has assessed the potential of a natural freshwater microalgal strain for bio-refinery that produces biodiesel, bioethanol, β-carotene and glycerol. A native freshwater microalgae was isolated and the phylogenetic positioning of isolated strain by 18S rRNA sequence analysis revealed that it belonged to genus *Scenedesmus*. The strain was named *Tetradesmus obliquus* SGM19. The preliminary optimization of the growth conditions showed sodium nitrate (1.5 g/L) as the required nitrogen source and 12L:12D photoperiod. The strain exhibited high lipid (28%), carbohydrate (24%) and protein (42%) concentrations, which makes it a promising feedstock for biofuels. The isolate was also rich in pigments such as chlorophyll and carotenoids (with high antioxidant activity), and thus, was a potential food and pharmaceutical supplement. The growth cycle of *Tetradesmus obliquus* SGM19 was further optimized using statistical experimental design for simultaneous production of lipid and β-carotene. Application of 33 kHz and 1.4 bar ultrasound at 10% duty cycle was revealed to enhance the lipid and β-carotene yields by 34.5% and 31.5%, respectively. Kinetic analysis of substrate and product profiles in control and test experiments revealed both lipid and β-carotene to be growth-associated products. The intracellular NAD(H) content during late log phase was monitored as a measure of relative kinetics of intracellular metabolism. Consistently higher NAD(H) concentrations were observed for sonicated samples; indicating faster metabolism. The viability of ultrasound-exposed microalgal cells (assessed with flow cytometry) was >80%. Further, the lipid in *T. obliquus* SGM19 biomass was subjected to transesterification for producing biodiesel. The biodiesel synthesis process was optimized in two steps, viz. (1) optimization of the conditions/pretreatment of biomass, and (2) statistical optimization of transesterification process parameters. Normal lipid extraction followed by transesterification was studied with the whole biomass (wet and

lyophilized) for *in-situ* transesterification. Extracted lipids/ whole biomass was subjected to transesterification with different acid/base catalysts. *In-situ* base-catalyzed transesterification of the lyophilized biomass had the highest biodiesel yield of 37.5% (w/w DCW). Next, statistical optimization of transesterification parameters (catalyst loading, methanol to biomass ratio, temperature and reaction time) was done. Finally, intensification of transesterification was attempted by replacing mechanical agitation of reaction mixture with sonication. Sonication reduced the overall activation energy of transesterification process from 24.66 to 19.82 kJ/mol. Furthermore, the FAME profile for ultrasound-assisted transesterification process was characterized with GC-MS. Major fatty acids present in the lipids were palmitic, heptadecanoic, linoleic, linolenic and arachidic acids. The biodiesel properties were found to be as per ASTM D6751 standards. Finally, the *T. obliquus* SGM19 biomass was subjected to sequential treatment for extraction and synthesis of β-carotene, biodiesel, bioethanol and glycerol. Both 2-step and *in-situ* transesterification was used in the sequential extraction of products from microalgae. It was observed that the *in-situ* transesterification resulted in higher yields of end-products in comparison to 2-step transesterification and were: 0.11 g β-carotene, 29 g biodiesel, 2.6 g glycerol and 12 g bioethanol. This thesis has thus presented a comprehensive study on lab-scale processes of cultivation and growth of a wild microalgal strain, extraction of lipids and nutraceutical (β-carotene), and further synthesis of green biofuels like biodiesel and bioethanol, and finally intensification of these processes with external stimulus of ultrasound.

LIST OF ABBREVIATIONS

CCD	Central composite design
CFPP	Cold filter plugging point
CN	Cetane number
CO_2	Carbon dioxide
DCW	Dry cell weight
DTG	Differential thermogravimetric
EDTA	Ethylene diamine tetraacetic acid
FAME	Fatty acid methyl ester
FTIR	Fourier transform infrared
GC-MS	Gas chromatograph-mass spectrometer
HHV	Higher heating value
IV	Iodine value
KV	Kinematic viscosity
PBR	Photobioreactor
PUFA	Poly unsaturated fatty acid
RSM	Response surface methodology
SV	Saponification value
TGA	Thermogravimetric analysis
T. obliquus	*Tetradesmus obliquus*

CONTENTS

LIST OF TABLES

Chapter 4

Chapter 5

LIST OF FIGURES

Chapter 3

Chapter 4

Chapter 5

CHAPTER 1

INTRODUCTION AND LITERATURE REVIEW

CHAPTER 1

Introduction and Literature Review

1.1 General Introduction

There is a continuous growth in world population surging the primary energy consumption. Milano et al. (2016) stated that the highest single–year growth of 5.6% in global primary energy consumption in past 4 decades was seen in 2010. Thereafter, the average growth rate of global primary energy consumption has been > 2.5%. Main sources of primary energy have been fossil fuels, namely coal, natural gas and petroleum. Fig. 1.1 depicts the world energy consumption for the year 2018. It can be clearly inferred that the contribution of fossil fuel is about 85% whereas the contribution of the renewable energy sources (e.g. biomass, hydropower, wind) to world energy consumption is only 14%. The extensive consumption of fossil fuels have triggered major issues of energy security and climate change risk in the world. The first one being energy crisis as these unsustainable fossil fuels are being depleted at a very high speed forcing the world to look for other fuel sources. Environmental pollution is the other issue associated with consumption of fossil

fuels, which also raises concern about global warming due to high emissions of carbon dioxide (CO_2) in the air.

Recently, the world is extensively trying to reduce the consumption of non–renewable fossil fuels to help mitigate CO_2 emission and mend the energy conversion efficiency (Brennan and Owende, 2010). The alternatives to fossil fuels could be liquid fuels derived from the renewable source of biomass. Biomass–based substrates for liquid biofuels could be edible food crops (e.g. palm, corn, sunflower), lignocellulosic materials (e.g. bamboo) and other non–edible crops (e.g. Jatropha). The plants ability to capture CO_2 and convert solar energy to chemical energy by photosynthesis, makes biofuels renewable, mitigate CO_2 emission and help reduce global warming and build green environment. Gupta and Tuohy (2013) reported that lignocellulosic materials approximately fix 77 Gigatons of CO_2 annually and produce 100 Gigatons biomass.

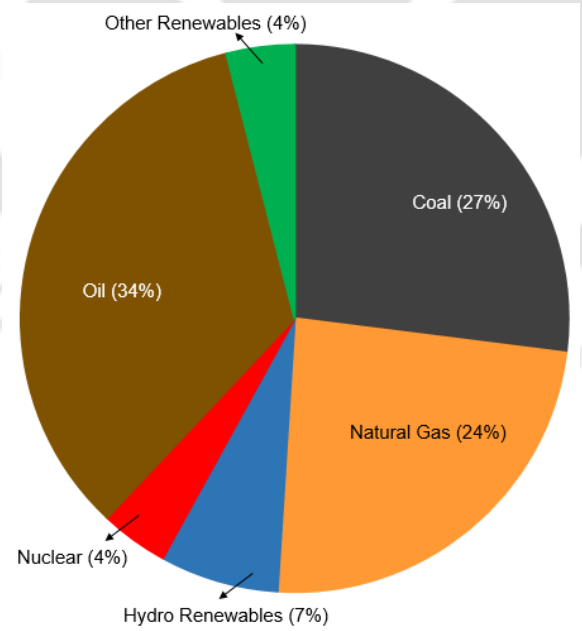

Figure 1.1. World primary energy consumption of the year 2018 (https://en.wikipedia.org/wiki/World_energy_consumption) – Accessed on 22–June–2020

In recent years, production of liquid biofuels has witnessed rapid growth globally. In Brazil, USA and the European Union, the first generation biofuels (edible crops) are being commercially used. Still, the scarcity of these sources is triggered by their competitive consumption as food and fodder. These limitations paved way for second generation biofuels derived from non–edible crops such as Castor, Jatropha, Palm oil and rubber seed. The second generation biofuels are mainly non–edible components of food crops, residues of agricultural and wood processing (Alam et al., 2012). Hence, they avoid any competition with food crops but they do require arable lands and exhibit low conversion rates. Microalgae have been considered as a promising third–generation biofuel feedstock as they possess numerous advantages, like higher photosynthesis efficiency, easy cultivation, usage of non–arable land, high lipid content and fast growth rate (Zhu et al., 2017). The various biofuel feedstocks are listed in Table 1.1.

Microalgae, or as the name suggest microscopic algae, are photosynthetic unicellular species which are present individually or in small clusters which can be noticed on the surface of water as colored patches. They are also known as phytoplankton (phyto meaning “plant” and planktos, meaning “drifter”), which mark the start of aquatic food chain or groups. A large variety of species of microalgae exist in a wide range of environmental conditions. Microalgae are prokaryotic or eukaryotic photosynthetic microorganisms that grow by the process of photosynthesis which produces carbohydrates, lipids and proteins. Some examples of microalgae are prokaryotic: cyanobacteria (Cyanophyceae) and eukaryotic: diatoms (Bacillariophyceae) and green algae (Chlorophyceae). Microalgae are capable of generating biomass with the help of solar energy (sunlight), nutrients (mainly nitrogen and phosphorus) and CO_2 in presence of water.

Table 1.1. Comparison of Microalgae with various feedstocks for biodiesel production (Adopted from Milano et al., 2016)

Crop	Seed oil (% oil by wt)	Oil yield (L oil/ha year)	Land area use (m^2 year/kg biodiesel)	Viscosity 40°C (mm^2/s)
1st Generation				
Canola	41	974–1190	12	33
Corn	44	172	66	31
Peanut	70	1059	–	22.7
Soybean	18	446–636	18	26
Sunflower	40	952–1070	11	–
2nd Generation				
Castor	48	1307–1413	9	–
Coconut	65–75	2689	–	29.6
Jatropha	20–60	1892	15	42.5
Palm	36	5366–5950	2	38
3rd Generation				
Microalgae	30–70	58.7–136.9k	0.1–0.2	36.6

Microalgae can photosynthetically convert these requirements into energy and utilize it for the cell development. Sizing from micrometers to millimeters, they float in the water where sunlight is available. Not only in the aquatic ecosystem, but microalgae are present in all ecosystem. They exist in all of the earth ecosystems, from aquatic to terrestrial as well, signifying a huge species variety living under varied environmental conditions. Researchers estimate that there might be more than 50,000 microalgal species that exist; out of which only around 30,000 species could be identified and studied (Mata et al., 2010). Microalgae possess the ability, like terrestrial plants, to fix CO_2 using sunlight or solar energy with efficiency far more than that of the terrestrial plants and have approximately 10% higher growth rate than the conventional food crops (Faried et al., 2017). Microalgae have been reported to utilize the sunlight more efficiently than the terrestrial plants, they can also consume many harmful pollutants for their growth, have very less requirements

for resources, and thus, are non–competitive with agriculture (food) for these valuable resources (Zhu et al., 2017). They own a very simple cell structure which can be unicellular or simple multicellular structure enabling them to rapidly grow and survive even in harsh conditions.

1.1.1 Chemical composition of microalgae

Metabolites are basically the intermediate products and the end–products of any metabolism. Metabolites can be divided into two types, viz. primary and secondary. The primary metabolites are the ones directly associated with the growth and development of microalgal cells. On the contrary, the secondary metabolites are not associated with the growth directly, but participate in other vital ecological functions and are induced by specific environmental conditions or stress (Tyagi et al., 2010).

The structure of a microalgal cell wall, depends on the strain and the microalgal growth conditions, especially the chemical composition and the thickness of the cell wall (Lee et al., 2017). The microalgal cell can also store different chemical constituents depending upon the environmental conditions. Major chemical constituents present in a microalgae are carbohydrates, lipids, and proteins stored in the microalgal cells with varying compositions. The major reason for considering microalgae as an alternative biodiesel feedstock is its high lipid productivity. Zhu et al. (2017) have reported that the microalgae yield could reach as high as 55 tons ha^{-1} $year^{-1}$ with about 60% lipid content within the microalgae cell under stress conditions. The lipid productivity in microalgae could be 15–300 times to that of the common oil crops (Zhu et al., 2017). These key primary metabolites (carbohydrates, lipids and proteins), have specific production pathways, and also produce high–value co–products that have applications as animal feed and human food supplements, industrial chemicals, transport fuels and pharmaceuticals.

The structural components of a microalgae differs widely from species to species. It also depends on the cultivation conditions, thus making it a non–intrinsic constant factor. Microalgae retort to environmental variability by modifying their chemical composition as they possess the ability to acclimate as per the changes in the environment around them. By altering the environmental factors such as light, pH, salinity, temperature, nutrients and available CO_2 concentration, it is feasible accumulate large extents of products in microalgae, as desired. The microalgae accumulate different products according to the changes in the environment. Microalgae are also known to produce chemical signals to avoid certain situations, defend and prey selection. They are called unconventional protein source as many species of microalgae are rich in protein content. Sugars, starch and various other polysaccharides provide microalgal species with high carbohydrate content. The microalgae are easily digestible due to its rich and diverse composition, thus, making it possible to use dried whole microalgae or extracted component as food and feed. Lipids are one of the major component in microalgae ranging in quantity from 1 to 70 wt% among several species and capable of achieving up to 90% dry cell weight in some conditions (Pal et al., 2019). The major lipid constituents are bases (sugars) and glycerol esterified to 12 – 22 carbon fatty acids (saturated or unsaturated). ω3 and ω6 family fatty acids are of specific interest compared to several other fatty acids present in the microalgal lipid.

Microalgal cells store two types of lipids, neutral lipids (which are free fatty acids and acyl–glycerides) and polar lipids (which are glycolipids and phospholipids). The polar lipids help in the formation of cell membranes, making them structural lipids, whereas the neutral lipids deals with the supply of energy. Table 1.2 highlights the major chemical compositions of few microalgal species. In general, lipids range from approx. 20%–50% of the dry cell weight in microalgal cells (Tan et al., 2018). Different species and their growth conditions allow microalgal cells to produce chemical constituents (viz.

carbohydrate, proteins and lipids) with varying content. Thus, the lipid content of microalgal cell can be manipulated by growing it in specific environment. The growth environment of the microalgae could be modified by several factors. Stress is one such major factor which induces enhanced lipid production in the microalgal cells. This stress can be due to nutrient starvation or any other external stimuli. Nitrogen deficiency can enhance triglyceride formation whereas sulphur and phosphorous depletion affect the production of neutral lipid. Other factors that affect the accumulation of lipid (composition and content) in microalgal cell are temperature, illumination, salinity, and other nutrients, such as carbon source (Alessandro and Antoniosi, 2016). Dong et al. (2016) reported that longer periods of cultivation and depletion of nutrients result in reduction of protein content with concurrent rise in lipids and carbohydrate content of microalgal biomass. However, the exact nature and extent of variation is species–dependent.

Other than the major components, there are also many minor constituents in microalgae. Pigments are minor constituents of microalgae which could be employed in several cosmetic, food and pharmaceutical industries (Alessandro and Antoniosi, 2016). Few examples of pigments are carotenoids (ranging from 0.1% – 0.2% dry cell weight on average but rising upto 14% of dry cell weight in specific cases such as β–carotene in *Dunaliella*), chlorophylls (0.5% – 1% of dry cell weight), and phycobiliproteins. Another minor yet essential constituents of microalgae are vitamins. Microalgae are store house for almost every essential vitamins (like, Vitamin A, B_1, B_2, B_3, B_5, B_6, B_7, B_8, B_9, B_{12}, C, E, H). Though, the quantity of vitamins in the cells vary due to environmental conditions, harvesting techniques and cell drying method, the algal cells nutritional value is improved by vitamins (Spolaore et al., 2006).

Table 1.2. Chemical composition of various microalgae suitable for biofuel production (% dry matter) (Kobayashi et al., 2013, Menetrez, 2012; Shuba and Kifle, 2018)

S. No.	Microalgae	Carbohydrate	Lipid (%)	Protein (%)
	Bacilliariophyceae			
1	*Chaetoceros calcitrans*	10	39	58
2	*Chaetoceros muellerii*	11–19	40–57	44–65
	Chlorophyceae			
3	*Botryococcus braunii*	20	25–75	4
4	*Chlamydomonas rheinhardii*	17	21	48
5	*Chlorella protothecoides*	12–17	14–56	15–58
6	*Chlorella pyrenoidosa*	25	2	57
7	*Chlorella vulgaris*	12–21	16–40	51–56
8	*Dunaliella salina*	32	6	57
9	*Haematococcus pluvialis*	15–40	20–37	17–45
10	*Scenedesmus dimorphus*	17–51	15–45	8–18
11	*Scenedesmus obliquus*	10–16	20–55	50–56
12	*Spirogyra* sp.	33–64	11–19	6–21
	Cyanophyceae			
13	*Anabaena cylindrical*	25–35	4–7	43–57
14	*Spirulina maxima*	13–16	6–7	60–71
	Euglenophyceae			
15	*Euglena gracilis*	7–25	21–38	30–45
	Rhodophyceae			
16	*Porphyridium cruentum*	40–58	11–20	29–40

1.1.2 Microalgal cultivation

The growth of microalgae depends on various factors such as cultivation condition, reaction type and reactor system. The microalgal cultivation conditions (e.g. CO_2, light, nutrients, pH, and temperature) influence the characteristics and constituents of microalgae. Carbon dioxide (CO_2) is basically the carbon source required for cell development (Tan et

al., 2018). Hasnain et al. (2018) suggested replacing pure CO_2 with flue gas to reduce the cost. Hasnain et al. (2018) also reported that 1 kg microalgal biomass can be produced from 1.8 kg CO_2. Light/illumination is the source of energy required for growth and photosynthesis. The pH of the growth media and temperature of the growth environment should be maintained at specific conditions to promote microalgal cell growth. The microalgal cells majorly require nitrogen and phosphorus for growth. These could be provided with both organic and inorganic sources, but inorganic source utilization can cause water pollution. Hence, wastewater management is important step in microalgae cultivation. An alternative approach can be utilization of wastewater for microalgal growth as they are rich in nitrogen and phosphorous. This approach is beneficial as not only the cost of microalgal cultivation reduces, it also helps in decontaminating the water (wastewater treatment). However, the hindrance in its use for microalgal growth are composition imbalance, and presence of toxic compounds. To consider wastewater as an alternative nutrient source, it is necessary to apply a systematic wastewater analysis (Tan et al., 2018).

The commercial production of microalgae–based biodiesel is a combination of various processes followed in a specific order. These processes are cultivation of microalgae, then, harvesting/dewatering, and lastly conversion of lipids to biodiesel (Roux et al., 2017). The microalgae can be cultivated in open raceway pond or in closed photo–bioreactor (PBR). A comparison of the open and closed systems for microalgae cultivation is shown in Table 1.3. Raceway pond (open system) as compared to photo–bioreactor require low capital cost, but are prone to contamination. In addition, there is huge water loss due to evaporation. This system does not utilize the carbon dioxide optimally due to no mixing; hence, require several improvements to the current system. A photo–bioreactor, on the other hand, is a

closed and controlled system, thus requires small area and is less contaminable, but involves higher production cost.

Table 1.3. Comparison of open and closed systems for culturing microalgae

Sr. No.	Open systems (Ponds)	Closed systems (PBRs)
1.	The open systems are simple, easy maintenance and low cost.	The closed systems are complex, require high maintenance and are expensive.
2.	These systems require low energy inputs. Hence, making it easier to scale–up for industrialization.	Closed systems require high energy inputs for various functions, thus, very hard to scale–up.
3.	Important growth factors such as temperature, pH, illumination, CO_2 cannot be controlled.	The system works under controlled and monitored growth factors. This also helps in enhanced CO_2 utilization efficiency. Temperature and light are uniformly distributed through the culture.
4.	Open system do not have sterilized conditions which results in growth and cultivation of multiple species.	Closed systems work under sterilized conditions procuring single species cultivation. Hence, the contamination risk is low and could be controlled.
5.	Uniform mixing is very difficult, thus the nutrients and other growth factors are not available in equal proportion to each organism. Thus, affecting the biomass productivity.	Uniform mixing can be achieved with help of agitators enabling proper availability of all nutrients to every organism. This helps in achieving high biomass productivity.

Microalgae can either be grown in pure or mixed cultures. The energy and carbon source for all heterotrophic cultures are same, but phototrophic cultures require different sources of each. Organic carbon (e.g. glucose) constitutes both energy and carbon source for heterotrophic cultures. On the other hand, light and CO_2 are the energy and carbon sources, respectively, for the phototrophic cultures (Zhu et al., 2017). A combination of phototrophic and heterotrophic cultures, termed as *mixotropic* culture, can result in increased cell production rate and higher lipid productivity as compared to the phototrophic culture. However, the organic substrate for microalgal growth makes up about 80% of the

total cultivation cost (Tan et al., 2018). Hence, to reduce the biodiesel production cost, proper selection and optimization of the cultivation conditions is essential.

Harvesting/dewatering is the process of removing water after cultivation from microalgae. It is the second step or process in cultivation of microalgae for biodiesel production. It can be divided into two steps, i.e., bulk harvesting followed by thickening. As the name suggest, bulk harvesting uses flocculation, flotation, or sedimentation processes to collect solid matter (microalgal biomass) from the bulk culture. The biomass slurry content can be enhanced by thickening (centrifugation and then filtration). The harvesting costs and energy requirements are important factors associated with microalgae–based biodiesel production (Tan et al., 2018). 20%–30% of the total production cost is incurred in harvesting (Alessandro and Antoniosi, 2016). Hence, it is crucial to select microalgal species that ease the harvesting process after growth.

Though the lipid content in microalgae is high, the cell walls are rigid, thick and protected by glycoproteins and complex carbohydrates. Similarly to the contents of microalgae, the thickness of their cell wall is also associated with the growth factors. This complexity of the microalgal cell wall restricts the extraction of algal oil. To obtain high oil extraction efficiency, higher rate of cell disruption is required. Hence, oil extraction should be preceded by a pretreatment method for cell wall disruption with ease, making the selection of species and culture medium a vital step for obtaining a fragile cell wall (Lee et al., 2017). Additionally, the growth parameters like pressure and temperature also need much attention. The biomass conditions (e.g. dry/wet biomass, its concentration) and the biomass stage of harvesting are few other factors to be monitored first.

Harvesting is generally followed by a drying step that reduces water content of biomass from 60% to ~ 10%. This step is crucial as high water content in microalgal biomass has adverse impact on conversion of lipids (Sitthithanaboon et al., 2015). Steriti et

al. (2014) reported that higher lipid yield could be achieved from dried microalgae as compared to wet biomass, dried microalgal cells possess more susceptible cell wall. Takisawa et al. (2013) supported this fact with a similar analysis. Takisawa et al. (2013) reported that wet microalgal biomass with 80% water content, when used directly (without drying) post harvesting for release of lipid/oil from the cells caused several difficulties. The drying step is an energy intensive process consuming up to 80% of the entire consumed energy (Dong et al., 2016). However, the elimination of this crucial step of drying can reduce the total energy consumption and eventually the total cost of production. Hence, it is necessary to develop new and advanced technologies which is capable of converting microalgal oil to biodiesel from wet biomass without hampering the capital cost and also achieve high conversion efficiency.

In summary, microalgae is a new alternate sustainable feedstock for biodiesel production with several distinct merits. However, commercial implementation of microalgal production would require significant study and optimization of the governing factors that would reduce the energy consumption and the associated capital and operating costs. Selection of proper microalgal species, optimization of growth conditions and proper extraction and conversion of lipids are the important features. Moreover, recovery of valuable byproducts from microalgal biomass is also crucially important as it forms another source of revenue for the microalgae refinery.

1.2 Microalgae–derived compounds and their applications

The extracted and purified products from microalgal biomass or microalgal biomass as a whole has many promising applications. These applications range from feedstock for biodiesel, feedstock for bioalcohol fermentation, aquaculture to animal feed, but also as a potential source of human health and nutritional products. Moreover, the microalgal

cultivation provides controlled quality of the cells to prevent contamination from pesticides, herbicides and other harmful substances. Almost every component of microalgal cell holds its own application in different industries. The microalgae as a whole is also used for various functions such as wastewater treatment and CO_2 mitigation. Hence, few applications of the microalgae and microalgae–derived products are briefly discussed below.

1.2.1 Lipids – For Biodiesel production

Microalgae produce two types of lipids. The polar lipids (e.g. glycerol–phospho lipids) play important role in cell structure, thus also called structural lipids. The non–polar lipids (e.g. triglycerides) play the vital role of energy storage. Polar or Structural lipids, generally, comprise of long–chains of polyunsaturated fatty acids (PUFAs). Some example of important PUFAs from microalgae are Docosahexaenoic acid (DHA), Docosapentaenoic acid (DPA) and Eicosapentaenoic acid (EPA). These lipids along with few sterols offer selectively permeable barrier protecting the microalgal cells. PUFAs from microalgae have multiple applications such as biofuel production (biodiesel), mitochondrial super complex formation and treatment of serious diseases such as Alzheimer, Atherosclerosis and Parkinson (Yates et al., 2014). The structural lipids also play important role in various biosynthetic and metabolic processes by maintaining the ideal fluidity of the membrane and directly contribute in several fusion events in intracellular membrane. Furthermore, one of the most important function of the polar lipids is cell signaling to protect the cells from environmental disturbances by promoting changes in the cellular environment.

The triglycerides (TAGs), on the other hand, are associated with energy storage in the cells. When the photosynthesis occurs, the solar energy is converted into chemical energy, so that it could be utilized by the microalgal cells for growth and other metabolic

functions. To be able to utilize this energy, the microalgal cells employ a carbon skeleton (glycerate–3–phosphate), which is converted to other special molecules (e.g. amino acids, lipids, pyruvate, etc.). A simple metabolic pathway of a microalgal cell is shown in Fig. 1.2. Hence, the microalgal cell growth, maintenance and other complex metabolism is facilitated by the intensive process of energy conversion and storage (Fan et al., 2017).

The lipid production by microalgae (in terms of quality and quantity) varies from species to species. Vasudevan and Briggs (2008) reported that microalgal strains with low oil (lipid) content grew faster as compared to those with high lipid content. Also, Francisco et al. (2010) stated that the microalgal strains with high lipid content have lower biomass productivity. Table 1.4 presents a brief summary of few species of microalgae with their biomass and lipid productivity. It can be observed that the microalgal species of Chlorophyceae generally have high lipid content, making them a suitable feedstock for biodiesel production.

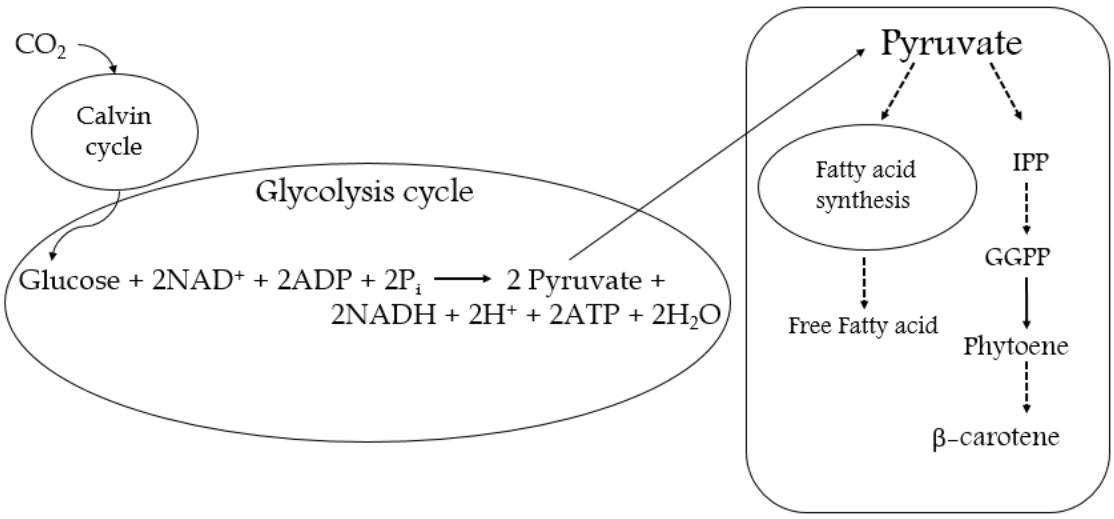

Figure 1.2. A simplified metabolic pathway of fatty acid and carotenoid production in microalgae

Table 1.4. Biomass and lipid productivity of various microalgae (Adopted from Mata et al., 2009)

Microalgae	Biomass productivity (g L^{-1} day^{-1})	Lipid content (% DCW)	Lipid productivity (mg L^{-1} day^{-1})
Botryococcus braunii	0.02	25.0–75.0	–
Chaetoceros calcitrans	0.04	14.6–16.4	17.6
Chlorella sorokiniana	0.23–1.47	19.0–22.0	44.7
Chlorella vulgaris	0.02–0.2	5.0–58.0	11.2–40.0
Chlorococcum sp.	0.28	19.3	53.7
Dunaliella salina	0.22–0.34	6.0–25.0	116.0
Dunaliella tertiolecta	0.12	16.7–71.0	–
Euglena gracilis	7.70	14.0–20.0	–
Haematococcus pluvialis	0.05–0.06	25.0	–
Nannochloropsis oculata	0.37–0.48	22.7–29.7	84.0–142.0
Phaeodactylum tricornutum	0.003–1.9	18.0–57.0	44.8
Porphyridium cruentum	0.36–1.5	9.0–18.8	34.8
Scenedesmus obliquus	0.004–0.74	11.0–55.0	–
Scenedesmus quadricauda	0.19	1.9–18.4	35.1
Spirulina platensis	0.06–4.3	4.0–16.6	–
Spirulina maxima	0.21–0.25	4.0–9.0	–
Tetraselmis suecica	0.12–0.32	8.5–23.0	27.0–36.4

Biodiesel is essentially alkyl esters of long–chain fatty acids, which has properties similar to those of diesel. It is the most potential biofuel from microalgae and is produced by a reaction called trans–esterification of microalgal oil (lipids). The trans–esterification reaction is generally conducted in a closed controlled reaction system to promote biodiesel production. When triglycerides and mixed with alcohol in presence of a catalyst (acid or alkali), the trans–esterification reaction starts and fatty acid esters are formed along with glycerol. Post the reaction, it is essential to separate the two products to obtain pure

biodiesel for commercial use. A funnel–type separator is used for separation of glycerol from esters. Thus, the separated esters are evaporated to remove any left alcohol and then rinsed thoroughly with water to remove any impurities. This simple process for biodiesel production makes it a potential fuel for commercial production as alternative to petroleum fuels (Hu et al., 2006).

For replacement of current feedstock for biodiesel (i.e. vegetable oils) with microalgal lipids, the fuel properties of biodiesel synthesized from these lipids have to meet certain standards. Cetane number, cold filter plugging point, viscosity, iodine value, ignition quality are a few examples of these properties. Two globally accepted standards for biodiesel properties are ASTM D6751 (United States) and EN 14214 (Europe), respectively. The fatty acid profile of the biodiesel, which governs these properties is dependent on the microalgal growth parameters like light intensity and temperature (Johnson and Wen, 2009). Table 1.5 shows the fatty acid content of few microalgal species. The biodiesel with higher oleic acids (C18:1) content shows balanced fuel properties, such as oxidation stability, combustion heat, ignition quality, viscosity and cold filter plugging point (Islam et al., 2013). For colder regions, the long storage and better oxidation stability is achieved due to higher content of oleic acid in the FAME (fatty acid methyl ester) profile of microalgae. Hence, microalgal species with high oleic acids in FAME profile are preferred for biodiesel production (Johnson and Wen, 2009). Some microalgal species, like *Botryococcus, Nannochloropsis*, *Picochlorum* and *Scenedesmus*, have high oleic acid content making them promising feedstocks for biodiesel production.

Table 1.5. Common fatty acid profiles of different microalgal species (%)

(Francisco et al., 2010, Islam et al., 2013, Milano et al., 2016)

Microalgae	C14:0 (Myristic)	C16:0 (Palmitic)	C16:1 (Palmitoleic)	C16:2 (Hexadienoic)	C18:0 (Stearic)	C18:1 (Oleic)	C18:2 (Linoleic)	C18:3 (Linolenic)	C20:0 (Arachidic)
Aphanothece	–	1.58	1.02	–	2.04	8.05	14.67	0.18	0.17
Bidulphia	21	–	57	6.1	1.5	0.6	–	–	–
Botryococcus	–	–	4.8	–	4.3	55.7	34.2	0.2	–
Chlorella	1.19	2.22	1.36	–	1.06	12.31	1.42	–	2.87
Dunaliella	1.47	1.16	11.71	–	4.91	11.96	27.8	–	0.01
Franceia	0.6	12.9	7.3	2.3	0.5	15.2	1.2	32.3	–
Mesotaenium	0.5	13.4	6.1	2.9	0.6	7.6	11.8	31.4	–
Nannochloropsis	5.8	–	62	–	20	1.3	–	–	–
Phaeodactylum	3.3	–	77.8	5.7	3.6	2.3	0.58	–	1.32
Phormidium	0.73	1.53	12.29	1.28	12.25	27.77	4.54	–	–
Picochlorum	0.5	–	18.2	8.6	16	36	15	2.1	–
Scenedesmus	0.5	15.8	5.16	2.36	0.6	21.7	1	25	1.97

1.2.2 Protein – In Food and Feed Industry

As shown in Table 1.2, microalgae are rich in proteins. This makes them capable of being used in food and feed industry. Microalgae are a rich source of proteins, and contain all essential amino acids at various concentration (depending on type of strain). Species such as *Spirulina* sp. may contain more than 60% dcw proteins, and have been used in human nutrition. Microalgae are typically consumed as a dietary supplement in the form of powder, pills and tablets. Amorim et al. (2012) showed that most of the bioactive compounds present in edible microalgae are deactivated after heat treatment.

Martínez–Hernández et al. (2018) reported that algal powders were excellent sources of amino acid and protein showing their potential application as nutritional supplements. Liang et al. (2004) reported that in China more than 100 industries are anxious about use of microalgae as food. Significant research has been carried out discovering the potential of microalgae or extracted microalgal proteins for human consumption as protein supplements (Becker, 2007; Raja et al., 2016). Gouveia et al. (2007) have suggested that the microalgal protein quality is similar or even higher than plant protein. For better yield and quality of egg, meat and milk, *Spirulina* and *Chlorella* are occasionally mixed with the feed in cattle and poultries industries (Desai and Sivakami, 2004).

Spirulina naturally grows in the lakes which have high salinity, generally in the subtropical climates. They have high pH tolerance upto 10 or 11. *Chlorella* has been reported to be easily digestible by animals when consumed in paste form (5%) with the animal feed and for pigs, their protein digestibility was approximately 56% (Harari et al., 2013). In sheep, *Chlorella* have been found to cause weight gain (Raja et al., 2018). Some microalgae companies, like Allma and Necton, are commercial suppliers of *Chlorella* and *Spirulina* in several forms such as juices, millets, soups, smoothies and dietary supplements (protein sources, antioxidant) for human consumption (Raja et al., 2018).

1.2.3 Pigments – In Pharmaceutical and Cosmetic Industry

In microalgae, there are many pigments present which are related to the light. Chlorophyll, one of the major pigments, is the primary photosynthetic compound along with other vital pigments like carotenoids and phycobiliproteins. The phycobiliproteins (e.g. phycoerythrin and phycocyanin) exclusive to algae are being used in cosmetics and food applications (Priyadarshani and Biswajit, 2012). The carotenoids present within the microalgae also have several industrial applications. Fig. 1.3 shows the chemical structures of major microalgal carotenoids. Astaxanthin extracted from *Haematococcus* is widely used as red colourant in aquaculture. β–carotene extracted from *Dunaliella* is used as vitamin–supplement in pharmaceuticals. Other carotenoids like canthaxanthin, lutein and zeaxanthin have pharmaceutical uses.

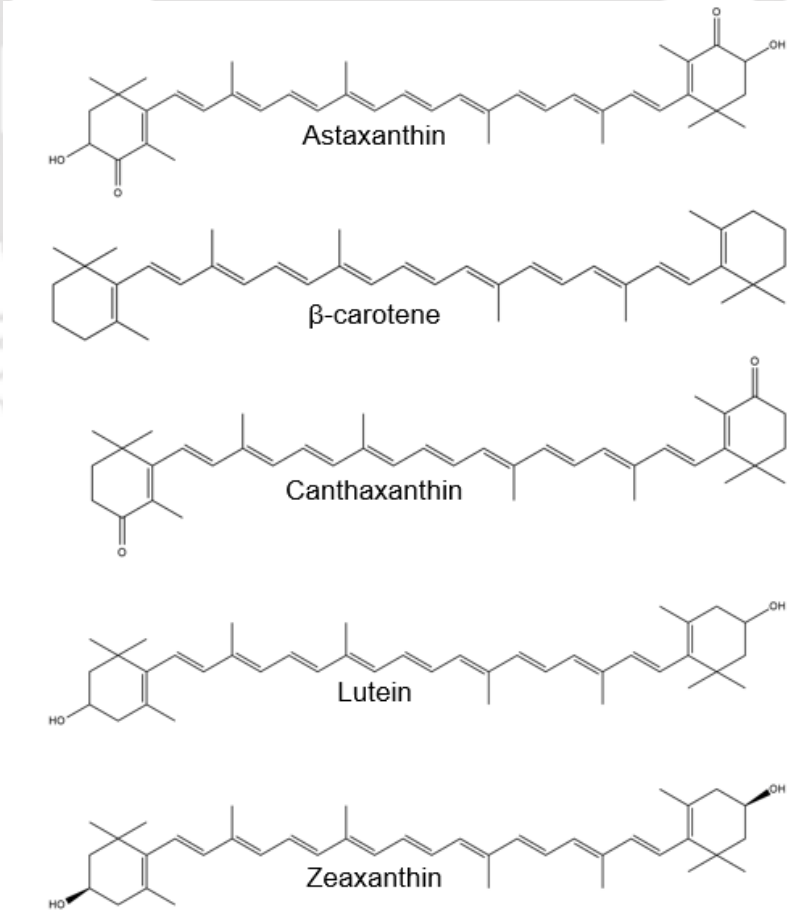

Figure 1.3. Chemical structure of major carotenoids from microalgae

Cosmetics: Microalgal species like *Arthrospira* and *Chlorella* are commonly applied in the skin care. Few cosmetic companies have their own cultivation systems for microalgae (Sharma and Sharma, 2017). Pigment extracts of few microalgae are already being used in cosmetics, like anti–aging creams, hair care, sunscreen and rejuvenating products (Spolaore et al., 2006). Microalgal extracts are also used as antioxidants, thickening agents and water–binding agents (Stolz and Obermayer, 2005). Many face and skin care products have microalgal extracts. *Alaria esculenta*, *Ascophyllum nodosum*, *Chlorella vulgaris*, *Chondrus crispus*, *Dunaliella salina*, *Nannochloropsis oculata* and *Spirulina platensis* are the common microalgal species with application in cosmetics. Sharma and Sharma (2017) have reported uses of Spirulina by various cosmetics companies in facial scrubs and masks for cleansing, removing dead skin and improving moisture balance, skin complexion and immunity.

Pharmaceuticals: The major reason for application of carotenoids in the pharmaceuticals is due to its biological activities. The biological activities of microalgae are as antioxidants, antiviral, antifungal and antibacterial. These biological activities are very important for human health. Antioxidants have free radical scavenging properties that acts as an anticancer activity. Astaxanthin is the most potential natural antioxidant from microalgae. Higuera–Ciapara et al. (2006) stated that the health benefits of astaxanthin are approximately 100 times more than that of tocopherol because of its antioxidant activity. There are several literatures that reports the potential use of astaxanthin against several diseases such as cancer, diabetes, metabolic and neurogenerative disorders (Yuan et al., 2011). β–carotene is a precursor for vitamin A, but also possess antioxidant property, making its way in the health foods (Bhattacharjee, 2016). β–carotene was declared as anticarcinogenic compound by National Cancer Institute. It also helps in prevention of heart disease and helps control cholesterol (Sharma and Sharma, 2017). Hu et al. (2008) reported

that *Dunaliella* derived β–carotene showed higher antioxidant properties than the synthetic β–carotene as only trans–isomers form the synthetic β–carotene whereas microalgal β–carotene is formed by both cis and trans isomers.

1.2.4 Carbohydrates – For Bioethanol production

The high carbohydrate content in microalgae make them a potential bioethanol producers. The carbohydrates in microalgae are converted to bioethanol by fermentation. Fermentation is an alcohol production process which involves conversion of sugars (starch or cellulose) present in the biomass. The microalgal biomass is subjected to pretreatment before fermentation. Pretreatment breaks the complex sugar such as cellulose into monomeric forms (glucose) to facilitate easy fermentation by the micro–organism. The bioethanol produced by the microbe requires purification by distillation for removal of impurities and excess water (McKendry, 2002). Microalgae rich in carbohydrate content like *C. vulgaris* are potential source for bioethanol production which can attain upto 65% bioethanol conversion (Brennan and Owende, 2010).

Ueno et al. (1998) has reported the possible use of *Chlorococcum littorale* (marine green microalgae) for production of bioethanol by dark fermentation. Approximately 27% of microalgal starch was consumed at 25°C in 24 h. John et al. (2011) have evaluated the algal biomass (like *Arthrospira*, *Chlamydomonas*, *Chlorella*, *Dunaliella*, *Euglena*, *Prymnesium*, *Scenedesmus* and *Spirulina*) potential to be bioethanol feedstock and persuade their usage as renewable sourced–biofuel, thus, delivering secured option. In Brazil, bioethanol is being commercially used in about 86% cars as sole fuel or as an additive to gasoline (Walker, 2010). However, bioethanol still have few limitations such as low energy density and low vapor pressure (Balat et al., 2008).

1.2.5 Other biofuels from microalgae

Biohydrogen: In recent years, bio–hydrogen production has gained much attention, as hydrogen is the cleanest fuel. However, the bio–hydrogen production on large scale is unfeasible as process is expensive and generates low biomass concentration. It has been reported in several works that the exposure of few algae species to stress conditions such as deprivation of light may help in triggering hydrogen gas in considerable amount. However, this technology still stands in initial stage and it can be further improved (Saifuddin and Priatharsini, 2016). There are three pathways through which hydrogen can be produced: direct photolysis, indirect photolysis and ATP driven pathway. Direct photolysis is feasible when hydrogen and oxygen produced are removed continuously. In this process, hydrogen and oxygen are produced together that increases the separation cost and imposes greater security risks. Moreover, this process makes use of hydrogenase enzyme that is highly oxygen sensitive, thus, indirect processes are comparatively more feasible. Under anaerobic conditions, starch present in algae cell walls is converted into hydrogen up to certain limit. Most of the previous literature reported that cyanobacteria mainly produce biohydrogen using hydrogenase and nitrogenase enzymes as catalyst (Guan, 2012).

Bio–methane: Biogas produced through aerobic digestion of biomass is a potential and popular means of deriving energy from biomass. An anaerobic digester contains synergistic microbial populations, which convert algal organic compounds (lipid, protein, carbohydrate) to biogas, which is a mixture of methane and carbon dioxide. Methane is widely used both as a fuel and chemical feedstock. Chynoweth et al. (1993) investigated the potential of different feedstocks such as algae, wood, grass, solid waste for biomethane production and found algae biomass as potential candidate. The biomass productivity of algae is generally higher than land plants, but its growth is influenced by limiting of

different nutrients. Wang et al. (2016) examined the thermal pretreatment of microalgae for enhancement of biomethane production by using *Chlorella* sp. Methane yields from untreated algae were 155 mL/g VS_{add}, while thermal pretreatment at 70°C and 90°C for 0.5 h increased the methane yield by 37% and 48%, respectively. Thermal pretreatment at 121°C for 0.3 h resulted in the highest methane yield (322 mL/g VS_{add}), which was 108% higher than the untreated algae.

Bio–oil: Bio–oils are produced by thermochemical conversion that can be used as a substitute to petroleum oils. The production process of bio–oil comprises of two steps, mainly pyrolysis and thermochemical liquefaction (Demirbas, 2000). Pyrolysis is performed at high temperatures of 350°–550°C for production of a liquid along with solid part and gaseous parts. The liquid part comprises of aqueous as well as non–aqueous phase, i.e. bio–oil or tar and the left out biomass is dried. The bio–oil is usually made up of different organic compounds such as proteins, lipids and carbohydrates. Various types of microalgae have been explored for production of bio–oil through pyrolysis or thermal liquefaction process. The bio–oil yield differs according to microalgae species, for instance, a bio–oil yield of about 41% was obtained in *Spirulina* (Jena and Das, 2011), up to 24 – 45% for *Scenedesmus* (Vardon et al., 2012), approximately 37% for *Dunaliella* (Minowa et al., 1995) and around 49% for *Desmodesmus* (Alba et al., 2012).

1.2.6 Other applications of microalgae

Aquaculture: Microalgae also serve as a vital food source of larvae of some marine gastropods, marine bivalve mollusks such as oysters, scallops, etc., few types of fishes, marine shrimps and zooplanktons. Thus, after cultivation of microalgae, they are concentrated to produce algae pastes or freeze–dried cubes and stored under refrigeration which can be directly used later by the aquaculture industrialists (Hemaiswarya et al.,

2011). The aquaculture feed formulations are generally kept in the form of paste. These formulations may contain one or more algae species so that a complete and balanced nutrition can be provided. Microalgae feed serves as a potential source of fatty acids to fish. It is known that Omega–3 fatty acids such as docosahexaenoic acid (DHA) and eicosapentaenoic acid (EPA) are extracted and sold as fish oil for human consumption. But, DHA and EPA are not synthesized by fish rather these are accumulated and stored from the microalgae in the fish.

Algae pastes are also freeze dried into ice cubes of specified amount for a ready usage. The freezing process helps in the extension of the algal shelf life. These ice cubes can be fed directly in the water tank or indirectly after dilution in water. The eukaryotic classes generally used to produce aquaculture feeds are Bacillariophyceae and Chlorophyceae. Further, the marine algae that are commercially important for the production of pastes are *Phaeodactylum tricornutum, Nannochloropsis oculata* and *Chaetoceros* sp. (Chini–Zittelli et al., 1999). These are mixed with seawater to produce 10% algal solution which is eventually frozen into ice cubes to provide uniform feeds in the aquaculture industry.

CO_2 mitigation: The various options explored for capturing CO_2 are either economically or environmentally not much feasible. Though, CO_2 sequestration into algal biomass could be profitable through the formation of high value products such as pigments and high–grade lipids that can be extracted from some of the microalgae species. Brennan and Owende (2010) also reported that animal feed supplements could be extracted from the microalgae species such *Scenedesmus, Chlorella* and *Spirulina*. Hence, biological CO_2 mitigation could be a solution to the immediate need of substantial reductions in CO_2 levels. In this sense, microalgae could prove beneficial as these can convert CO_2 as well as some other supplementary nutrients into biomass by photosynthesis at higher rates in comparison to conventional biofuel crops. The obtained biomass can be further transformed into methane

or hydrogen by anaerobic bacteria, rendering microalgae useful for the hydrothermal production of methane (Li et al., 2008). The oil production via microalgae has gained much attention recently due to the ease of synthesis in which scarcity of nitrogen source generally triggers a kind of secondary metabolism. Then, lipid extraction and re–esterification is attained through short–chain alcohols (Li et al., 2008). After extraction, obtained oils could be hydrolyzed followed by re–esterification with methyl/ethyl alcohol moieties in order to produce biodiesel. In order to achieve sustainable biofuel production and microalga–mediated CO_2 fixation, the biomass production of microalgae should be coupled wastewater treatment infrastructures (Mostafa et al., 2012).

Wastewater treatment: Microalgae are capable of utilizing poor–quality or wastewater, like agricultural runoff, industrial and municipal wastewaters, for the growth medium as the source of water, phosphorus, nitrogen and other minor nutrients (Mostafa et al., 2012). Nitrogen and phosphorous present in wastewater can serve as the nutrients for microalgae thus serving a two–way purpose of microalgal growth along with biological cleaning. In this way, nutritional requirements of microalgae can be completed by the utilization of organic compounds such as nitrogen and phosphorous present in industrial or some other wastewater. In addition, microalgae can help in reducing the severe effects of sewage effluent and nitrogenous waste from industrial wastewater treatment or fish aquaculture thereby contributing to biodiversity. Further, by removal of carbon and nitrogen from water, microalgae help in reducing eutrophication in the aquatic environment. Aslan and Kapdan (2006) reported a removal efficiency of 72% (3 – 8 mg/L NH_4^+) and 28% (1.5–3.5 mg/L PO_4^{3-}) from wastewater for N_2 and P, respectively, using microalgae *C. vulgaris*. *Chlorella* and *Spirulina* species are common microalgae species used for nutrient removal (Gonzales et al., 1997). Also, *Nannochloris*, *Botryococcus brauinii* and cyanobacterium

Phormidium bohneri have been explored to investigate their potential for nutrient removal (Dumas et al., 1998, Olguín et al., 2003). Hence, combining the potential of microalgae for biodiesel production or other bio–products with processes such as wastewater and flue gas treatment could be more cost effective, economical and environmentally sustainable. Thus, many studies have shifted their focus onto exploration of combined use of microalgae for simultaneous production of valuable products as well as aid in environmental applications.

1.3 Intensification strategies for enhanced lipid (biodiesel) production

Various species of microalgae have different types and varied amounts of lipids (Zhu et al., 2016) however these amounts can also be varied by altering lipid metabolism in different ways. The quantity and composition of lipids are species–dependent and may be affected by the external cultivation conditions, such as temperature, light intensity and carbon dioxide. Application of stress, in the form of nutrient stress or other external stimuli such as ultrasonication, can also boast lipid metabolism in the microalgae. Another approach can be genetic engineering that involves the manipulation of specific genes related to lipid metabolism to improve synthesis, storage and lipid's structural contents inside the microalgae cell. The related techniques are discussed below in detail.

1.3.1 Optimization of medium components and process parameters

A biochemical engineering approach is one method that involves the alteration in the nutritional and cultivation conditions. The cultivation conditions refers to exposure to different carbon dioxide levels, temperature, light intensity, available nutrients (Widjaja et al., 2009), salinity stress (Zhu et al., 2016), and usage of nanoparticles.

Carbon dioxide: For microalgae and other photosynthetic microorganisms, the major sources of CO_2 are the atmospheric CO_2 and also the CO_2 appearing in industrial exhaust.

The inorganic carbon derived from CO_2 is used to produce biomass and other chemical compounds in the presence of sunlight (Wang et al., 2008). A few examples of CO_2 effect on lipid accumulation in various microalgae are given in Table 1.6. The growth and metabolic activity of microalgae depends on specific CO_2 levels. The optimal CO_2 levels influence the production and accumulation of lipids within the cell. The increase in CO_2 level could improve the lipid production and their accumulation in the microalgae cells, however excessive CO_2 after the threshold levels can cause disruptive effects in cell growth and thereby lipid production.

Table 1.6. Carbon dioxide concentration effect on lipid accumulation in various microalgae species

Microalgae	**CO_2 concentration**	**Effect on lipid**	**References**
Attheya longicornis	20–25%	No significant effect	Artamonova et al., 2017
Chlamydomonas sp. JSC4	4% (v/v)	Lipid content (65.3%) and productivity (169.1 mg/L/day)	Nakanishi et al., 2014
Chlorella sp. BTA 9031	3% (v/v)	Lipid content (25%)	Mondal et al., 2016
Chlorella vulgaris	30%	Lipid content (45.68%) and productivity (86.03 mg/L/day)	Huang and Su, 2014
Chlorococcum littorale	5% (v/v)	Lipid content (34%)	Ota et al., 2009
Nannochloropsis oculata	3% (v/v)	Lipid content (53.2%)	Krishnan et al., 2015
Porosira glacialis	20–25%	Lipid content (10.57%)	Artamonova et al., 2017
Scenedesmus sp.	10%	Lipid productivity (20.65 mg/L/day)	Yoo et al., 2010
Synechocystis sp. PCC6803	3% (v/v)	Lipid content (14%)	Cuellar–Bermudez et al., 2015

It has been reported earlier that the best production of microalgae cells requires high CO_2 resource. Initial experiments performed with *Nannochloropsis* species showed no

inhibition at high CO_2 levels. However, continuous exposure to high levels of CO_2 resulted in reduction in growth. In few cases, high CO_2 levels were even proven lethal for some microalgal cultures (Hoshida et al., 2005; Singh and Singh, 2014).

When a microalgae culture is exposed to high CO_2 concentrations, some carbon is used for photosynthesis, while the remaining carbon is converted to carbonic acid. The carbonic acid generated may lead to the acidification of medium, thus hindering cell growth and related metabolic pathways. Ying et al. (2014) studied pH alterations in the medium while exposing the cells to different CO_2 levels. It was reported that the sudden and drastic change in pH levels led to the damage of enzymes involved in the photosynthesis. Thus, optimum pH levels should be maintained depending on the microalgae species to achieve optimal biomass growth and lipid production.

Various related works have tried to investigate the effect of different concentrations of carbon dioxide on microalgae. Ying et al. (2014) showed that the growth of *D. Salina* culture was inhibited due to the exposure to 0.02 mol CO_2/L concentration. It was also discovered that the concentration higher than 0.02 mol CO_2/L was highly poisonous for the cell growth. In another work by Montoya et al. (2014), it was determined that with 8% CO_2 concentration high amount of fatty acids with enhanced lipid productivity (29.5 mg/L/day) was achieved in a culture of *C. vulgaris*. Moreover, cultivation of *Chlorella Pyrenoidosa* under 5% CO_2 concentration (v/v) led to the attainment of high lipid productivity of approximately 107 mg/L/day. Further, a maximum lipid productivity of 169 mg/L/day was obtained with cultivation of green microalgae of *Chlamydomonas* sp. under 4% CO_2 concentration (v/v) (Nakanishi et al., 2014).

Temperature: The microalgae growth and lipid production increase exponentially with the increase in temperature up to a certain extent (Zhu and Hiltunen, 2016). The optimal temperature at which the highest biomass growth can be attained varies in different species.

The temperature of 25°C was observed to be optimum for microalgae *C. vulgaris* to produce maximum lipids (Converti et al., 2009). Xin et al. (2011) reported that microalgae *Scenedesmus* accumulated high lipid content at an optimal temperature of 20°C. The lipid concentration ranged between 18 – 40% dcw in microalgae *S. obliquus*, when the temperature was varied from 20° – 27.5°C (Vitova et al., 2015). In another study, Converti et al. (2009) observed that with the increase in temperature from 20° to 25°C, the lipid content gradually increased from 7.9 to 14.9% dcw.

The rise in temperature is accompanied by rise in lipid content till an optimum value. However, this trend is not seen for all types of lipids. Wei et al. (2015) investigated the effect of temperature on lipids present in microalgae *Nannochloropsis oculata* and *Tetraselmis subcordiformis*. It was observed that elevated temperature caused a decrease in neutral lipids and polyunsaturated fatty acids, while an increase in saturated and monounsaturated fatty acids. Similarly, James et al. (2013) studied the effect of modulation of temperature in microalgae *Chlamydomonas reinhardtii* and reported that the temperature less than 25°C led to a decrease in the stored fatty acids while an increase in the unsaturated fatty acids.

Light intensity: The light is an important factor required during photosynthesis in microalgae (Zhu, 2015). An adequate amount of light intensity usually favors the production of lipids in microalgae as sufficient light is beneficial for excessive storage of photo assimilates that are converted to chemical energy (Solovchenko et al., 2008). The high amount of lipid accumulation (47% DCW) was obtained in microalga *Nannochloropsis* sp. under a light intensity of 700 μmol photons m^{-2} s^{-1} (Pal et al., 2011). Further, Takeshita et al. (2014) observed that *C. vulgaris*, *C. viscosa*, *P. beijerinckii*, *P. kessleri* CCALA255 and *C. emersonii* exhibited increased lipid productivity under high

light intensity (600 μmol photons m^{-2} s^{-1}). Further, it was observed that the lipid content in microalgae *Scenedesmus abundans* increased drastically from 21.2% to 32.8% with the increase in light intensity from 3000 to 6000 lux, respectively (Mandotra et al., 2016). The other study demonstrated that *Botryococcus* sp. exhibited the highest lipid content of approximately 36% at 6000 lux (Yeesang and Cheirsilp, 2011). Thus, it can be inferred that the highest lipid content in different microalgae species varied with light intensities, as the efficiency of light utilization is different in each species. Hence, the ability to utilize light is specific to microalgae species. When the light intensity is considerably low such as below a threshold value, the concentration of microalgal biomass is compromised that impacts the cell growth and lipid accumulation negatively (Zhu, 2015). On the contrary, microalgal growth increases with the increase in the light intensity above the threshold value, also maximum photosynthetic efficiency is achieved at the light saturation point (Vitova et al., 2015). However, excessively high light intensity may result in photo–inhibition and damaging of microalgal photosystems, thereby reducing lipid accumulation.

Nutrient starvation: The inorganic nutrients such as carbon, nitrogen, iron, sulfur, phosphorus, etc. have a significant impact on the growth, metabolism and reproduction of microalgae cells. Nutrient starvation is an effective technique for altering and controlling the cell cycle and biochemical pathways in microalgae related to the production of lipids and their storage. The limitation of nutrients generates a response causing more lipid compounds to accumulate (Arguelles et al., 2018).

The cell growth is directly linked to the concentration of nutrients present in the culture medium. During the early stages of cell growth; a medium rich composition favors the enhancement of biomass productivity. After attaining a significant biomass, nutrient limitation can develop an environmental stress and shoot up lipid production, especially in the late stages of cell growth. Table 1.7 briefly discusses various microalgae cultivation in

nutrient–limited environment. Many literatures reported that various microalgae species produce and accumulate higher amount of lipids such as triacylglycerides in a nitrogen limited mixotrophic conditions (Hsieh and Wu, 2009; Li et al., 2014; Yeh and Chang, 2011). However, the nutrient limitation might impact other biochemical pathways in the cells affecting the lipid production indirectly (Srinuanpan et al., 2018).

Table 1.7. Studies on effect of nutrient starvation on lipid content of various microalgae

Microalgae	Nutrient	Culture conditions	Lipid (%)	References
Ankistrodesmus falcatus	Nitrogen starvation; phosphorus starvation	Autotrophic at 20°C for 16 days	34.4; 45.9	Álvarez–Díaz et al., 2014
Chlorella lobophora	Sulfur deprivation	Autotrophic at 20°C for 21 days	50.0	Mizuno et al., 2013
Chlorella protothecoides	Phosphorus starvation	Mixotrophic at 28°C for 7 days	32.8	Li et al., 2014
Chlorella vulgaris	Nitrogen starvation	Autotrophic at 25°C for 10 days	53	Mujtaba et al., 2012
Chlorella zofingiensis	Nitrogen starvation; phosphorus starvation	Autotrophic at 25°C for 28 days	65.1; 44.7	Feng et al., 2012
Chlorella zofingiensis	Nitrogen starvation; phosphorus starvation	Mixotrophic at 25°C for 8 days	41.2; 42.7	Zhu et al., 2013
Monoraphidium sp.	Nitrogen starvation	Autotrophic at 25°C for 5 days	44.4	Zhao et al., 2016
Parachlorella kessleri	Sulfur deprivation	Autotrophic at 20°C for 14 days	50.7	Ota et al., 2016
Scenedesmus sp.	Nitrogen starvation	Mixotrophic at 25°C for 10 days	31	Xin et al., 2010

Several works have investigated different types of nutrient limitation methods in variety of strains to understand and optimize different parameters. Yang et al. (2018)

demonstrated that under conditions of nitrogen and phosphorus limitation, the yield of fatty acids is considerably increased in *Chlamydomonas reinhardtii*. Cordeiro et al. (2017) investigated the effects of nitrogen and phosphorus on the growth of *Microcystis* species and reported that the obtained lipid performance exhibited an inverse and direct correlation with concentrations of nitrogen (35.8%) and phosphorus (31.7%) in *Microcystis panniformis* and *Microcystis novacekii*, respectively. Nevertheless, Mata et al. (2013) demonstrated that by increasing the nitrogen concentration by ten folds in the culture medium, lipid content and productivity enhanced by 33.5% and 47.4 mg/L/day, respectively in microalgae *Dunaliella tertiolecta*. It was also shown that ten times increase of the iron concentration in the standard culture medium, increased the lipid productivity from 14.6 to 28 mg/L/day.

Salinity stress: Salts play an important role in the growth and metabolism of fatty acids in microalgae, hence, salinity stress is also an effective technique for increasing lipid accumulation and content of microalgal biomass (Guo et al., 2017). Saline stress can cause a difference in osmotic pressure within microalgae cells that leads to stress–response causing alteration in their metabolism causing microalgae to adapt to new conditions (Kan et al., 2012). The modifications at the metabolic level causes fluctuation in the saline level within cell, considerably enhancing the lipid content. It has been observed that variations in the saline concentration in the growth medium not only enhances the lipid content, but may also change its composition (Sharma et al., 2012). Bartley et al. (2013) studied the effects of saline stress on the cell growth of marine microalgae *Nannochloropsis salina.* The microalgae were grown at 22 PSU (particle salinity unit) until the stationary phase was reached later increasing the salt concentrations to 34, 46 and 58 PSU. The lipid content was found to increase at these salt concentrations, with the highest total content of fatty acids (36% dry tissue mass) achieved at 34 PSU.

Further, Salama et al. (2013) reported that the maximum growth was achieved with a concentration of 25 mM NaCl for *C. Mexicana* and *S. obliquus* exhibiting maximum lipid content of 37% and 34%, respectively. They also studied the fatty acid composition reporting the oleic acids (41%) and linoleic acids (41%) to be the major fractions. Though the reports on the effect of salt concentrations on the composition of fatty acids in microalgal lipids are limited and variable, it has also been shown that high salt concentrations in microalgae such as *C. Mexicana* and *S. obliquus* can improve the fatty acid composition. Thus, different salt (NaCl) levels can be used to alter the composition of fatty acids, depending on the type of lipid in microalgae. Pandit et al. (2017) reported that high lipid content of 49% and 43% was obtained with the growth of *C. vulgaris* and *A. obliquus*, respectively, in a culture medium containing different salt concentration ranging from 0.06 to 0.4 M NaCl. Moreover, considerable lipid accumulation of 33.40 ± 2.29% was observed in *Acutodesmus dimorphus* with 200 mM NaCl; that increased to 43% on extending the salinity stress to 3 days (Chokshi et al., 2017).

The lipid accumulation in microalgae also gets affected by the type of salt used to give salinity stress. Srivastava and Goud (2017) carried out the cultivation of *Chlorella sorokiniana* and *Desmodesmus* with different types of salts such as NaCl, KCl, $CaCl_2$, etc. They reported that the maximum production of lipids was obtained with $CaCl_2$. It was assumed that calcium played a vital role in cell signaling under conditions of salt stress that may have increased the production of lipid compounds.

1.3.2 Application of sonication during fermentation

The kinetics and yield of fermentation processes (such as bioalcohol fermentation) can be improved with application of both low and high intensity ultrasound (Sinisterra, 1992). The pretreatment processes (such as enzymatic hydrolysis of biomass) prior to

fermentation can also be enhanced with application of ultrasound (Jeon et al., 2013). Sonication induces modifications in the physicochemical properties of the algal cell that facilitates an improved cellular transport with better accessibility to the carbohydrate substrates in the fermentation media, thus, enhancing their utilization and conversion during fermentation. Sonication at low intensity has been reported to promote cell growth or cell density in the medium and improve the porosity of the cell membrane that results in higher protein production (Chaunyan et al., 2004). For example, the cell membrane porosity was observed to increase in *Pseudomonas aeruginosa* by sonication that resulted in an increased uptake of 16–doxylstearic acid through the membrane (Rapoport et al., 1997). Also, diffusion rates can be enhanced due to the increased cell permeability ultimately boosting the overall growth rate and cell productivity (Pitt and Ross, 2003). Literature review reveals very little activity in the area of sonication-enhanced lipid production by microalgae.

Most of the previous literature reports application of sonication in downstream processing, i.e. biomass pretreatment and extraction of lipids from microalgae. Han et al. (2016) have demonstrated that application of sonication during the end of log phase was most effective for enhancing fermentative lipid production. Sonication under optimum conditions could enhance extent as well as rate of lipid accumulation by 57.5%.

1.3.2.1 Basic principles of ultrasound and cavitation

Ultrasound: Ultrasound are basically the longitudinal acoustic waves that are beyond the upper limit of human hearing range which is above 20 kHz. The frequency of ultrasound waves ranges from 20 kHz – 20 MHz. Since ultrasound is a longitudinal wave, it can pass in the form of alternate compression and rarefaction cycles through a compressible medium like air or water. A periodic variation is generated in bulk pressure and density of the

medium due to the propagation of ultrasound waves in the medium. Such a propagation causes an oscillatory motion of fluid elements in the medium (Shah et al. 1999). The ultrasound wave is characterized by physical properties of frequency, velocity and pressure amplitude. The properties of the sound wave in gaseous medium are strongly influenced by the static pressure in the medium. Since the liquid properties are comparatively insensitive to moderate variations of static pressure, the ultrasound waves in liquid medium are practically uninfluenced by the static pressure.

Cavitation: Cavitation refers to the growth, nucleation, oscillation or collapse of gas bubbles due to variation in the bulk pressure of the medium. Such a pressure may arise due to propagation of an acoustic wave, variation in the flow geometry, or energy dissipation in the system. The efficiency of any process whether it is biological, physical or chemical, is usually dependent on the method through which energy is introduced into the system. Cavitation is one of the methods that is efficient in introducing the energy into the system for intensification of large number of biological processes. Ultrasound uniquely provides energy available on very small time and spatial scales that are generally unavailable from any other kind of source.

Physical effects of cavitation and sonication on system: Both cavitation and ultrasound exhibit different physical effects on a particular reaction system. However, the primary purpose of the final outcome is the induction of intense micro–mixing and micro–convection in the reaction system. The physical effects generated due to cavitation and ultrasound are briefly described below (Young, 1989; Shah et al., 1999):

Micro–streaming: It refers to an oscillatory motion of fluid elements having small amplitude around a mean position that is generated due to propagation of ultrasound wave.

The micro–streaming velocity is approximately 0.08 m/s for an ultrasound wave having a pressure amplitude of 120 kPa in water (C = 1500 m/s; ρ = 1000 kg/m^3).

Acoustic streaming: The wave momentum is absorbed by the medium during propagation of ultrasound wave due to finite viscosity. Such phenomenon leads to generation of unidirectional currents of fluid having low velocity and is referred to as acoustic streaming (Nyborg, 1958).

Micro–turbulence: The oscillatory motion of fluid generated due to oscillations of the bubble is known as micro–turbulence. This process usually comprises of two phases. During the expansion phase of the radial motion of cavitation bubble, the liquid is pushed away from the bubble interface. While in the collapse phase the liquid is attracted towards the bubble as filling the generated vacuum in the liquid due to the size reduction of bubble. The mean velocity of micro–turbulence is dependent on amplitude of the bubble oscillation.

Acoustic (or shock) waves: In the compression phase of radial motion, a contraction of the cavitation bubble takes place, generating a void space in the liquid. The fluid elements are then spherically converged with high velocity in the void space created during compression, thus transferring kinetic energy to the bubble. Thus, work is done on the bubble. In a cavitation bubble that contains a non–condensable gas (air), the adiabatic compression leads to a rapid rise of the pressure within the bubble. At the minimum radius i.e. maximum compression, the bubble wall experience a sudden halt. At this point, the fluid elements reflect from the interface that were converged towards the bubble. Such a reflection generates a highly pressurized shock wave that travels through the entire medium. Finally, the pressure within the bubble due to non–condensable gas results in rebounce of the bubble.

Micro–jets: If the motion of liquid in proximity of the cavitation bubble is uniform and symmetric, a spherical geometry can be maintained by radial motion due to ultrasound

waves such that pressure gradient is not there. If the location of the bubble is in close proximity to a phase boundary– solid–liquid, liquid–liquid or gas–liquid, the motion of liquid is altered in its vicinity, thereby leading to emergence of pressure gradient. Such a non–uniform pressure results in the loss of bubble's spherical geometry. In the asymmetric radial motion, the bubble portion which is exposed to a higher pressure ruptures faster in comparison to other bubbles, thereby resulting in the formation of a high speed liquid jet directed towards the boundary. The velocity of such micro–jets were predicted to be in the range of 120 to 150 ms^{-1} which can cause acute damage such as cell disruption, particle size reduction, polymer degradation or particle size reduction.

1.3.3 Genetic modification of microalgae

The genetic modification in microalgae using molecular biology can be an alternative to enhance the lipid productivity. Genetic engineering involves the inhibition or over expression of one or more genes responsible for the production of a particular metabolite. In case of microalgae, these genes are related to photosynthesis, growth rate, resistance to extreme pH, high salinity, elevated temperature and genes that are responsible for the lipid metabolism (Dickinson et al., 2017). The application of genetic engineering is restricted due to the reliance on the available data to carry out genetic modifications, sequencing the microalgae genomes and precision of the genes according to these genomes. Till date, the available genomes of microalgae are limited.

There are various bioengineering methods for the genetic modification of microalgae such as Clustered Regularly Interspaced Short Palindromic Repeats—CRISPR associated with the protein 9 (CRISPR–Cas9), Transcription Activator–Like Effector Nucleases (TALEN), Random Mutagenesis and Zinc–Finger Nucleases (ZFN) generally employed in the gene sequence alteration (Sizova et al., 2013). Further, homologous

recombination, short interfering RNA (siRNA) and micro RNA (miRNA) can be used for the activation or repression of gene expression (Yao et al., 2015). Moreover, for the transfer of DNA into microalgae cells, agitation assisted by glass or silicon bead, electroporation, carbide whiskers, biolistic micro–particle bombardment and *Agrobacterium tumefaciens*–mediated gene transfer could be used (Sizova et al., 2013). Most of the genetic manipulation reported on microalgae have been carried out in the study models as *Chlorella* and *Chlamydomonas* to increase the production of lipids. RNA silencing technique has been reported among the best methods in the genetic engineering approach.

Moreover, the basic problem with genetically modified (GM) microalgae is the environmental concern and the related ethics pertaining to their release. It is worth mentioning that the release of any genetically modified organism into the nature must be analyzed thoroughly, and moreover should pass through the acceptance of various international committees comprising of experts. In the erroneous situation, their consensual release may affect the natural habitat where they can further reproduce and spread undesirably (Beacham et al., 2017). Thus, the GM microalgae related concerns and its impact on human health and environment needs to be scrutinized before making a final decision about their release to prevent negative ecological effects like alteration in food web structure, displacement of native species like phytoplankton, local extinctions, and societal as well as economic effects for various toxic strains (Campbell, 2011).

1.4 Catalytic and non–catalytic microalgal biodiesel production

The production of biodiesel from microalgae generally involves the lipid extraction from microalgae cell followed by transesterification. The lipid extraction by cell rupture (i.e. the breakdown of the rigid cell wall) facilitates almost complete release of intracellular lipids, thus making lipid extraction easy and efficient. The disruption of the cell wall can

be achieved by either mechanical methods (grinding with mortar and pestle or microwave or sonication) or non–mechanical methods such as biological or chemical treatments. Though mechanical methods are energy intensive, higher yield of lipids can be obtained in less extraction time. These methods are also easy to scale-up. Comparatively, chemical methods do not require energy and make use of salts, solvents, acids, surfactants that are selective as well as efficient. Huang and Kim (2017) reported the use of methanol and trimethylamine as solvents for the simultaneous cell wall disruption and lipid extraction in wet *Chlorella vulgaris*. The reported process was shown to exhibit a 95% lipid yield.

Further, biological methods involve the usage of enzymes such as protease, lipase and cellulase or different multiple enzymes for the cell wall disruption. The advantages of this method are mild operating conditions along with low energy consumption. Wu et al. (2017) carried out the alkaline pretreatment assisted lipid extraction employing various enzymes from microalgae *Nannochloropsis* sp. It was reported that 90% lipid yield was obtained under an extraction temperature of 50°C and extraction time of 30 min. However, the high cost of enzyme and longer reaction time limits its usage, thus making enzymatic disruption a challenging method (Lee et al., 2017).

Thus, an efficient yet economic method for lipid extraction and recovery would involve combination of mechanical and non-mechanical methods (Lee et al., 2017; Zhu et al., 2017). Table 1.8 compares the techniques reported in previous literature on biodiesel production from microalgae. An example of an economic and energy efficient technique for lipid extraction is reported by Kim et al. (2016). This technique involves ultrasound-based pretreatment followed by solvent extraction using methanol that yielded ~ 42 wt% lipid extraction from *Chlorella protothecoides* (Kim et al., 2016).

Table 1.8. Comparison of different techniques used for biodiesel production

Sr. No.	Techniques	Advantages	Disadvantages	References
1	Micro–emulsion	It is very easy and convenient.	The biodiesel produced does not have good stability and volatility. It also has high viscosity.	Namasivayam et al., 2010
2	Pyrolysis	This is a simple process as well as non–polluting.	The apparatus used is expensive and requires high temperature. The biodiesel produced has low purity.	Maher and Bressler, 2007
3	Supercritical methanol	The process does not require any catalyst and has a short reaction time with high conversion.	The process demands high energy consumption along with expensive apparatus.	Xin et al., 2008
4	Transesterification	The process is cost efficient with higher conversion efficiency. The properties of the biodiesel produced are closer to diesel making it suitable for blending/ substitution making it convenient for industrialization.	The products of the process must be washed and neutralized before use.	Habibullah et al., 2014; Patil and Deng, 2009

Biodiesel can be obtained by transesterification, the reaction of microalgae oil with excessive alcohol such as methanol, ethanol, propanol or butanol. Most commonly used alcohol is methanol as it inexpensive and reactive. Further, acids, base, and enzymes are often employed as catalysts in transesterification. Fig. 1.4 shows the overall transesterification reaction. Enzyme based catalysts offer the advantages of mild operating conditions, higher yield, and a need of simple purification. However, these catalysts are comparatively more expensive than other and require longer reaction time. Though base

catalyst provide a fast reaction rates, however, those are unsuitable for microalgae oil due to its high FFA content. Chen et al. (2012) observed that the FFA content of microalgae oil can possibly reach up to 70.3%. Similarly, Krohn et al. (2011) reported the FFA content of 84% in microalgae oil extracted from *D. tertiolecta*. Hence, for oils having high FFA content, the use of acid catalyst could be a best option for biodiesel production, even though it requires higher temperature, longer reaction time and quite typical product purification process (Park et al., 2015; Zhu et al., 2017). The homogeneous catalysts impose a problem of product separation (Park et al., 2015). On the contrary, heterogeneous catalysts can be separated and recovered easily and are ecofriendly (Daniel et al., 2017).

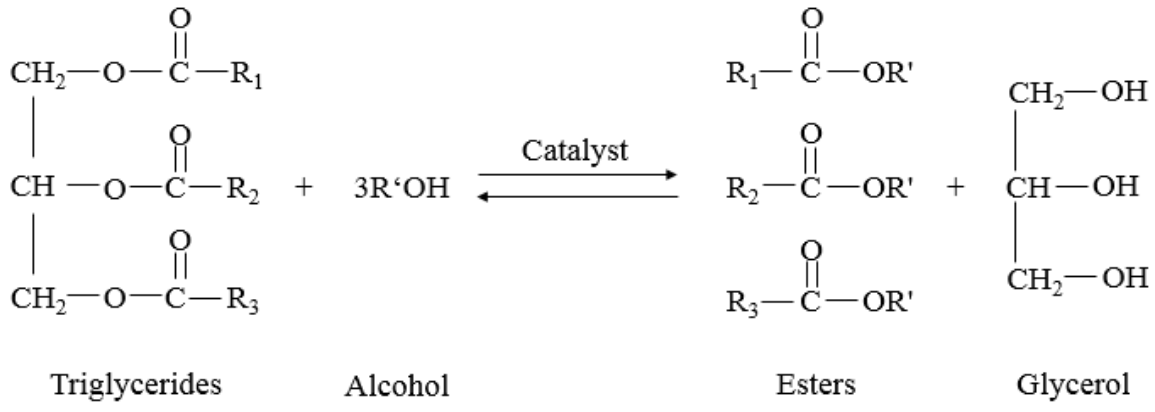

Figure 1.4. Overall reaction of transesterification of triglycerides

Wet *in situ* transesterification has been introduced to convert lipids into biodiesel with a minimum energy consumption. In *in situ* transesterification, extraction and transesterification are carried out simultaneously resulting in a higher biodiesel due loss of oil is prevented during solvent extraction. A peculiar feature of such processes is that methanol plays a dual role, i.e. solvent for lipid extraction and a reagent of transesterification reaction. Thus, methanol is needed in relatively larger quantities in such process. Moreover, wet microalgae retain water in higher amount that can lead to hydrolysis

of biodiesel into alcohol and FFA. Water in wet microalgae leads to formation of a thin layer (Park et al., 2015) that is miscible with the reactant (Park et al., 2017), thus preventing lipid extraction and transesterification. To overcome the problems of water as well as requirement of alcohol in larger amounts, the addition of co–solvents like hexane or chloroform can be a good option. Co–solvents are reported to improve the lipid extraction and facilitate the mass transfer of reactant (Park et al., 2017). Im et al. (2014) showed that the addition of chloroform as a co–solvent resulted in approximately 90% biodiesel yield during *in situ* transesterification of wet microalgae having high water content (65%). Another work reported by Im et al. (2015) showed that the biodiesel yield can improve up to 13.44% by using chloroform as a co–solvent. Nevertheless, Kim et al. (2015a) reported that pure methanol was comparatively more effective in wet in situ transesterification leading to > 99% biodiesel yield. Another factor to be considered is ratio of chloroform to alcohol that could affect the biodiesel yield. Higher the alcohol in the solvent mixture, higher amount of oil can be converted to biodiesel, as the co–solvent helps in improving the lipid extraction and mass transfer between alcohol and oil (Park et al., 2015; Skorupskaite et al., 2016). Although the usage of co–solvent is beneficial, its separation and environmental issues should be taken into consideration.

The other prominent factors affecting biodiesel conversion in wet *in situ* transesterification are microalgae species, water content, temperature, and ratio of biomass to alcohol as well as catalyst, agitation rate and reaction time (Salam et al., 2016). The severe operating conditions could result in a higher biodiesel yield, as with the increase in temperature, mass transfer, reaction rates can increase (Skorupskaite et al., 2016). Among the acid catalysts, sulfuric acid is preferred since it is cost effective. However, according to Kim et al. (2015b), the use of HCl in comparison to H_2SO_4 as the catalyst could result in 15 wt% higher FAME. A higher FAME yield of 90% was achieved even in the conditions

of high moisture content (80%). Also, the biodiesel yield remained unaffected by moisture content, co–solvent addition, and temperature change on using HCl as the catalyst. Nevertheless, usage of enzyme as a catalyst is beneficial due to operation at lower reaction temperature and its easier separation. López et al. (2016) reported that 99.5% FAME was obtained during in situ transesterification using enzyme as the catalyst in the high–pressure homogenization (HPH) pretreatment process. However, high cost, low reaction rate and low stability limits their application as the catalyst. Table 1.9 summarizes the literature on biodiesel production from microalgae with different catalysts and modus operandi of *in situ* transesterification and two–step transesterification.

The commercial production of microalgae–based biodiesel has not been realized yet. The major causes are energy intensive processes and high fixed and operating costs. Especially, drying of biomass is the cost intensive and limiting factor (Pan et al., 2017). Processes with direct use of wet biomass (thus skipping the drying step) may have higher merits in terms of energy consumption. Another challenge in this process is the dilution of catalyst due to moisture content of biomass. Use of catalysts with higher activity (which is relatively insensitive to presence of moisture) could be a solution to this issue.

The non–catalytic transesterification process can be carried out under either supercritical or subcritical condition. Both of these processes need high temperature and pressure conditions in comparison to catalytic processes. Even though these processes are energy intensive, their distinct merits are: (1) conversion of biodiesel is relatively independent of initial feedstock conditions (such as water or FFA content) under sub– or supercritical conditions. This facilitates the direct usage of microalgae as a feedstock that has moisture content of up to 90% and high FFA content, (2) high conversion in short reaction time, (3) simpler and easier product separation and purification (Jazzar et al., 2015; Nan et al., 2015).

Table 1.9. Catalytic biodiesel production from various microalgae

Sr. No.	Microalgae	Process	Catalyst	Operating conditions	Yield (%)	References
1	*Tetradesmus obliquus* IPPAS S–2023	Transesterification	H_2SO_4 (5 wt%)	t = 1.5 h, 0.01% 2,6–di–tert–butyl–4–methylphenol as antioxidant	–	Ismagulova et al., 2018
2	Mixed culture	Two–step transesterification	H_2SO_4 (1.5 wt%) and KOH (3 wt%)	1st step: T = 55°C, t = 90 min, methanol/oil molar ratio = 7:1, 2nd step: T = 60°C, t = 1 h, methanol/oil molar ratio = 6:1	96	Karmakar et al., 2018
3	*Chlorella* sp. (dry powder)	*In situ* transesterification	Impregnated pumice (20 wt%)	T = 80°C, t = 3 h, agitation = 500 rpm, methanol/biomass = 12:1 mL/g	42	Daniel et al., 2017
4	*Botryococcus* sp. (dry)	Ultrasound–assisted *in situ* transesterification	Immobilized lipase (*Candida antartica* lipase B) 10%	Ultrasound: 30 kHz, 200 W, T = 50°C, t = 4 h, reactant: dimethyl carbonate = 5 mL/g, distilled water = 1%	88	Sivaramakrishnan and Incharoensakdi, 2017
5	*Botryococcus* sp. (dry)	*In situ* transesterification	Immobilized lipase (*Candida antartica* lipase B) 20%	T = 50°C, t = 36 h, reactant: dimethyl carbonate = 5 mL/g, distilled water = 1%	78	Sivaramakrishnan and Incharoensakdi, 2017
6	*Chlorella pyrenoidosa*	Microwave–assisted *in situ* transesterification	Graphene oxide (5 wt%)	Microwave: 600 W (heating) 500 W (holding), T = 90°C, t = 40 min, methanol/chloroform = 1:1 (v/v)	95.1	Cheng et al., 2016
7	*Nannochloropsis gaditana* B–3 (25% dry biomass)	*In situ* transesterification	Novozym 435 (N435)	Pre–treatment: high pressure homogenization, T = 40°C, t = 56 h, methanol/oil = 4.6: 1 (mL/g), t–butanol/oil = 7.1:1 (mL/g), N435/oil = 0.32:1	99.5	López et al., 2016

Table 1.9. (*continued*…..)

Sr. No.	Microalgae	Process	Catalyst	Operating conditions	Yield (%)	References
8	*Chlamydomonas* sp. JSC4 (slurry: 31.3% dry biomass)	Two–step transesteri-fication	NaOH (0.5 wt%)	Pretreatment: microwave (350 W, 10 min), solvent extraction: methanol/hexane = 3:1, T = 45°C, t = 80 min, transesterification: hexane + oil/methanol = 6:1 (v/v), T = 45°C, t = 15 min, agitation = 600 rpm	95	Chen et al., 2015
9	*Chlamydomonas* sp. JSC4 (Cake, solid content: 56.6%–60.5%)	*In situ* transesteri-fication	NaOH (0.5 wt% in methanol)	T = 45°C, t = 15 min, agitation = 600 rpm, hexane/methanol/biomass = 6:4:1 (mL/mL/g)	101 ± 2.7	Chen et al., 2015
10	*Nannochloropsis salina* (moisture: 76.5 ± 1%)	*In situ* transesteri-fication	H_2SO_4 (50 µL)	T = 100°C, t = 1 h, wet biomass = 200 mg, methanol = 2 mL	99.7	Kim et al., 2015(a)
11	*Nannochloropsis gaditana* (80% moisture)	*In situ* transesteri-fication	HCl (0.3 mL)	T = 95°C, t = 2 h, methanol/chloroform = 1:2 (v/v)	85.7 ± 1.7	Kim et al., 2015(b)
12	*Scenedesmus obliquus* (Trup.) Kutz. (SAG 276–3a)	Transesteri-fication	HCl	T = 65°C, t = 6.4 h, methanol/HCl/oil = 82:4:1	68.3 ± 1.6	Patnaik and Mallick, 2015

Table 1.9. (*continued*…..)

Sr. No.	Microalgae	Process	Catalyst	Operating conditions	Yield (%)	References
13	*Chlorella* sp.	*In situ* transesterification	H_2SO_4 (0.6 mL)	T = 90°C, t = 2 h, hexane/ethanol = 1:2 (v/v), solvent = 6 mL	90.02 ± 0.55	Zhang et al., 2015
14	*Chlorella* sp. FC2 IITG	Two–step direct transesterification	NaOH and H_2SO_4	T = 90°C, agitation = 150 rpm 1st step: t = 20 min, catalyst/biomass = 0.67 (w/w), methanol/biomass = 49.51 (v/w), 2nd step: t = 10 min, catalyst/biomass = 2.07 (v/w), methanol/biomass = 61.07 (v/w)	98.96	Kumar et al., 2014
15	*Nannochloropsis*	*In situ* transesterification	$Mg_2Zr_5O_{12}$	T = 65°C, t = 4 h, methanol/methylene dichloride (10 wt%) = 3:1 (v/v)	60	Li et al., 2011

It has been reported in previous literature that both *in situ* and two–step transesterification can be carried out under the critical conditions. Two–step transesterification comprises of solvent or subcritical water extraction in the first step, followed by transesterification carried out under supercritical condition in the subsequent step. As the process is sequential in nature it becomes energy intensive, thus, *in situ* transesterification carried out under supercritical condition could help in reducing energy consumption.

Further, temperature is an important factor in the sub– or supercritical process. When the temperature is equal or above its critical temperature, water or methanol not only exhibit an ability to extract lipids but also facilitate the conversion of these extracted lipids into biodiesel (Patil et al., 2011). Under sub– or super critical condition water or methanol possess similar properties to that of an organic solvent that makes them feasible to exclude the extraction step carried out separately without the addition of catalyst. Moreover, *in situ* transesterification under a supercritical condition requires a higher temperature and pressure in comparison to a subcritical condition. Therefore, in order to lower the critical temperature of mixture, addition of a co–solvent becomes a necessity. The addition of a co–solvent leads to a positive effect on increasing the lipid extraction efficiency (Abedini et al., 2015). Besides temperature, the other factors such as pressure, amount of alcohol and reaction time also affect the conversion of biodiesel in the sub– or supercritical process. Higher biodiesel yield can be obtained at higher temperatures. However, alkyl esters may undergo decomposition at high temperature, thus lowering the yield. Thus, the decomposition temperature limit for the respective microalgae strain should be known (Abedini et al., 2015). Though pressure is temperature dependent it was reported to have a slight positive impact on biodiesel yield.

Further, the alcohol is required in high amount in the supercritical condition. Alcohol serves a variety of purpose like as a solvent in the lipid extraction, as a feed to produce biodiesel, and as a catalyst precursor (Cheng et al., 2016). However, excessive alcohol should be avoided as it can decrease the final yield (Patil et al., 2013). Although, the supercritical process requires lower reaction times, the optimum reaction time must be known because a reaction completed before the optimum reaction time may lead to an incomplete reaction (Li et al., 2011; Tsigie et al., 2012) while a reaction running longer than the optimum time may reduce the biodiesel since the presence of water favors the hydrolysis of FAME to free fatty acids (Nan et al., 2015; Patil et al., 2013).

In addition, the temperature and pressure requirement in the subcritical process are comparatively lower than supercritical process, but still result in a high yield of FAME. The subcritical process thus requires less energy for biodiesel production. Sitthithanaboon et al. (2015) and Tsigie et al. (2012) converted wet microalgae with moisture content up to 80% into biodiesel under a subcritical condition using methanol. However, different operating conditions and two different algae strains were used in both the works obtaining a maximum FAME yield of and 59.28% and 88.65%, respectively. The factors affecting conversion under a subcritical condition are quite similar to those under supercritical conditions.

1.5 Biorefinery approach for microalgal biodiesel production

Microalgae serves as a potential feedstock in biofuel production as well as a source of bioactive compounds. Fig. 1.5 shows few biofuels produced from microalgae. Although the lipid content in microalgae cell is high, microalgae lipid conversion to produce biodiesel only makes it economically feasible. The generation of valuable products from other cell constituents of microalgae can be profitable from the economic aspect (Chew et al., 2017).

The constituents of a microalgae cell can be divided into major and minor components. The major components include proteins, lipids and carbohydrates while the minor components include vitamins, pigments and fatty acids (Parniakov et al., 2015).

Among the major components, derivatives of carbohydrate compounds such as glucose, cellulose, starch, etc. can generate chemicals that are valuable. Cellulose based derivatives can yield co–products during production of biodiesel using wet *in situ* transesterification. Im et al. (2015) reported that ethyl formate, diethyl ether and ethyl levulinate were formed together with biodiesel using C_2H_5OH as the solvent and H_2SO_4 as the catalyst. Ethyl formate (EF) can be used as a fumigant in the food stores. Diethyl ether (DEE) can be used as additive in biodiesel to improve the fuel property thereby reducing emissions. Ethyl levulinate (EL) can be used as flavoring agent or its addition to biodiesel can improve the low temperature properties of biodiesel (Im et al., 2015). Generally, *in situ* transesterification is carried out in optimum temperature conditions, however, elevated temperatures are needed for the concurrent synthesis of co–products (example EL, EF, DEE). These co–products can be produced only at temperatures higher than 100°C. The approximate yields of 10%, 52%, and 23% can be obtained for EF, DEE and EL, respectively, with biomass having 65% moisture content. The amount of catalyst and alcohol, in addition to moisture content of biomass affects the formation of co–products. The increase in the catalyst amount can positively affect the formation of co–products, particularly EL and DEE. Larger quantities of alcohol in reaction mixture promote co–product yield because it helps in the esterification of FA and LA. However, the amount needs to be regulated since the acidity reduction due to the catalyst dissolution in alcohol may lead to reduced hydrolyzed algal product and lesser esterification (Im et al., 2015). Furthermore, the moisture content enhances HMF rehydration and cellulose hydrolysis, however, excessive water can hinder dehydration and result in a low EF and EL yield.

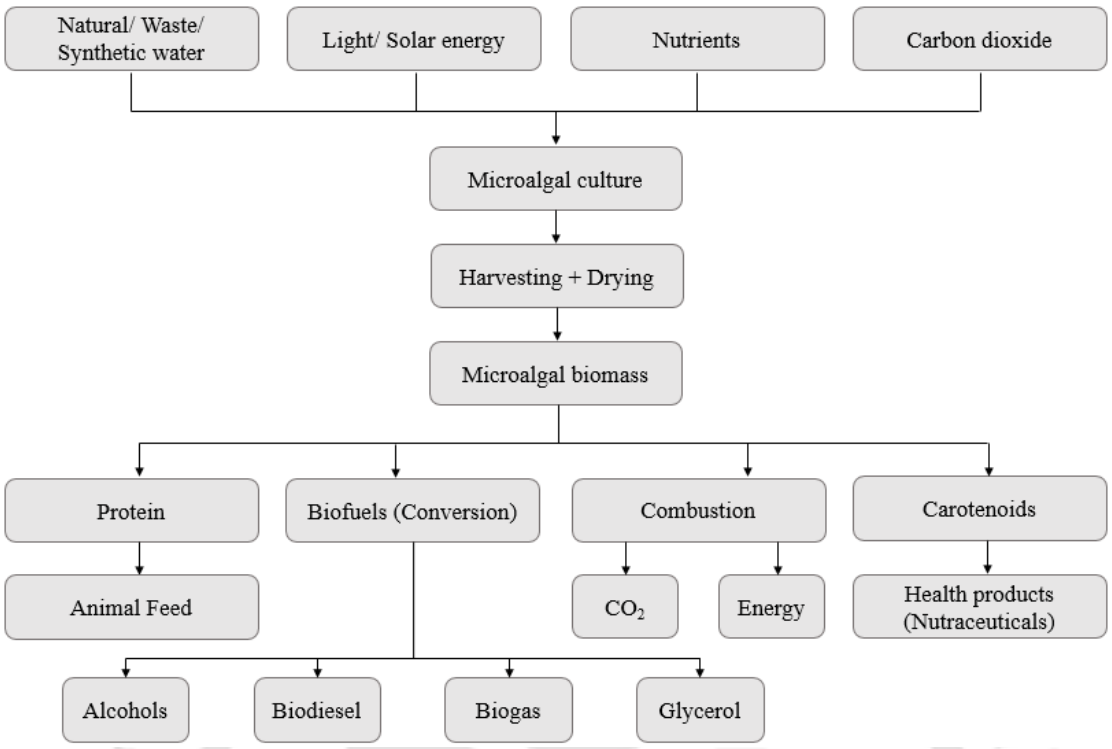

Figure 1.5. Flow diagram depicting various biofuels from microalgae

Pigments, which constitute one of the minor components of microalgal cell, are valuable products. Common pigments present in microalgae strains of all genre are chlorophylls, carotenoids, etc. These pigments have gradually gained importance in the food, cosmetics and pharmaceutical industries (Chew et al., 2017). The major carotenoids found in microalgae are β–carotene, astaxanthin, canthaxanthin, lycopene, and lutein. Astaxanthin and canthaxanthin play role in mechanisms of cell protection. The carotenoids are involved in the photosynthesis of microalgae. For example, lutein absorbs light thereby diminishing excessive energy in the photosynthetic metabolism. The content of carotenoids in microalgae is relatively higher than other sources such as vegetables. The lutein, astaxanthin and β–carotene content in microalgae was approximately 4, 48 and 50 mg/g under stress cultivation conditions (Gong and Bassi, 2016). Carotenoids have also gained attention in the market due to their antioxidant properties involving health benefits. Further,

they could be employed as an agent for anti–cancerous, anti–inflammatory and protection from radiation. Among all the carotenoids, astaxanthin is known to be the strongest antioxidant (Gong and Bassi, 2016). Astaxanthin holds high potential as an antioxidant in comparison to β–carotene (Yen et al., 2013). Astaxanthin or β–carotene are abundant in *Haematococcus, Chlorella and Dunaliella* (Schüler et al., 2017; Singh et al., 2013). These carotenoids can be separated from microalgae cell using supercritical fluid or organic solvent extraction. Organic solvents most commonly used are methanol, ethanol, and acetone along with grinding, homogenization or sonication as a pretreatment for the disruption of the cell wall (Khanra et al., 2018).

Ultrasound has been reported to disrupt the cell wall of microalgae facilitating release of lipids as well as carotenoids. Jaeschke et al. (2017) reported that the ultrasound intensity and solvent concentration affected the carotenoid extraction. The high yields of 1.31 ± 0.04 mg/g were obtained under 50% ultrasound intensity and 75% ethanol concentration. However, the high power of ultrasound and longer exposure to solvents may result in the degradation of compound. Thus, a green solvent may be an alternative solution for the extraction of carotenoids. Damergi et al. (2017) carried out the carotenoid extraction using 2–methyltetrahydrofuran along with ethanol from *C. vulgaris*. At a temperature of 110°C and extraction time of 30 min, the carotenoids obtained were 277 ± 3.8 μg/g DCW from wet microalgae (50% moisture). Also, Singh et al. (2013) reported that sonication followed by maceration resulted in the highest carotenoid extraction that was found to be 16.39 mg/g comprising of 31% β–carotene and 69% zeaxanthin.

The primary limitation in the usage of organic solvents is their toxic nature causing harm to the environment. In such case, supercritical fluid extraction (SFE) can be a better option. Carbon dioxide is most commonly used as a fluid since it is abundant, inert, inexpensive and non–flammable (Khanra et al., 2018). Other solvents that can be used are

ethane, propane, butane and dimethyl ether (DME) (Feller et al., 2018). The supercritical fluid extraction process is highly selective in extracting target compounds of non-polar nature. However, this technique is unsuitable for extraction of polar compounds because of low polarity of solvent commonly employed in supercritical extraction. Supplementation of the main solvent of supercritical extraction with a polar cosolvent can enhance the extraction of carotenoids. Liau et al. (2010) reported the lipids and carotenoid extraction under supercritical CO_2 by the addition of ethanol as a co–solvent at 323 K and 350 bar; yielding 7.6 mg carotenoids/g and 239.7 mg triglycerides/g. Feller et al. (2018) carried out the lipid and carotenoid extraction from *P. cruentum* using n–butane with a yield of 5.2 ± 0.7 mg carotenoids/g. Goto et al. (2015) employed subcritical dimethyl ether for the carotenoid extraction from *U. pinnatifida*, that yielded 390 μg fucoxanthin/g biomass. Marcías–sánchez et al. (2009) showed that the extraction under SFE condition at 60°C and 300 bar yielded 14.9 ± 0.9 μg carotenoids/mg of dry microalgae.

Lastly, the purification of extracted carotenoids generally involves a saponification–solvent extraction based on the Willstatter method. The saponification agent employed are alkalis such as NaOH or KOH that help in releasing carotenoids at a low temperature of 60°C. The solvent extraction using hexane or ethanol–water–CH_2Cl_2 mixture is further used for the separation of water insoluble compounds from the saponified extract. The carotenoid purification can also be conducted via chromatography or crystallization. Generally, carotenoids are obtained in a separate extraction process. However, lutein can be obtained along with biodiesel in one process that resulted in 6 mg lutein/g and 94 mg FAME/g (Gong and Bassi, 2016). Thus, the inclusion of carotenoids as a product during biodiesel production can greatly enhance the economic feasibility. However, the improvement in technologies to reduce the cost of carotenoid separation and purification is mandatory to make the entire process economical.

1.6 Objectives, Approach and Scope of the present Thesis

It can be clearly inferred from the previously described review of literature that microalgae serve as a potential source of various renewable biofuels. Some of these biofuels are biodiesel form lipids (microalgal oil), methane generated from the algal biomass by anaerobic digestion and biohydrogen produced photo–biologically. Traditionally, microalgae were considered as a source of omega-3 fatty acids and as fish food. Due to issues of energy security and global warming (climate change), the microalgae are being looked at as a source of lipids for green liquid fuel production. Despite encouraging results on laboratory scale studies, commercial scale production of biofuels through microalgal route hasn't been possible due to several constraints in large scale cultivation that adversely affect the economy of production. Large production of lipid–rich biomass could not be achieved as advanced technologies are still being developed. Hence, the microalgal route of lipid production has low economic potential. Proper recovery and purification of other value-added products from microalgal biomass that can fetch higher revenue is being sought as a solution to boost economy of microalgal route. Research in microalgae cultivation should also address issues of enhancing the content of nutritional side products from the microalgal biomass. This biorefinery approach can help overcome the bottlenecks in commercialization of biodiesel.

The present thesis is directed towards finding new avenues for microalgae cultivation and growth that would result in enhanced yields of lipids and other nutritional value-added products. The thesis also deals with synthesis of biodiesel from the microalgal lipids and its extensive characterization. The microalgae used in the present study are isolated native strains of *Tetradesmus obliquus* (isolated from local natural habitat). Our studies are based on native strains due to their stability in the environment and resistance towards fluctuations in conditions such as temperature, humidity or external contaminations. The microalgal

cultivation has been statistically optimized for the media components and physio–chemical parameters of growth (viz. incubation temperature, initial pH, substrate concentration and light intensity) for enhancing the lipid and β–carotene content of biomass. To further enhance the yields of these metabolites, external stimuli (sonication) was given. The sonication was provided at optimized duty cycle to intensify the production of metabolites without having any effect on the cells mortality. A kinetic analysis of the process was done. All possible products were synthesized/extracted from biomass such as biodiesel, bioethanol, glycerol and β-carotene. The biorefinery approach of present thesis is shown below in Fig. 1.6.

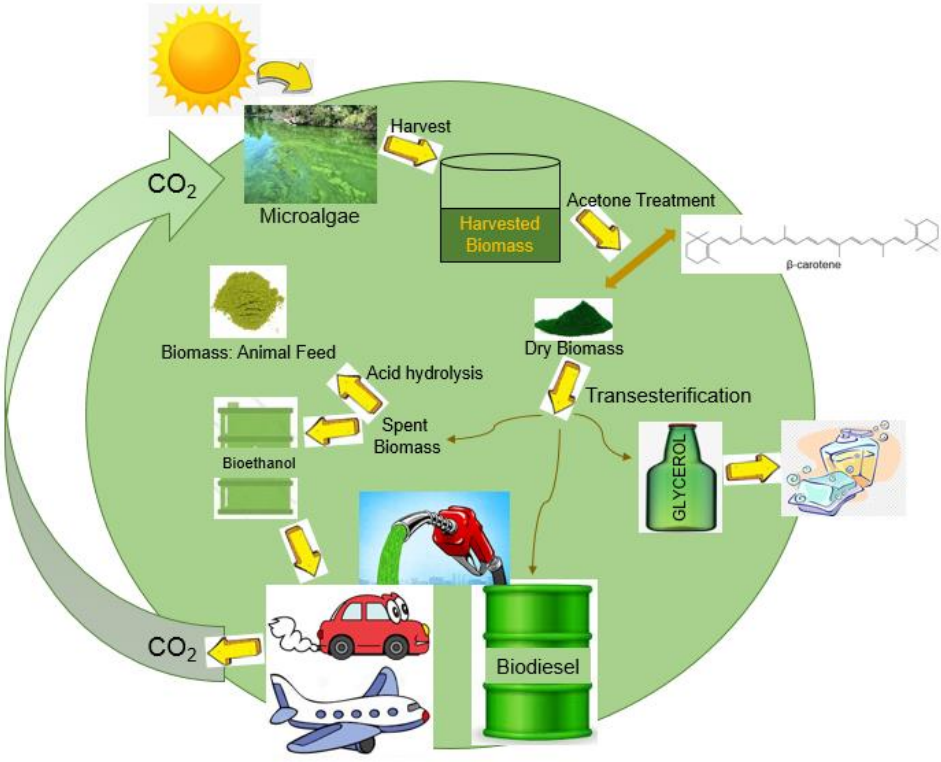

Figure 1.6. Pictorial representation of biodiesel production from isolated microalgae with other value–added products

In addition to this chapter, this thesis includes 5 more chapters that address various facets of microalgae cultivation and growth, extraction of lipids and nutraceuticals from biomass and biodiesel production and characterization. The content of each chapters are briefly outlined below:

- Chapter 2 outlines the process of isolation and biochemical characterizations of wild microalga *Tetradesmus obliquus* SGM19. An initial assessment of this microalgal strain for production of lipids is also done.
- Chapter 3 describes the statistical optimization of simultaneous lipid and β–carotene production from the microalgal strain of *Tetradesmus obliquus* SGM19. Intensification of lipid and β–carotene production with sonication is also attempted. A kinetic analysis of the process is done.
- Chapter 4 explains the *in situ* and two–step transesterification of *Tetradesmus obliquus* SGM19 strain biomass/extracted lipid with further enhancement in transesterification process by optimization and sonication.
- Chapter 5 details a sequential (bio-refinery) approach for synthesis or extraction of biofuels (biodiesel, bioethanol) and other value-added products (β-carotene, glycerol) from *Tetradesmus obliquus* SGM19.
- Chapter 6 presents an overview of conclusions and contributions of all chapters in the thesis. Some suggestions are also given for taking ahead the research work.

References

Abedini H., Vossoughi M., Pazuki G., 2015. The role of cosolvents in improving the direct transesterification of wet microalgal biomass under supercritical condition. Bioresour. Technol. 193, 90–96.

Alam F., Date A., Rasjidin R., Mobin S., Moria H., Baqui A., 2012. Biofuel from algae – is it a viable alternative? Procedia Eng. 49, 221–227.

Alba L.G., Torri C., Samori C., Spek J.V., Fabbri D., Kersten S.R.A., Brilman D.W.F., 2012. Hydrothermal treatment of microalgae: Evaluation of the process as conversion method in an algae biorefinery concept. Energy Fuels 26, 642–657.

Alessandro E.B.D., Antoniosi N.R., 2016. Concepts and studies on lipid and pigments of microalgae: a review. Renew. Sustain. Energy Rev. 58, 832–841.

Álvarez–Díaz P.D., Ruiz J., Arbib Z., Barragán J., Garrido–Pérez C., Perales J.A., 2014. Lipid production of microalga *Ankistrodesmus falcatus* increased by nutrient and light starvation in a two–stage cultivation process. Appl. Biochem. Biotechnol. 174(4), 1471–1483.

Arguelles E.D, Laurena A.C., Monsalud R.G., Martinez–G M.R., 2018. Fatty acid profile and fuel–derived physico–chemical properties of biodiesel obtained from an indigenous green microalga, *Desmodesmus* sp. (I–AU$_1$), as potential source of renewable lipid and high quality biodiesel. J. Appl. Phycol. 30(1), 411–419.

Artamonova E., Vasskog T., Eilertsen H.C., 2017. Lipid content and fatty acid composition of *Porosira glacialis* and *Attheya longicornis* in response to carbon dioxide (CO_2) aeration. PLoS ONE. 12(5), e0177703.

Aslan S., Kapdan I.K., 2006. Batch kinetics of nitrogen and phosphorus removal from synthetic wastewater by algae. Ecol. Eng. 28(1), 64–70.

Balat M., Balat H., Oz C., 2008. Progress in bioethanol processing. Prog. Energy Combust. Sci. 34, 551–573.

Bartley M.L., Boeing W.J., Corcoran A.A., Holguin F.O., Schaub T., 2013. Effects of salinity on growth and lipid accumulation of biofuel microalga *Nannochloropsis salina* and invading organisms. Biomass Bioenerg. 54, 83–88.

Beacham T.A., Sweet J.B., Allen M.J., 2017. Large scale cultivation of genetically modified microalgae: a new era for environmental risk assessment. Algal Res. 25, 90–100.

Becker E.W., 2007. Microalgae as a source of protein. Biotechnol. Adv. 25, 207–210.

Bhattacharjee M., 2016. Pharmaceutically valuable bioactive compounds of algae. Asian J. Pharm. Clin. Res. 9, 43–47.

Brennan L., Owende P., 2010. Biofuels from microalgae—a review of technologies for production, processing, and extractions of biofuels and co–products. Renew. Sustain. Energy Rev. 14(2), 557–577.

Campbell M.L., 2011. Assessing biosecurity risk associated with the importation of non–indigenous microalgae. Environ. Res. 111(7), 989–998.

Chaunyan D., Bochu W., Haun Z., Conglin H., Chuanren D., Wangqian L., Toyama Y., Sakanishi A., 2004. Effect of low frequency ultrasonic stimulation on the secretion of riboflavin produced by *Ecemothecium ashbyii*. Colloid Surf. B 34, 7–11.

Chen L., Liu T., Zhang W., Chen X., Wang J., 2012. Biodiesel production from algae oil high in free fatty acids by two–step catalytic conversion. Bioresour. Technol. 111, 208–214.

Chen C., Huang C., Ho K., Hsiao P., Wu M., 2015. Biodiesel production from wet microalgae feedstock using sequential wet extraction/transesterification and direct transesterification processes. Bioresour. Technol. 194, 179–186.

Cheng J., Qiu Y., Huang R., Yang W., Zhou J., Cen K., 2016. Biodiesel production from wet microalgae by using graphene oxide as solid acid catalyst. Bioresour. Technol. 221, 344–349.

Chew K.W., Yap J.Y., Show P.L., Suan N.H., Juan J.C., Ling T.C., 2017. Microalgae biorefinery: high value products perspectives. Bioresour. Technol. 229, 53–62.

Chini–Zittelli G., Lavista F., Bastianini A., Rodolfi L., Vincenzini M., Tredici M.R., 1999. Production of eicosapentaenoic acid by *Nannochloropsis* sp. cultures in outdoor tubular photobioreactors. J. Biotech. 70, 299–312.

Chokshi K., Pancha I., Ghosh A., Mishra S., 2017. Salinity induced oxidative stress alters the physiological responses and improves the biofuel potential of green microalgae *Acutodesmus dimorphus*. Bioresour. Technol. 244, 1376–1383.

Chynoweth D.P., Turick C.E., Owens J.M., Jerger D.E., Peck M.W., 1993. Biochemical methane potential of biomass and waste feedstocks. Biomass Bioenerg. 5, 95–111.

Converti A., Casazza A.A., Ortiz E.Y., Perego P., Borghi M.D., 2009. Effect of temperature and nitrogen concentration on the growth and lipid content of *Nannochloropsis oculata* and *Chlorella vulgaris* for biodiesel production. Chem. Eng. Process. Process Intensif. 48(6), 1146–1151.

Cordeiro R.S., Vaz I.C.D., Magalhães S.M.S., Barbosa F.A.R., 2017. Effects of nutritional conditions on lipid production by cyanobacteria. Anais da Academia Brasileira de Ciências. 89, 2021–2031.

Cuellar–Bermudez S.P., Romero–Ogawa M.A., Vannela R., Lai Y.J.S., Rittmann B.E., Parra–Saldivar R., 2015. Effects of light intensity and carbon dioxide on lipids and fatty acids produced by *Synechocystis* sp. PCC6803 during continuous flow. Algal Res. 12, 10–16.

Damergi E., Schwitzguébel J., Refardt D., Sharma S., Holliger C., Ludwig C., 2017. Extraction of carotenoids from *Chlorella vulgaris* using green solvents and syngas production from residual biomass. Algal Res. 25, 488–495.

Daniel M., Luna G., De M.L., Doliente T., Ido A.L., Chung T., 2017. *In situ* transesterification of *Chlorella* sp. microalgae using LiOH pumice catalyst. J. Environ. Chem. Eng. 5(3), 2830–2835.

Demirbas A., 2000. Mechanisms of liquefaction and pyrolysis reactions of biomass. Energy Convers. Manag. 41, 633–646.

Desai K., Sivakami S., 2004. *Spirulina* the wonder food of the 21st century. APBN 8(23), 1298–1302.

Dickinson S., Mientus M., Frey D., Hajibashi A.A., Ozturk S., Shaikh F., Sengupta D., El–Halwagi M.M., 2017. A review of biodiesel production from microalgae. Clean Technol. Environ. Policy 19(3), 637–668.

Dong T., Van W.S., Nagle N., Pienkos P.T., Laurens L.M.L., 2016. Impact of biochemical composition on susceptibility of algal biomass to acid–catalyzed pretreatment for sugar and lipid recovery. Algal Res. 18, 69–77.

Dumas A., Laliberte G., Lessard P., De la Noue J., 1998. Biotreatment of fish farm effluents using the cyanobacterium *Phormidium bohneri*. Aquacult. Eng. 17(1), 57–68.

Fan J., Yu L., Xu C., 2017. A central role for triacylglycerol in membrane lipid breakdown, fatty acid β–oxidation, and plant survival under extended darkness. Plant Physiol. 174(3), 1517–1530

Faried M., Samer M., Abdelsalam E., Yousef R.S., Attia Y.A., Ali A.S., 2017. Biodiesel production from microalgae: processes, technologies and recent advancements. Renew. Sustain. Energy Rev. 79, 893–913.

Feller R., Matos Â.P., Mazzutti S., Moecke E.H.S., Tres M.V., Derner R.B., Oliveira J.V., Junior A.F., 2018. Polyunsaturated ω–3 and ω–6 fatty acids, total carotenoids and antioxidant activity of three marine microalgae extracts obtained by supercritical CO_2 and subcritical n–butane. J. Supercrit. Fluids 133, 437–443.

Feng P., Deng Z., Fan L., Hu Z., 2012. Lipid accumulation and growth characteristics of *Chlorella zofingiensis* under different nitrate and phosphate concentrations. J. Biosci. Bioeng. 114(4), 405–410.

Francisco E.C., Neves D.B., Jacob–Lopes E., Franco T.T., 2010. Microalgae as feedstock for biodiesel production: Carbon dioxide sequestration, lipid production and biofuel quality. J. Chem. Technol. Biotechnol. 85, 395–403.

Gao K., Orr V., Rehmann L., 2016. Butanol fermentation from microalgae–derived carbohydrates after ionic liquid extraction. Bioresour. Technol. 206, 77–85.

Gong M., Bassi A., 2016. Carotenoids from microalgae: a review of recent developments. Biotechnol. Adv. 34(8), 1396–1412.

Gonzales L.E., Canizares R.O., Baena S., 1997. Efficiency of ammonia and phosphorus removal from a Colombian agro industrial wastewater by the microalgae *Chlorealla vulgaris* and *Scenedesmus dimorphus*. Bioresour. Technol. 60, 259–262.

Goto M., Kanda H., Machmudah S., 2015. Extraction of carotenoids and lipids from algae by supercritical CO_2 and subcritical dimethyl ether. J. Supercrit. Fluids 96, 245–251.

Guan Q.Q., Savage P.E.; Wei C.H., 2012. Gasification of alga *Nannochloropsis* sp in supercritical water. J. Supercrit. Fluids 61, 139–145.

Guo D.S., Ji X.J., Ren L.J., Li G.L., Huang H., 2017. Improving docosahexaenoic acid production by *Schizochytrium* sp. using a newly designed high–oxygen–supply bioreactor. AIChE J. 63(10), 4278–4286.

Gupta V.K., Tuohy M.G., 2013. Biofuel technologies: recent developments. Berlin Heidelberg: Springer.

Habibullah M., Masjuki H.H., Kalam M.A., Fattah I.M.R., Ashraful A.M., Mobarak H.M., 2014. Biodiesel production and performance evaluation of coconut, palm and their combined blend with diesel in a single–cylinder diesel engine. Energy Convers. Manag. 87, 250–257.

Han F., Pei H., Hu W., Zhang S., Han L., Ma G., 2016. The feasibility of ultrasonic stimulation on microalgae for efficient lipid accumulation at the end of the logarithmic phase. Algal Res. 16, 189–194.

Harari A., Abecassis R., Relevi N., Levi Z., Ben–Amotz A., Kamari Y., Harats D., Shaish A., 2013. Prevention of atherosclerosis progression by 9–cis–β–carotene rich alga *Dunaliella* in apoE–deficient mice. Biomed. Res. Int. 2013, 169–517.

Hasnain S., Ahmed I.R., Rizwan M., Rashid N., Mahmood Q., Ali F., Shah F.A., Pervez A., 2018. Potential of microalgal biodiesel production and its sustainability perspectives in Pakistan. Renew. Sustain. Energy Rev. 81(1), 76–92.

Hemaiswarya S., Raja R., Kumar R.R., Ganesan V., Anbazhagan C., 2011. Microalgae: a sustainable source for feed in aquaculture. Wr. J. Microbiol. Biotechnol. 27, 1737–1746.

Higuera–Ciapara I., Felix–Valenzuela L., Goycoolea F.M., 2006. Astaxanthin: a review of its chemistry and applications. Crit. Rev. Food Sci. Nutr. 46, 185–196.

Hoshida H., Ohira T., Minematsu A., Akada R., Nishizawa Y., 2005. Accumulation of eicosapentaenoic acid in *Nannochloropsis* sp. in response to elevated CO_2 concentrations. J. Appl. Phycol. 17(1), 29–34.

Hsieh C.H., Wu W.T., 2009. Cultivation of microalgae for oil production with a cultivation strategy of urea limitation. Bioresour. Technol. 100(17), 3921–3926.

Hu Q., Zhang C., Sommerfeld M., 2006. Biodiesel from algae: lessons learned over the past 60 years and future perspectives. J. Phycol. 42(1), 7–12.

Hu C., Lin J., Lu F., Chou F., Yang D., 2008. Determination of carotenoids in *Dunaliella salina* cultivated in Taiwan and antioxidant capacity of the algal carotenoid extract. Food Chem. 109, 439–446.

Huang Y., Su C., 2014. High lipid content and productivity of microalgae cultivating under elevated carbon dioxide. Int. J. Environ. Sci. Technol. 11(3), 703–710.

Huang W., Kim J., 2017. Simultaneous cell disruption and lipid extraction in a microalgal biomass using a nonpolar tertiary amine. Bioresour. Technol. 232, 142–145.

Im H., Lee H., Park M.S., Yang J., Lee J.W., 2014. Concurrent extraction and reaction for the production of biodiesel from wet microalgae. Bioresour. Technol. 152, 534–537.

Im H., Kim B., Lee J.W., 2015. Concurrent production of biodiesel and chemicals through wet *in situ* transesterification of microalgae. Bioresour. Technol. 193, 386–392.

Islam M.A., Ayoko G.A., Brown R., Stuart D., Magnusson M., Heimann K., 2013. Influence of fatty acid structure on fuel properties of algae derived biodiesel. Procedia Eng. 56, 591–596.

Ismagulova T., Chekanov K., Gorelova O., Baulina O., Semenova L., Selyakh I., Chivkunova O., Lobakova E., Karpova O., Solovchenko A., 2018. A new subarctic strain of *Tetradesmus obliquus* – part I: identification and fatty acid profiling. J. Appl. Phycol. 30, 2737–2750.

Jaeschke D.P., Rech R., Marczak L.D.F., Mercali G.D., 2017. Ultrasound as an alternative technology to extract carotenoids and lipids from *Heterochlorella luteoviridis*. Bioresour. Technol. 224, 753–757.

James G.O., Hocart C.H., Hillier W., Price G.D., Djordjevic M.A., 2013. Temperature modulation of fatty acid profiles for biofuel production in nitrogen deprived *Chlamydomonas reinhardtii*. Bioresour. Technol. 127, 441–447.

Jazzar S., Olivares–carrillo P., Pérez A., Ríos D.L., Néjib M., Quesada–medina J., 2015. Direct supercritical methanolysis of wet and dry unwashed marine microalgae (*Nannochloropsis gaditana*) to biodiesel. Appl. Energy 148, 210–219.

Jena U., Das K.C., 2011. Comparative evaluation of thermochemical liquefaction and pyrolysis for bio–oil production from microalgae. Energy Fuels 25, 5472–5482.

Jeon B.H., Choi J.A., Kim H.C., Hwang J.H., Abou–Shanab R.A., Dempsey B.A., Regan J.M., Kim J.R., 2013. Ultrasonic disintegration of microalgal biomass and consequent improvement of bioaccessibility/bioavailability in microbial fermentation. Biotechnol. Biofuels 6, 1–9.

John R.P., Anisha G., Nampoothiri K.M., Pandey A., 2011. Micro and macroalgal biomass: a renewable source for bioethanol. Bioresour. Technol. 102, 186–193.

Johnson M.B., Wen Z., 2009. Production of biodiesel fuel from the microalga *Schizochytrium limacinum* by direct transesterification of algal biomass. Energy Fuels 23(10), 5179–5183.

Kan G., Shi C., Wang X., Xie Q., Wang M., Wang X., Miao J., 2012. Acclimatory responses to high–salt stress in *Chlamydomonas* (Chlorophyta, Chlorophyceae) from Antarctica. Acta. Oceanol. Sin. 31(1), 116–124.

Karmakar R., Rajor A., Kundu K., Kumar N., 2018. Production of biodiesel from unused algal biomass in Punjab, India. Pet. Sci. 15, 164–175.

Khanra S., Mondal M., Halder G., Tiwari O.N., Gayen K., Bhowmick T.K., 2018. Downstream processing of microalgae for pigments, protein and carbohydrate in industrial application: a review. Food Bioprod. Process 110, 60–84.

Kim T.H., Suh W.I., Yoo G., Mishra S.K., Farooq W., Moon M., Shrivastav A., Park M.S., Yang J.W., 2015a. Development of direct conversion method for microalgal biodiesel production using wet biomass of *Nannochloropsis salina*. Bioresour. Technol. 191, 438–444.

Kim B., Im H., Lee J.W., 2015b. *In situ* transesterification of highly wet microalgae using hydrochloric acid. Bioresour. Technol. 185, 421–425.

Kim D.Y., Vijayan D., Praveen R.K., Han J.I., Lee K., Park J.Y., Chang W.S., Lee J.S., Oh Y.K., 2016. Cell–wall disruption and lipid/astaxanthin extraction from microalgae: *Chlorella* and *Haematococcus*. Bioresour. Technol. 199, 300–310.

Kobayashi N., Noel E.A., Barnes A., Watson A., Rosenberg J.N., Erickson G., Oyler G.A., 2013. Characterization of three *Chlorella sorokiniana* strains in anaerobic digested effluent from cattle manure. Bioresour. Technol. 150, 377–386.

Krishnan V., Uemura Y., Thanh N.T., Khalid N.A., Osman N., Mansor N., 2015. Three types of Marine microalgae and *Nannocholoropsis oculata* cultivation for potential source of biomass production. J. Phys: Conf. Ser. 622(1), 012034.

Krohn B.J., Mcneff C.V., Yan B., Nowlan D., 2011. Production of algae based biodiesel using the continuous catalytic Mcgyan Ó process. Bioresour. Technol. 102(1), 94–100.

Kumar V., Muthuraj M., Palabhanvi B., Ghoshal A.K., Das D., 2014. Evaluation and optimization of two stage sequential *in situ* transesterification process for fatty acid methyl ester quantification from microalgae. Renew. Energy 68, 560–569.

Lee S.Y., Cho J.M., Chang Y.K., Oh Y.K., 2017. Cell disruption and lipid extraction for microalgal bio–refineries: a review. Bioresour. Technol. 244, 1317–1328.

Li Y., Horsman M., Wu N., Lan C.Q. Dubois–Calero N., 2008. Biofuels from microalgae. Biotechnol. Prog. 24(4), 815–820.

Li Y., Lian S., Tong D., Song R., Yang W., Fan Y., Qing R., Hu C., 2011. One step production of biodiesel from *Nannochloropsis* sp. on solid base Mg–Zr catalyst. Appl. Energy 88(10), 3313–3317.

Li Y., Han F., Xu H., Mu J., Chen D., Feng B., Zeng H., 2014. Potential lipid accumulation and growth characteristic of the green alga *Chlorella* with combination cultivation mode of nitrogen (N) and phosphorus (P). Bioresour. Technol. 174, 24–32.

Liang S., Liu X., Chen F., Chen Z., 2004. Current microalgal health food R&D activities in China. In: Ang P.O. (eds) Asian Pacific Phycology in the 21st Century: Prospects and Challenges. Developments in Hydrobiology, vol 173. Springer, Dordrecht, 45–48.

Liau B., Shen C., Liang F., Hong S., Hsu S., 2010. Supercritical fluids extraction and anti–solvent purification of carotenoids from microalgae and associated bioactivity. J. Supercrit. Fluids 55(1), 169–175.

López E.N., Medina A.R., Cerdán L.E., González Moreno P.A., Macías Sánchez M.D., Grima E.M., 2016. Fatty acid methyl ester production from wet microalgal biomass by lipase–catalyzed direct transesterification. Biomass Bioenerg. 93, 6–12.

Macías–sánchez M.D., Mantell C., Rodríguez M., De E.M., Lubián L.M., Montero O., 2009. Comparison of supercritical fluid and ultrasound–assisted extraction of carotenoids and chlorophyll a from *Dunaliella salina*. Talanta 77, 948–952.

Maher K.D., Bressler D.C., 2007. Pyrolysis of triglyceride materials for the production of renewable fuels and chemicals. Bioresour. Technol. 98, 2351–2368.

Mandotra S.K., Kumar P., Suseela M.R., Nayaka S., Ramteke P.W., 2016. Evaluation of fatty acid profile and biodiesel properties of microalga *Scenedesmus abundans* under the influence of phosphorus, pH and light intensities. Bioresour. Technol. 201, 222–229.

Martıńez–Hernández G.B., Castillejo N., Carrión–Monteagudo M.M., Artés F., Artés–Hernández F., 2018. Nutritional and bioactive compounds of commercialized algae powders used as food supplements. Food Sci. Technol. Int. 24(2), 172–182.

Mata T.M., Martins A.A., Caetano N.S., 2010. Microalgae for biodiesel production and other applications: a review. Renew. Sustain. Energy Rev. 14, 217–232.

Mata T.M., Almeidab R., Caetanoa N.S., 2013. Effect of the culture nutrients on the biomass and lipid productivities of microalgae *Dunaliella tertiolecta*. Chem. Eng. 32, 973–978.

McKendry P., 2002. Energy production from biomass (part2): conversion technologies. Bioresour. Technol. 83(1), 47–54.

Menetrez M.Y., 2012. An overview of algae biofuel production and potential environmental impact. Environ. Sci. Technol. 46(13), 7073–7085.

Milano J., Ong H.C., Masjuki H.H., Chong W.T., Lam M.K., Loh P.K., Vellayan V., 2016. Microalgae biofuels as an alternative to fossil fuel for power generation. Renew. Sustain. Energy Rev. 58, 180–197.

Minowa T., Yokoya S.Y., Kishimoto M., Okakura T., 1995. Oil production from algae cells of *Dunaliella tereiolata* by direct thermochemical liquefaction. Fuel 74, 1731–1738.

Mizuno Y., Sato A., Watanabe K., Hirata A., Takeshita T., Ota S., Sato N., Zachleder V., Tsuzuki M., Kawano S., 2013. Sequential accumulation of starch and lipid induced

by sulfur deficiency in *Chlorella* and *Parachlorella* species. Bioresour. Technol. 129, 150–155.

Mondal M., Khanra S., Tiwari O.N., Gayen K., Halder G.N., 2016. Role of carbonic anhydrase on the way to biological carbon capture through microalgae—a mini review. Environ. Prog. Sustain. Energy 35(6), 1605–1615.

Montoya E.Y.O., Casazza A.A., Aliakbarian B., Perego P., Converti A., Carvalho J.C.M., 2014. Production of *Chlorella vulgaris* as a source of essential fatty acids in a tubular photobioreactor continuously fed with air enriched with CO_2 at different concentrations. Biotechnol. Prog. 30(4), 916–922.

Mostafa S.S.M., Shalaby E.A., Mahmoud G.I., 2012. Cultivating microalgae in domestic wastewater for biodiesel production. Not. Sci. Biol. 4(1), 56–65.

Mujtaba G., Choi W., Lee C.G., Lee K., 2012. Lipid production by *Chlorella vulgaris* after a shift from nutrient–rich to nitrogen starvation conditions. Bioresour. Technol. 123, 279–283.

Namasivayam A.M., Korakianitis T., Crookes R.J., Bob–Manuel K.D.H., Olsen J., 2010. Biodiesel, emulsified biodiesel and dimethyl ether as pilot fuels for natural gas fuelled engines. Appl. Energy 87, 769–778.

Nakanishi A., Aikawa S., Ho S.H., Chen C.Y., Chang J.S., Hasunuma T., Kondo A., 2014. Development of lipid productivities under different CO_2 conditions of marine microalgae *Chlamydomonas* sp. JSC4. Bioresour. Technol. 152, 247–252.

Nan Y., Liu J., Lin R., Tavlarides L.L., 2015. Production of biodiesel from microalgae oil (*Chlorella protothecoides*) by noncatalytic transesterification in supercritical methanol and ethanol: process optimization. J. Supercrit. Fluids 97, 174–182.

Nyborg W.L., 1958. Acoustic streaming near a boundary. J. Acoust. Soc. Am. 30, 329–339.

Olguín E.J., Galicia S., Mercado G., Perez T., 2003. Annual productivity of *Spirulina* (Arthrospira) and nutrient removal in a pig wastewater recycle process under tropical conditions. J. Appl. Phycol. 15, 249–257.

Ota M., Kato Y., Watanabe H., Watanabe M., 2009. Fatty acid production from a highly CO_2 tolerant alga, *Chlorocuccum littorale*, in the presence of inorganic carbon and nitrate. Bioresour. Technol. 100(21), 5237–5242.

Ota S., Oshima K., Yamazaki T., Kim S., Yu Z., Yoshihara M., Takeda K., Takeshita T., Hirata A., Bišová K., Zachleder V., Hattori M., Kawano S., 2016. Highly efficient lipid production in the green alga *Parachlorella kessleri*: draft genome and transcriptome endorsed by whole–cell 3D ultrastructure. Biotechnol. Biofuels 9(13), 1–10.

Pal D., Khozin–Goldberg I., Cohen Z., Boussiba S., 2011. The effect of light, salinity, and nitrogen availability on lipid production by *Nannochloropsis* sp. Appl. Microbiol. Biotechnol. 90(4) 1429–1441.

Pal P., Chew K.W., Yen H.W., Lim J.W., Lam M.K., Show P.L., 2019. Cultivation of oily microalgae for the production of third–generation biofuels. Sustainability 11, 5424–5440.

Pan Y., Alam M.A., Wang Z., Huang D., Hu K., Chen H, Yuan Z., 2017. One–step production of biodiesel from wet and unbroken microalgae biomass using deep eutectic solvent. Bioresour. Technol. 238, 157–163.

Pandit P.R., Fulekar M.H., Karuna M.S.L., 2017. Effect of salinity stress on growth, lipid productivity, fatty acid composition, and biodiesel properties in *Acutodesmus obliquus* and *Chlorella vulgaris*. Environ. Sci. Pollut. Res. 24(15), 13437–13451.

Park J., Park M.S., Lee Y., Yang J., 2015. Advances in direct transesterification of algal oils from wet biomass. Bioresour. Technol. 184, 267–275.

Park J., Kim B., Chang Y.K., Lee J.W., 2017. Wet *in situ* transesterification of microalgae using ethyl acetate as a cosolvent and reactant. Bioresour. Technol. 230, 8–14.

Parniakov O., Barba F.J., Grimi N., Marchal L., Jubeau S., Lebovka N., Vorobiev E., 2015. Pulsed electric field assisted extraction of nutritionally valuable compounds from microalgae *Nannochloropsis* spp. using the binary mixture of organic solvents and water. Innov. Food Sci. Emerg. Technol. 27, 79–85.

Patil P.D., Deng S., 2009. Optimization of biodiesel production from edible and non–edible vegetable oils. Fuel 88, 1302–1306.

Patil P.D., Gude V.G., Mannarswamy A., Deng S., Cooke P., Munson–McGee S., Rhodes I., Lammers P., Nirmalakhandan N., 2011. Optimization of direct conversion of wet algae to biodiesel under supercritical methanol conditions. Bioresour. Technol. 102(1), 118–122.

Patil P D , Reddy H , Muppaneni T , Ponnusamy S , Cooke P , Schuab T , Deng S., 2013. Microwave–mediated noncatalytic transesterification of algal biomass under supercritical ethanol conditions. J. Supercrit. Fluids 79, 67–72.

Patnaik R., Mallick N., 2015. Utilization of *Scenedesmus obliquus* biomass as feedstock for biodiesel and other industrially important co–products: An integrated paradigm for microalgal biorefinery. Algal Res. 12, 328–336.

Pitt W.G., Ross S.A., 2003. Ultrasound increases the rate of bacterial cell growth. Biotechnol. Prog. 19, 1038–1044.

Potts T., Du J., Paul M., May P., Beitle R., Hestekin J., 2012. The production of butanol from Jamaica bay macro algae. Environ. Prog. Sustain. Energy 31, 29–36.

Priyadarshani I., Biswajit R., 2012. Commercial and industrial applications of micro algae – a review. J. Algal Biomass. Utln. 3, 89–100.

Raja R., Hemaiswarya S., Ganesan V., Carvalho I.S., 2016. Recent developments in therapeutic applications of cyanobacteria. Cri. Rev. Microbiol. 42(3), 394–405.

Raja R., Coelho A., Hemaiswarya S., Kumar P., Carvalho I.S., Alagarsamy A., 2018. Applications of microalgal paste and powder as food and feed: An update using text mining tool. Beni–Suef Uni. J. Appl. Sci. 7, 740–747.

Rapoport N., Smirnov A.I., Timoshin A., Pratt A.M., Pitt W.G., 1997. Factors affecting the permeability of *Pseudomonas aeruginosa* cell walls toward lipophilic compounds: effects of ultrasound and cell age. Arch. Biochem. Biophys. 344, 114–124.

Roux J.M., Lamotte H., Achard J.L., 2017. An overview of microalgae lipid extraction in a biorefinery framework. Energy Procedia 112, 680–688.

Saifuddin N., Priatharsini P., 2016. Developments in bio–hydrogen production from algae: a review. Res. J. Appl. Sci. Eng. Technol. 12, 968–982.

Salam K.A., Velasquez–orta S.B., Harvey A.P., 2016. A sustainable integrated *in situ* transesterification of microalgae for biodiesel production and associated coproduct – a review. Renew. Sustain. Energy Rev. 65, 1179–1198.

Salama E.S., Kim H.C., Abou–Shanab R.A.I., Ji M.K., Oh Y.K., Kim S.H., Jeon B.H., 2013. Biomass, lipid content, and fatty acid composition of freshwater *Chlamydomonas mexicana* and *Scenedesmus obliquus* grown under salt stress. Bioprocess Biosyst. Eng. 36(6), 827–833.

Schüler L.M., Schulze P.S.C., Pereira H., Barreira L., León R., Varela J., 2017. Trends and strategies to enhance triacylglycerols and high–value compounds in microalgae. Algal Res. 25, 263–273.

Sharma N., Sharma P., 2017. Industrial and biotechnological applications of algae: a review. J. Adv. Plant Biol. 1(1), 1–25.

Sharma K.K., Schuhmann H., Schenk P.M., 2012. High lipid induction in microalgae for biodiesel production. Energies. 5(5), 1532–1553.

Shuba E.S., Kifle D., 2018. Microalgae to biofuels: 'Promising' alternative and renewable energy, review. Renew. Sustain. Energy Rev. 81, 743–755.

Singh D., Puri M., Wilkens S., Mathur A.S., Tuli D.K., Barrow C.J., 2013. Characterization of a new zeaxanthin producing strain of *Chlorella saccharophila* isolated from New Zealand marine waters. Bioresour. Technol. 143, 308–314.

Singh S., Singh P., 2014. Effect of CO_2 concentration on algal growth: a review. Renew. Sustain. Energy Rev. 38, 172–179.

Sinisterra J.V., 1992. Application of ultrasound to biotechnology: an overview. J. Ultrasonics 30, 180–185.

Sitthithanaboon W., Reddy H.K., Muppaneni T., Ponnusamy S., Punsuvon V., Holguim F., Dungan B., Deng S., 2015. Single–step conversion of wet *Nannochloropsis gaditana* to biodiesel under subcritical methanol conditions. Fuel 147, 253–259.

Sivaramakrishnan R., Incharoensakdi A., 2017. Direct transesterification of *Botryococcus* sp. catalysed by immobilized lipase: ultrasound treatment can reduce reaction time with high yield of methyl ester. Fuel 191, 363–370.

Sizova I, Greiner A., Awasthi M., Kateriya S., Hegemann P., 2013. Nuclear gene targeting in *Chlamydomonas* using engineered zinc–finger nucleases. Plant J. 73(5), 873–882.

Skorupskaite V., Makareviciene V., Gumbyte M., 2016. Opportunities for simultaneous oil extraction and transesterification during biodiesel fuel production from microalgae: a review. Fuel Process Technol. 150, 78–87.

Solovchenko A.E., Khozin–Goldberg I., Didi–Cohen S., Cohen Z., Merzlyak M.N., 2008. Effects of light intensity and nitrogen starvation on growth, total fatty acids and arachidonic acid in the green microalga *Parietochloris incisa*. J. Appl. Phycol. 20(3), 245–251.

Spolaore P., Joannis–Cassan C., duran E, Isambert A., 2006. Commercial applications of microalgae. J. Biosci. Bioeng. 101(2), 87–96.

Srinuanpan S., Cheirsilp B., Prasertsan P., Kato Y., Asano Y., 2018. Strategies to increase the potential use of oleaginous microalgae as biodiesel feedstocks: nutrient starvations and cost–effective harvesting process. Renew. Energy 122, 507–516.

Srivastava G., Goud V.V., 2017. Salinity induced lipid production in microalgae and cluster analysis (ICCB 16–BR_047). Bioresour. Technol. 242, 244–252.

Steriti A., Rossi R., Concas A., Cao G., 2014. A novel cell disruption technique to enhance lipid extraction from microalgae. Bioresour. Technol. 164, 70–77.

Stolz P., Obermayer B., 2005. Manufacturing microalgae for skin care. C&T 120, 99–106.

Takeshita T., Ota S., Yamazaki T., Hirata A., Zachleder V., Kawano S., 2014. Starch and lipid accumulation in eight strains of six *Chlorella* species under comparatively high light intensity and aeration culture conditions. Bioresour. Technol. 158, 127–134.

Takisawa K., Kanemoto K., Kartikawati M., Kitamura Y., 2013. Simultaneous hydrolysis esterification of wet microalgal lipid using acid. Bioresour. Technol. 149, 16–21.

Tan X.B., Lam M.K., Uemura Y., Lim J.W., Wong C.Y., Lee K.T., 2018. Cultivation of microalgae for biodiesel production: a review on upstream and downstream processing. Chinese J. Chem. Eng. 26, 17–30.

Tsigie Y.A., Huynh L.H., Ismadji S., Engida A.M., Ju Y.H., 2012. *In situ* biodiesel production from wet *Chlorella vulgaris* under subcritical condition. Chem. Eng. J. 213, 104–108.

Tyagi S., Singh G., Sharma A., Aggarwal G., 2010. Phytochemicals as candidate therapeutics: an overview. Int. J. Pharma. Sci. Rev. Res. 3(1), 53–55.

Ueno Y., Kurano N., Miyachi S., 1998. Ethanol production by dark fermentation in the marine green alga, *Chlorococcum littorale*. J. Ferment. Bioeng. 86, 38–43.

Vardon D.R., Sharma B.K., Blazina G.V., Rajagopalan K., Strathmann T.J., 2012. Thermochemical conversion of raw and defatted algal biomass via hydrothermal liquefaction and slow pyrolysis. Bioresour. Technol. 109, 178–187.

Vasudevan P.T., Briggs M., 2008. Biodiesel production—current state of the art and challenges. J. Ind. Microbiol. Biotechnol. 35, 421–430.

Vitova M., Bisova K., Kawano S., Zachleder V., 2015. Accumulation of energy reserves in algae: from cell cycles to biotechnological applications. Biotechnol. Adv. 33(6), 1204–1218.

Walker D.A., 2010. Biofuels—for better or worse? Ann. Appl. Biol. 156, 319–327.

Wang B., Li Y., Wu N., Lan C.Q., 2008. CO_2 bio–mitigation using microalgae. Appl. Microbiol. Biotechnol. 79(5), 707–718.

Wang M., Lee E., Dilbeck M.P., Liebelt M., Zhang Q., Ergas A.J., 2016. Thermal pretreatment of microalgae for biomethane production: experimental studies, kinetics and energy analysis. J. Chem. Tech. Biotechnol. 92, 399–407.

Wei L., Huang X., Huang Z., 2015. Temperature effects on lipid properties of microalgae *Tetraselmis subcordiformis* and *Nannochloropsis oculata* as biofuel resources. Chin. J. Oceanol. Limnol. 33(1), 99–106.

Widjaja A., Chien C.C., Ju Y.H., 2009. Study of increasing lipid production from fresh water microalgae *Chlorella vulgaris*. J. Taiwan Inst. Chem. Eng. 40(1), 13–20.

Wu C., Xiao Y., Lin W., Li J., Zhang S., Zhu J., Rong J., 2017. Aqueous enzymatic process for cell wall degradation and lipid extraction from *Nannochloropsis* sp. Bioresour. Technol. 223, 312–316.

Xin J., Imahara H., Saka S., 2008. Oxidation stability of biodiesel fuel as prepared by supercritical methanol. Fuel 87, 1807–1813.

Xin L., Hong H., Jia Y., 2010. Lipid accumulation and nutrient removal properties of a newly isolated freshwater microalga, *Scenedesmus* sp. LX1, growing in secondary effluent. New Biotechnol. 27(1), 59–63.

Xin L., Hong H., Yu Z., 2011. Growth and lipid accumulation properties of a freshwater microalga *Scenedesmus* sp. under different cultivation temperature. Bioresour. Technol. 102(3), 3098–3102.

Yang L, Chen J., Qin S., Zeng M., Jiang Y., Hu L., Xiao P., Hao W., Hu Z., Lei A., Wang J., 2018. Growth and lipid accumulation by different nutrients in the microalga *Chlamydomonas reinhardtii*. Biotechnol. Biofuels 11(1), 40–52.

Yao L., Cengic I., Anfelt J., Hudson E.P., 2015. Multiple gene repression in cyanobacteria using CRISPRi. ACS Synth. Biol. 5(3), 207–212.

Yates C.M., Calder P.C., Rainger G.E., 2014. Pharmacology and therapeutics of omega–3 polyunsaturated fatty acids in chronic inflammatory disease. Pharmacol. Ther. 141(3), 272–282.

Yeesang C., Cheirsilp B., 2011. Effect of nitrogen, salt, and iron content in the growth medium and light intensity on lipid production by microalgae isolated from freshwater sources in Thailand. Bioresour. Technol. 102(3), 3034–3040.

Yeh K.L., Chang J.S., 2011. Nitrogen starvation strategies and photobioreactor design for enhancing lipid content and lipid production of a newly isolated microalga *Chlorella vulgaris* ESP–31: implications for biofuels. Biotechnol. J. 6(11), 1358–1366.

Yen H., Hu I., Chen C., Ho S., Lee D., Chang J., 2013. Microalgae–based biorefinery – from biofuels to natural products. Bioresour. Technol. 135, 166–174.

Ying K., Zimmerman W., Gilmour D., 2014. Effects of CO_2 and pH on growth of the microalga *Dunaliella salina*. J. Microbial Biochem. Technol. 6(3), 167–173.

Yoo C., Jun S.Y., Lee J.Y., Ahn C.Y., Oh H.M., 2010. Selection of microalgae for lipid production under high levels carbon dioxide. Bioresour. Technol. 101(1), 71–74.

Young F.R., 1989. Cavitation. McGraw Hill, London. Zelitch, I.H., 1951. Simultaneous use of molecular nitrogen and ammonia by *Clostridium pasteurianum*. Proc. Natl. Acad. Sci. U S A. 37(9), 559–565.

Yuan J.P., Peng J., Yin K., Wang J.H., 2011. Potential health–promoting effects of astaxanthin: a high–value carotenoid mostly from microalgae. Mol. Nutr. Food Res. 55, 150–165.

Zhang Y., Li Y., Zhang X., Tan T., 2015. Biodiesel production by direct transesterification of microalgal biomass with cosolvent. Bioresour. Technol. 196, 712–715.

Zhao Y., Li D., Ding K., Che R., Xu J.W., Zhao P., Li T., Ma H., Yu X., 2016. Production of biomass and lipids by the oleaginous microalgae *Monoraphidium* sp. QLY–1 through heterotrophic cultivation and photo–chemical modulator induction. Bioresour. Technol. 211, 669–676.

Zhu L., 2015. Microalgal culture strategies for biofuel production: a review. Biofuel Bioprod. Bior. 9(6), 801–814.

Zhu L.D., Hiltunen E., 2016. Methylation of *DACT2* accelerates esophageal cancer development by activating Wnt signaling. Renew. Sustain. Energy Rev. 54, 1285–1290.

Zhu L.D., Takala J., Hiltunen E., Wang Z.M., 2013. Recycling harvest water to cultivate *Chlorella zofingiensis* under nutrient limitation for biodiesel production. Bioresour. Technol. 144, 14–20.

Zhu L., Li Z., Hiltunen E., 2016. Strategies for lipid production improvement in microalgae as a biodiesel feedstock. BioMed Res. Int. 2016, 8792548.

Zhu L., Nugroho Y.K., Shakeel S.R., Li Z., Martinkauppi B., Hiltunen E., 2017. Using microalgae to produce liquid transportation biodiesel: what is next? Renew. Sustain. Energy Rev. 78, 391–400.

CHAPTER 2

ISOLATION AND CHARACTERIZATION OF WILD FRESH WATER MICROALGAE

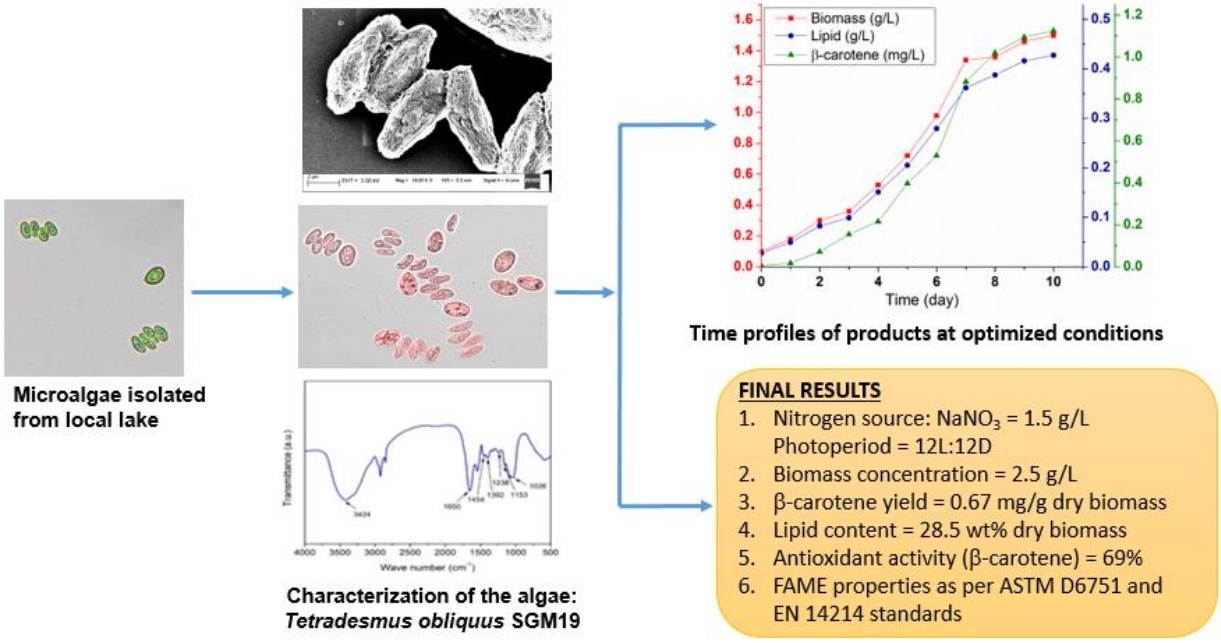

CHAPTER 2

Isolation and Characterization of Wild Fresh Water Microalgae

2.1 Introduction

Despite highly encouraging laboratory research, the commercial production of microalgae has suffered from an unattractive economy. Relatively low lipid content of natural isolates (approx. 15-20%) and low shelf life of lipids are some of the major operational hurdles. Boosting the revenue of the microalgal biorefinery is utmost essential to make it sustainable and financially viable. In addition to lipids, the microalgae are also a rich source of several products with high nutritional value such as carbohydrates, omega-3 fatty acids (for example docosahexanoic acid), and pigments and nutraceuticals (e.g. β-carotene and astaxanthin, which have antioxidant activity).

Previous authors have reported different approaches for enhancing the lipid productivity in microalgal cells; however, only a few studies have addressed the simultaneous production of other valuable products. Patnaik and Mallick (2015) have reported synthesis of multiple products from microalgal biomass of *Scenedesmus obliquus* under autotrophic and mixotrophic modes. At optimized nutrient composition, 100 g *S. obliquus* biomass yielded 0.06 g β-carotene, 38 g biodiesel, 17 g bioethanol, 3 g

glycerol, and 2 g of omega-3 fatty acids. Chandra et al. (2016) have reported a 2-fold increase in the *Scenedesmus obtusus* biomass productivity by changing the nitrogen source from sodium nitrate to urea and further enhancement by supplementation with acetate and bicarbonate. Maximum lipid content of 21 wt% in biomass with total carotenoid content of 11 mg/g was obtained for urea as the nitrogen source. Xu et al. (2019) reported biodiesel and bioethanol production of 127.1 mg/g dry wt and 0.558 g/g dry wt, respectively, by recycling waste glycerol as supplemental carbon source. A summary of the literature on lipid and β-carotene production from various strains of genus *Scenedesmus* is given in Table 2.1.

Table 2.1. Summary of previous literature on lipid and β-carotene production from different strains belonging to genus *Scenedesmus*

Microalgae	Biomass (g/L)	Lipid content (% dry biomass)	β-carotene content (mg/g dry biomass)	References
Scenedesmus acutus PVUW12	0.74	28.8 ± 2.05	NA	Doria et al., 2012
Scenedesmus quadricauda	2.8	33.1	NA	Zhao et al., 2012
Scenedesmus sp. KGU-0002	NA	NA	0.71 ± 0.04	Aburai et al., 2013
Scenedesmus sp. strain R-16	3.46	43.4	NA	Ren et al., 2013
Scenedesmus sp. KMN4	0.92 ± 0.06	28.63 ± 3.81	NA	Tale et al., 2014
Scenedesmus obliquus	1.92	56.4 ± 0.55	0.64	Patnaik and Mallick, 2015
Scenedesmus obtusus	0.766 ± 0.032	28	NA	Chandra et al., 2016
Scenedesmus obliquus	NA	NA	0.778	Patias et al., 2017
S. obliquus	1.36 ± 0.27	22.48	NA	Ferro et al., 2018
Tetradesmus obliquus SGM19	2.5±0.7	28.5±1.3	0.56±0.1	This study

Note: It may be noted that the cultivation methods adopted by previous authors may differ from present study. However, we have compared only the final biomass yield along with lipid and β-carotene content.

A large fraction of this literature on microalgae-derived products (or microalgal biorefineries) is based on genetically modified strains, which have been studied in highly controlled environment. However, these genetically engineered strains may not be stable and viable in an open environment of large-scale biorefineries using raceway ponds, as these strains cannot aggressively consume nutrients and substrate for survival and growth in competition with the wild species. These species are also susceptible to contaminations in the medium. In such circumstances, it is imperative to employ wild strains of algae in biorefineries. These natural isolates have relatively much lesser content of lipids and other products. However, this can be enhanced by proper optimization of growth conditions and medium.

The present study has demonstrated the potential of a native or wild microalgal species (isolated from a lake on campus of Indian Institute of Technology Guwahati) for a biorefinery that simultaneously produces lipids and β-carotene. β-carotene is a vital nutraceutical and precursor for production of vitamin A in human bodies, in addition to being an antioxidant. Moreover, β-carotene is also known to support and enhance lung strength in humans.

The initial characterization of microalga after isolation included: (1) strain identification, (2) microscopic (using simple light microscope, FE-SEM, and confocal microscope) assessment of cell morphology, and (3) preliminary estimation of biochemical composition. The strain was grown under different nitrogen sources, carbon sources, salinity levels, and photoperiods to assess the influence of these basic parameters on biomass growth profile and associated β-carotene production. Moreover, the thermogravimetric analysis (TGA) and differential thermogravimetric (DTG) analysis of microalgal biomass (in raw form and post extraction of lipids) was also carried out. Finally, the transesterification of extracted lipids has been carried out and FAME profile

of the biodiesel has been determined with GC-MS analysis.

2.2 Materials and Methods

2.2.1 Sampling, isolation and maintenance of culture

Samples containing microalgae were collected in 50 mL centrifuge tubes from ponds located in I.I.T. Guwahati. For isolation of axenic unialgal culture from the water samples, the standard plating method, as described by Lee et al. (2014), was used. The algal cells were allowed to grow for 15 days each time. For all analysis, the isolated microalgae (initial biomass = 0.01 g/L) was cultured in 200 mL liquid BG-11 medium (pH 7.0; $MgSO_4 \cdot 7H_2O$ – 0.075 g/L, EDTA – 0.001 g/L, Ammonium ferric citrate – 0.006 g/L, $CaCl_2$ – 0.036 g/L, $NaNO_3$ – 1.5 g/L, K_2HPO_4 – 0.04 g/L, Na_2CO_3 – 0.02 g/L, Citric acid – 0.006 g/L, and Trace elements: H_3BO_3, $MnCl_2$, $ZnSO_4$, $Na_2MoO_4 \cdot 2H_2O$, $CuSO_4$, $Co(NO_3)_2$) in 500 mL Erlenmeyer flask. The flask was incubated at $30^o \pm 0.5^oC$ in an incubator shaker at 150 rpm and 5000 lux light intensity. Continuous aeration in the flask was provided using a pump for uniform mixing of culture with 0.5 vvm atmospheric air. The dissolved oxygen (DO) was monitored in the broth by Thermo Scientific DO meter (Model: Eutech DO 700). The DO content of the culture was found to be close to saturation, i.e. 8±0.5 ppm, during the entire 15-day batch. The microalgae were maintained by reviving in a fresh medium every month.

2.2.2 Morphological and taxonomic investigations

The isolation process involved preliminary identification of morphological characteristics under a light microscope (Nikon Eclipse Ti-S) at 40× magnification. The surface structures and morphologies, and subcellular structures were analyzed using FE-SEM micrographs (Make: Zeiss, Model: Sigma 300). For FE-SEM analysis, the cells

were first washed with phosphate buffer saline (PBS) followed by fixation with glutaraldehyde at 4°C for 2 h after which the cells were dehydrated gradually with ethanol (50-100%, 10 min per concentration), followed by drying with acetone then filtration with 0.2 μm filter paper. The taxonomic identification was conducted by Yaazh Xenomics, Coimbatore by sequencing the 18S ribosomal RNA. The forward and reverse primers used for partial sequencing were ITS1 (5′-TCCGTAGGTGAACCTGCGG-3′) and ITS4 (5′-TCCTCCGCTTATTGATATGC-3′), respectively. The generated nucleotide sequences were compared (using the Blast program) and then submitted to the GenBank database. Fourier Transform Infrared (FTIR) spectrum of the microalgal biomass was recorded between 4000-400 cm^{-1} using Perkin Elmer Spectrum Two (USA) spectrophotometer. The samples of lyophilized microalgal biomass for the FTIR analysis were prepared as per the procedure outlined by Akhtar et al. (2017).

2.2.3 Monitoring of microalgal growth

The growth of the microalgae was observed with optical density (OD) on a UV-Vis spectrophotometer (Thermo Fisher Scientific, USA) at 680 nm by collecting aliquots at regular intervals. The standard curve (R^2 = 0.96) was used for calculating dry cell weight (DCW) for samples. Specific growth rate (μ_m, d^{-1}) and maximum biomass productivity (P_m, g/L/d) were determined from the growth profile of biomass using eqs. 2.1 and 2.2, respectively:

$$P_m = (X_m - X_0)/\tau \qquad [2.1]$$

$$\ln\left(X/X_0\right) = \mu_m t \qquad [2.2]$$

Notations: X_o - initial biomass concentration in the broth, X - biomass concentration at any time t, X_m – maximum biomass concentration attained in the broth, τ - the time

required to achieve maximum biomass concentration in broth.

2.2.4 Influence of growth conditions on biomass and associated products

Nitrogen sources: Growth experiments were carried out with seven different nitrogen sources: sodium nitrate (SN), beef extract (BF), urea (UR), peptone (PE), yeast extract (YE), ammonium nitrate (AN) and glycine (GL).The initial concentration of each source was 1.5 g/L and the rest of the growth mixture was BG-11 media with pH 7.0. The experiment was conducted at 30^{o}C and 5000 lux light intensity.

Carbon sources: The growth medium containing the optimum nitrogen source was also supplemented with different carbon sources to study its promotional effect on growth and product formation in microalgae. These sources were glucose (GLU), fructose (FRU), xylose (XYL), sucrose (SUC) and maltose (MAL). The results of these experiments were compared against control (sole nitrogen source and no carbon source).

Salinity: The cell cultures were subjected to different NaCl concentrations, viz. 25, 50, 75 and 100 mM to assess the influence of salinity on growth and product formation. The control culture was devoid of NaCl. The cultures were grown normally on BG-11 medium supplemented with NaCl at pH 7.0 and 30^{o}C.

Photoperiod: The experiments for photoperiod were conducted by exposing cultures to fluorescence light of intensity 5000 lux with varying photoperiods, like 12:12, 16:8 and 24:0 light to dark cycle. A digital lux meter was used to measure the light intensity. The experiments were conducted in batch and triplicates for a period of 10 days.

2.2.5 Biochemical characterization

***Total protein*:** Total proteins in the microalgae were analyzed by Lowry assay against the reference standard of bovine serum albumin (BSA).

***Total carbohydrates*:** The analysis of total soluble carbohydrates was conducted by following phenol-sulphuric acid method. D-glucose was used as a reference standard.

***Total lipids*:** For extraction of lipids, the Bligh and Dyer method was used with modified solvent ratio, i.e., chloroform/methanol at a ratio 2:1 (v/v). More recently, Huang et al. (2019) have reported a rapid technique based on fluorescence spectroscopy for estimation of lipid content of microalgal strains.

Nile Red staining: Staining of the lipid in microalgal cells was conducted by mixing 0.05 mL of 0.1 mg/mL of Nile red solution in acetone with the microalgal cells followed by incubation in dark at 37°C for 10 min. The fluorescence of the stained cells of microalgae was detected using confocal microscope (Make: Zeiss, Model: JSM-7610F) with excitation: 450 to 500 nm and emission > 528 nm.

***Pigment composition*:** For the estimation of pigment content of microalgae, 2 mL culture was withdrawn and centrifuged. The collected pellet was mixed vigorously with 2 mL 99.9% methanol and incubated overnight in dark at 4^{o}C. The mixture was then centrifuged (10,000 rpm, 5 min) for separation of supernatant for pigment estimation. Using the absorbance at a particular wavelength (denoted by *A*), the concentrations of different pigments were determined using eqs. 2.3, 2.4 and 2.5 as follows (Lichtenthaler, 1987):

Chlorophyll a: $Chl\text{-}a\ (\mu g/mL) = 16.72 \times A_{665} - 9.16 \times A_{652}$ [2.3]

Chlorophyll b: $Chl\text{-}b\ (\mu g/mL) = 34.09 \times A_{652} - 15.28 \times A_{665}$ [2.4]

Carotenoids: $Carotenoids\ (\mu g/mL) = (1000 \times A_{470} - 1.63 \times Chl\text{-}a - 104.9 \times Chl\text{-}b)/221$ [2.5]

***β-carotene estimation from microalgae*:** β-carotene was extracted from microalgal biomass using a 3-step protocol, viz. cell disruption, saponification followed by solvent

extraction. Initially, the sample was centrifuged at 6000 rpm for 10 min. The resulting pellet was washed with distilled water twice and lyophilized. Dry biomass was suspended in 75% acetone and vortex mixed until a white precipitate appeared. Next, the sample was mixed with 1/10th volume of 60% KOH at 49^{o}C, vortexed and again centrifuged. The supernatant was collected and mixed with acetone, i.e., the solvent for extraction. After centrifugation, the supernatant was collected and analyzed with HPLC (1220 Infinity, Agilent, USA) using a C18 reverse-phase column.

Anti-oxidant property assay: Antioxidant capacity of dried biomass was evaluated using two methods, viz. DPPH method and FRAP method.

***DPPH (2,2-diphenyl-1-picrylhydrazyl) assay*:** The DPPH assay was done by following the protocol described by Yen and Chen (1995). Ascorbic acid and methanol were used as standard and blank, respectively. The antioxidant activity was calculated using eq. 2.6:

$$Activity(\%) = [(Ac - At)/Ac] \times 100 \quad [2.6]$$

where *Ac* is the absorbance of the control (DPPH), and *At* is the absorbance of the tested sample.

***FRAP (ferric reducing antioxidant power) assay*:** The FRAP assay involves preparation of samples, reactions, and measurement of the absorbance at 700 nm spectrophotometrically. Ascorbic acid is used as standard antioxidant.

2.2.6 Thermogravimetric analysis (TGA) and determination of structural composition

Structural composition: The holocellulose and lignin content of raw (whole algae) and spent (lipid extracted algae) biomass were estimated according to TAPPI's protocol, whereas hemicellulose content was quantified using the method by Goering and Van Soest (1970). The cellulose content was estimated as the difference between holocellulose

and hemicellulose.

Dilute acid hydrolysis: The raw and spent biomass were subjected to dilute acid hydrolysis with 4 wt% sulphuric acid at 121^{o}C and 20 psi pressure using an autoclave (Equitron - PAD) for 1 h. The steam was rapidly released after completion of the hydrolysis. Post hydrolysis, the solids were separated from hydrolysate by centrifugation followed by filtration through a 0.2 μm nylon filter to ensure complete removal of solids.

Total reducing sugar (TRS) estimation: The hydrolysate obtained for the raw and spent biomass were quantified for sugar release. The TRS was estimated by following Nelson protocol. The monomeric sugars (hexoses and pentoses) in the hydrolysate were determined by HPLC (Perkin Elmer, Series 200) equipped with Hi-Plex CA column (300 ×7.7 mm) using refractive index (RI) detector and Milli Q water as mobile phase (flow rate - 0.6 mL/min).

TGA of biomass samples: The thermogravimetric profiles of both raw and spent microalgal biomass were studied using a Perkin Elmer STA 8000 analyer. In order to achieve high heat transfer between the thermocouples and crucibles, platinum crucibles were used. Each experimental run was conducted using 6-10 mg of sample. The crucibles were not covered so as to suppress char formation reactions. The temperature range for the TGA was 40^{o} – 900^{o}C at atmospheric pressure with a constant heating rate of 10^{o}C/min. The analysis was carried out under both inert atmosphere, with high purity nitrogen as the carrier gas, and also in an oxidative environment with air as the carrier gas. In both cases, the flow rate of carrier gas was 100 mL/min. The weight loss of the biomass with temperature was recorded for analysis. Using TGA curves, the rate of thermal decomposition at different temperatures (or differential thermogravimetric curves) was also determined.

2.2.7 Fatty acid methyl esters (FAME) analysis

Transesterification of lipids and FAME analysis: Transesterification of neutral lipids was carried out with methanol using a 2-step procedure reported by Mishra and Mohanty (2019). The resultant FAME were further analyzed for the profiles (or composition) using gas chromatograph–mass spectrometer (GC–MS) system. The GC-MS system comprised of a gas chromatograph (Clarus 680, Perkin Elmer, USA) employing Elite-5MS capillary column (dimensions 60 m × 0.25 mm × 0.25 μm with stationary phase of 5% diphenyl and 95% dimethylpolysiloxane) and a Clarus 600C mass spectrophotometer (Perkin Elmer, USA). The peaks were identified using data analysis software NIST-2008.

Fourier transform infrared (FTIR) spectrophotometer analysis: FTIR spectrophotometer (Shimadzu, IR-Affinity-1) was used to obtain infrared spectra of FAME in the range 500 to 4000 cm^{-1} for analysis of functional groups present in the algal biodiesel.

2.3 Results and Discussion

2.3.1 Preliminary analysis of biochemical characteristics of isolated strains

2.3.1.1 Morphological and molecular identification

Two different strains of microalgae were isolated into axenic cultures by repeated plating and microscopic observations employing basic microbial techniques. The isolated strains were identified on the basis of the preliminary morphological characteristics such as cell size and shape, which indicated that they might belong to Chlorophyta (*Tetradesmus* sp.). The isolated strains possessed pale green to dark green color in broth. *Scenedesmus* species is reported and known to exhibit diverse morphology and biochemical composition under different environmental conditions (Vasileva et al., 2015). Microscopic image (Fig. 2.1A) and FE-SEM analysis (Fig. 2.1B) suggested initial

identification as of genus *Tetradesmus*. The identified strain SGM19 was green-colored, small single or colonial microalgae. Most of the colonies comprised of 2–4 oval-shaped cells. Both the isolated microalgae showed similarity in some of the morphological characteristics. Hence, genetic identification of both the strains was conducted using sequence analysis of 18S rRNA to attain a clear distinction between them.

At molecular level, the strains were further distinguished by relative sequence analysis of the ITS regions of ribosomal RNA. The sequencing of the 18S rRNA showed 921 and 702 bp long nucleotide sequences in the isolated microalgal strains. The pairwise alignment of the isolate sequences with the NCBI database sequences, demonstrated that strains were 98% identical to *Scenedesmus* sp. The sequences of the isolated microalgae were submitted to NCBI database. Accession numbers - MG760624.1 (*Tetradesmus obliquus* SGM19) and MG754459.1 (*Tetradesmus obliquus* SGM09).

The microalgal identification was also verified by phylogenetic tree analysis. For constructing the phylogenetic tree, other microalgal gene sequences from Genbank were compared with the sequence of the isolates by employing the use of Neighbor-Joining method in Mega 5.0 as described by Saitou and Nei (1987). The isolated microalgal strains were labeled by NCBI as *Tetradesmus obliquus* SGM19 and *Tetradesmus obliquus* SGM09. Fig. 2.1C depicts the Neighbour-Joining phylogenetic tree with the location of respective strains based on 18S rRNA sequence.

Fig. 2.1D depicts the FTIR spectrum of raw biomass in the wavenumber range of 500 – 4000 cm^{-1}. The major peaks in the spectrum and their assignment are as follows: 1026 cm^{1} = P=O bond in phospholipids and nucleic acids; 1153, 1238, 1392 and 1454 cm^{-1} = bending and stretching of various bonds in polysaccharide, aliphatic groups and carbonate ions (C-O-C, C=O stretching and C-H bending); 1705–1460 cm^{-1} = proteins, 3000–2800 cm^{-1} = lipids; 3424 cm^{-1} = O-H stretching; 1650 cm^{-1} = ester groups.

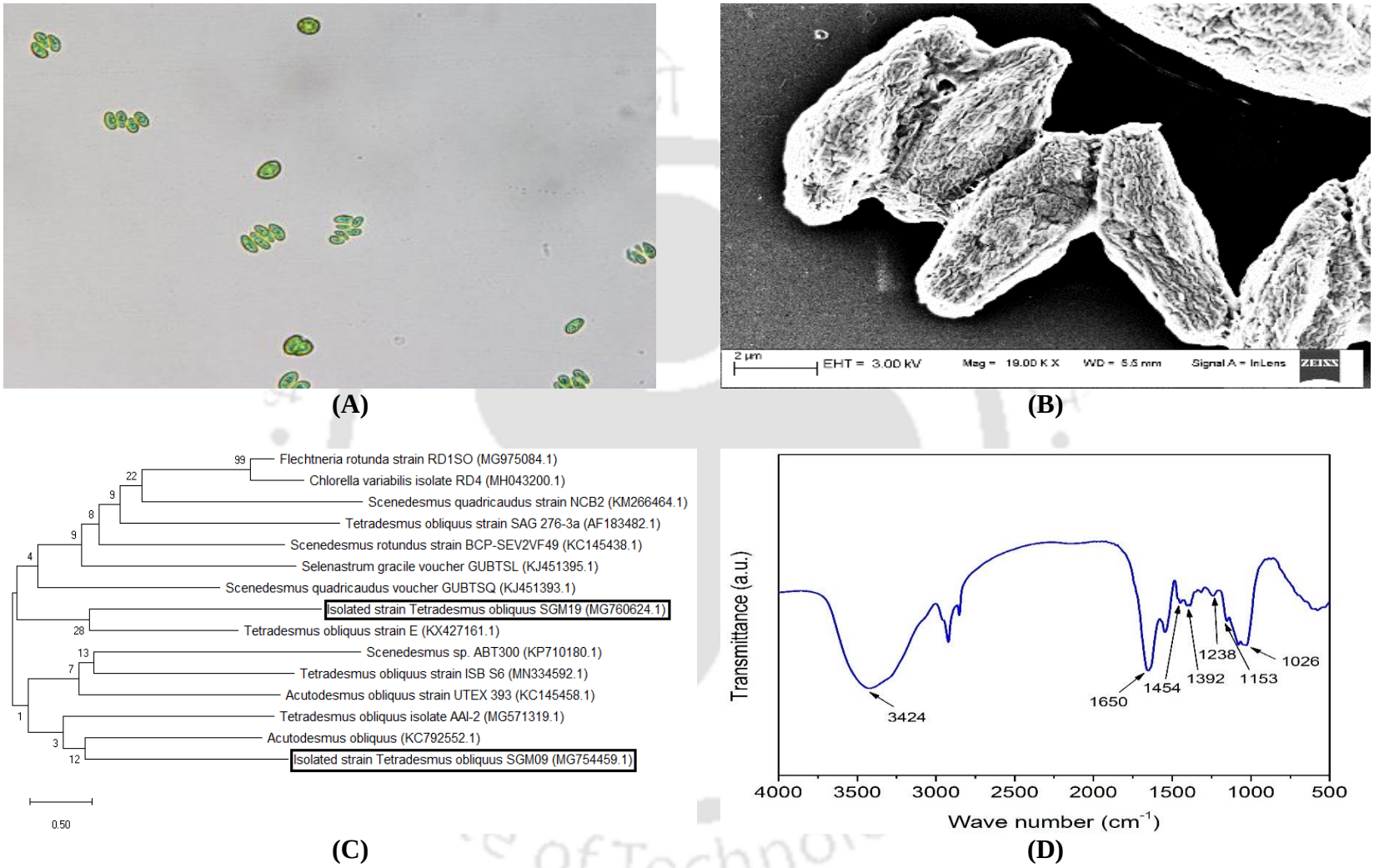

Figure 2.1. Characterization of isolated microalgae *T. obliquus* SGM19. (A) light micrograph, (B) FE-SEM micrograph, (C) phylogenetic tree based on 18S rRNA sequences, (D) FTIR spectrum of raw biomass

2.3.1.2 Biomass and lipid content

The growth and biochemical compositions of the isolated microalgae are presented in Table 2.2. *T. obliquus* SGM19 exhibited a significant growth, displaying maximum specific growth rate of 0.177 ± 0.014 d^{-1}. The sigmoidal growth curve (Fig. 2.2A) showed 1 d lag-phase and a gradual shift to stationary phase, which promotes production of storage substances. On 15th day from inoculation, the final biomass concentration attained was 2.3 ± 0.8 g/L.

Table 2.2. Growth and biochemical characteristics of the isolated microalgae

Parameters	*T. obliquus* SGM19	*T. obliquus* SGM09
Specific growth rate, μ (d^{-1})	0.177±0.014	0.161±0.011
Biomass concentration (g/L)	2.3±0.8	1.51±0.62
Biomass productivity (g/L/d)	0.17±0.03	0.15±0.02
Chlorophyll a (μg/mL)	17.71±1.1	17.82±1.8
Chlorophyll b (μg/mL)	10.43±0.8	9.28±1.2
Total Chlorophyll (μg/mL)	28.14±1.9	24.49±1.5
Total Carotenoid (μg/mL)	7.91±0.5	8.45±0.43
Protein (% DCW)	19.7±2.1	19.2±1.6
Carbohydrate (% DCW)	21.5±1.2	19.6±1.2
Lipid (% DCW)	27.5±1.5	20.5±2.2
β-carotene (mg/g DCW)	0.61±0.1	0.55±0.13
Antioxidant activity (%)	69.1±6.3	63.8±5.4

The lipid content was 27.5 ± 1.5 % of DCW, and the maximum lipid productivity was found to be 41 mg/L/d. The microalgal strain with lipid content > 20% and lipid productivity of higher than 40 mg/L/d are considered as potential lipid producers for biofuels (Chen et al., 2017). Based on this criterion, *T. obliquus* SGM19 is worth of further investigation. Furthermore, with the Nile red staining, the microalgae displayed

lipid bodies as small red dots, indicating high content of intracellular lipid (Fig. 2.2B).

T. obliquus was found to be a promising biomass producer. Biomass and lipid production by the *T. obliquus* SGM19 strain varied proportionately. The highest lipid content noted in *T. obliquus* SGM19 was 27.5± 1.5% DCW.

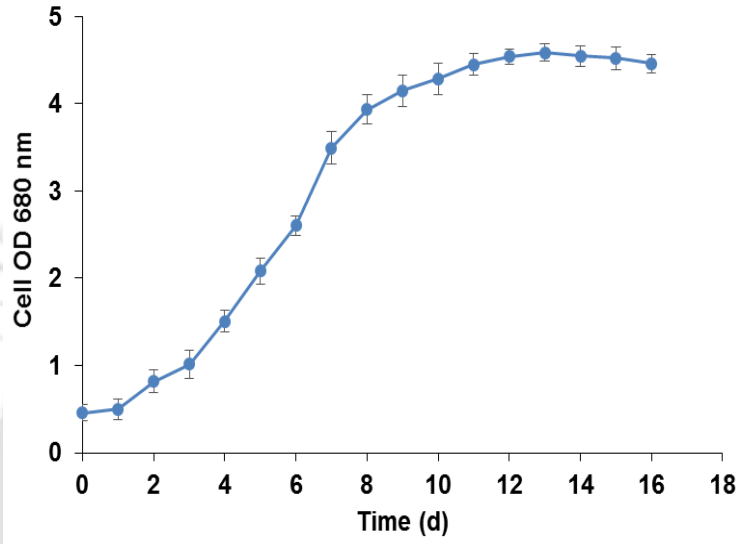

(A)

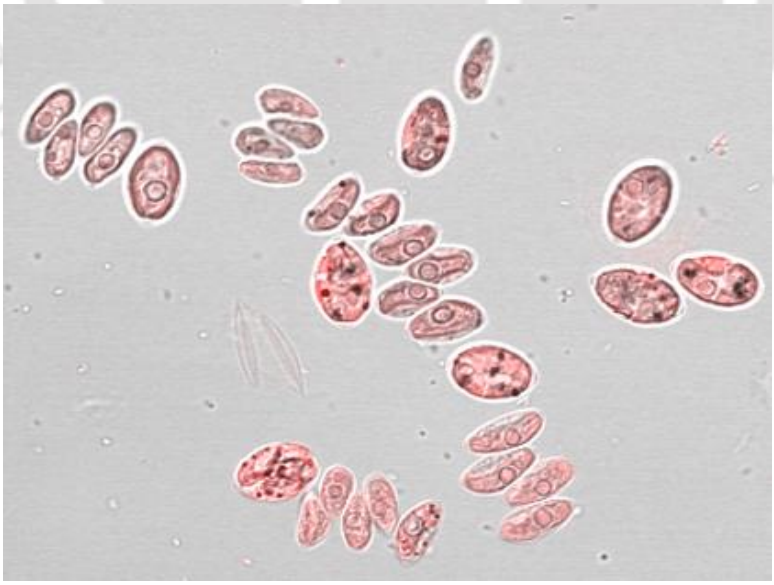

(B)

Figure 2.2. (A) growth profile in BG-11 medium, (B) Nile red stained micrograph

2.3.1.3 Protein and carbohydrate content

Microalgae are potential feedstock for food and pharmaceutical industry because of their high carbohydrate and protein content. With procedure outlined in section 2.2.5, protein content of *T. obliquus* SGM19 was determined as 19.7% dry biomass, while carbohydrate content was 21.5% dry biomass. Comparing these values with previous literature (Selvarajan et al., 2015), we find that protein content of *T. obliquus* SGM19 is at par with microalgal strains of other genres such as *Chlorella*, *Dunaliella*, and *Chlamydomonas*. However, carbohydrate content of *T. obliquus* SGM19 was relatively smaller than other species. Carbohydrate content of the biomass can be enhanced by full optimization of growth conditions supplementation of the medium with CO_2 and other promoters. Chandra et al. (2016) reported an increase in carbohydrate content of biomass from 7.73% to 23.91% by sparging CO_2 at 20% v/v. Similarly, Patnaik and Mallick (2015) reported that the carbohydrate content could be enhanced from 22.2 to 55.1% DCW by supplementing growth medium with acetate and citrate.

2.3.1.4 Pigment composition analysis

Chl-a, Chl-b and total carotenoid contents of *T. obliquus SGM19* were determined as 17.71, 10.43 and 7.91 µg/mL, respectively, which can be attributed to significant photosynthetic rate and biomass production. Among the two microalgal strains isolated by us, carotenoids/total chlorophyll and chlorophyll a/b ratio were higher in *T. obliquus* SGM09 which indicates active stress conditions caused by reduction in light-harvesting complex and PS II activity (Zhang et al., 2013). β-carotene yield in both the isolated strains, viz., *T. obliquus* SGM09 and *T. obliquus* SGM19 was estimated to be 0.55 and 0.61 mg/g DCW, respectively.

2.3.1.5 Antioxidant assay

The extract from microalgae was further fractionated with methanol, acetone (75%),

ethanol (70%), and water. For the DPPH method, the standard antioxidant showed highest antioxidant activity of 94.6%. The methanolic extract of *T. obliquus* SGM19 registered the highest activity of 69.1%, followed by methanolic extract of *T. obliquus* SGM09 (activity = 63.8%) and water extracts of *T. obliquus* SGM19 (activity = 63.5%). Other extracts of both microalgal strains showed activities below 60%. The antioxidant activities determined with FRAP assay showed similar trend as the DPPH scavenging method with the highest antioxidant activity of 92% for standard, followed by methanolic extract of *T. obliquus* SGM19 (72.2 %). The other extracts showed activities below 65%.

As the preliminary analysis of biochemical facets of the two isolated microalgal strains (viz. biomass productivity, lipid/carbohydrate/protein/pigment content and antioxidant activities, as described in preceding sections) indicated performance of both the strains to be more or less similar, thus, further studies on simultaneous production of lipids and β-carotene were carried out using *T. obliquus* SGM19.

2.3.2 Growth of *T. obliquus* SGM19 and associated product synthesis

2.3.2.1 Influence of nitrogen sources

The trends in growth of *T. obliquus* SGM19 and associated β-carotene synthesis under different nitrogen sources are shown in Fig. 2.3A. It can be inferred from Fig. 2.3A that *T. obliquus* SGM19, for growth as well as β-carotene accumulation, can consume both organic and inorganic nitrogen sources. Sodium nitrate as nitrogen source yielded highest biomass of 2.3 g/L with specific growth rate of 0.177 d^{-1} which was followed by medium supplemented with urea (2.1 g/L) and yeast extract (2 g/L). This result was in accordance with previous literature. Arumugam et al. (2013) reported nitrate at lower concentrations (up to 10 mM) as the ideal nitrogen source for *Scenedesmus bijugatus*. Ren et al. (2013) also achieved 3.46 g/L biomass with sodium nitrate for *Scenedesmus* sp.

strain. The β-carotene content of biomass varied proportionately with quantity of biomass. As seen in Fig. 2.3A, the highest β-carotene content of 0.63 mg/g dry biomass was obtained for $NaNO_3$ as the nitrogen source.

2.3.2.2 Influence of carbon sources

Fig. 2.3B depicts the effect of mixotrophic medium (supplemented with different carbon sources in presence of $NaNO_3$ as the nitrogen source) on the biomass and β-carotene content of *T. obliquus* SGM19. The profiles in Fig. 2.3B show moderate increase in biomass production (from 2.4 g/L in control to 3.2 g/L) with 10 g/L glucose as carbon source, but it had an inverse effect on β-carotene content. The β-carotene content drops sharply from 0.62 mg/g dry biomass to 0.08 mg/g dry biomass with 10 g/L of glucose. For other carbon sources like sucrose, maltose and fructose, β-carotene production reduces to negligible levels. Previous authors have reported the augmentative effect of carbon sources on biomass growth (for example, Wang et al., 2012). However, as evident from the present work, the synthesis of β-carotene is adversely affected by carbon source in the medium.

2.3.2.3 Effect of salinity (NaCl concentration)

The growth profiles of *T. obliquus* SGM19 cultivated with varying levels of salinity are shown in Fig. 2.3C. It can be observed that the microalga *T. obliquus* SGM19 could only bear salinity up to 25 mM. The growth of the culture was hampered by higher concentrations (i.e., 50 and 100 mM), causing the cells to turn from green to pale yellow by the eighth day. The biomass productivity and the growth rate of *T. obliquus* SGM19 grown with 25 mM NaCl and control samples were almost similar. This result was in accordance with the results reported by Chandra et al. (2016).

2.3.2.4 Effect of photoperiod

Fig. 2.3D represents the growth profiles of *T. obliquus* SGM19 under three photoperiods, viz. 12L:12D, 16L:08D and 24L:00D. Biomass growth profiles for 12L:12D and 16L:08D match closely, while marginal reduction in biomass concentrations is observed for the 24L:00D period. Thus, it could be concluded that continuous illumination restricts the growth of *T. obliquus* SGM19. As the final biomass yield (1.7 g/L) was the highest with 12L:12D photoperiod, it was used for all the experiments.

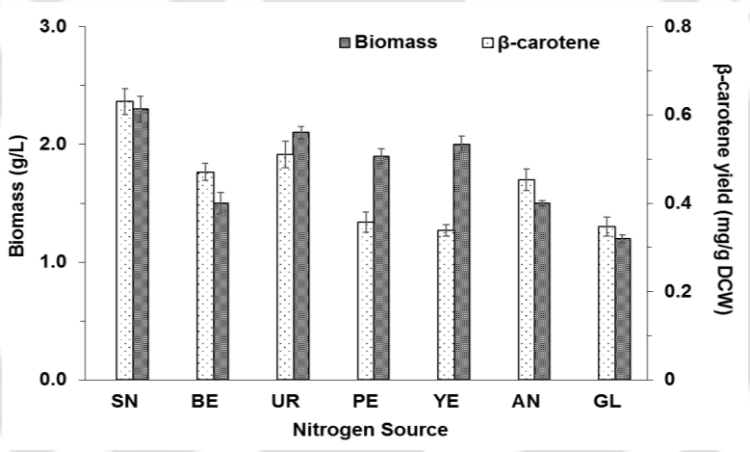

(A)

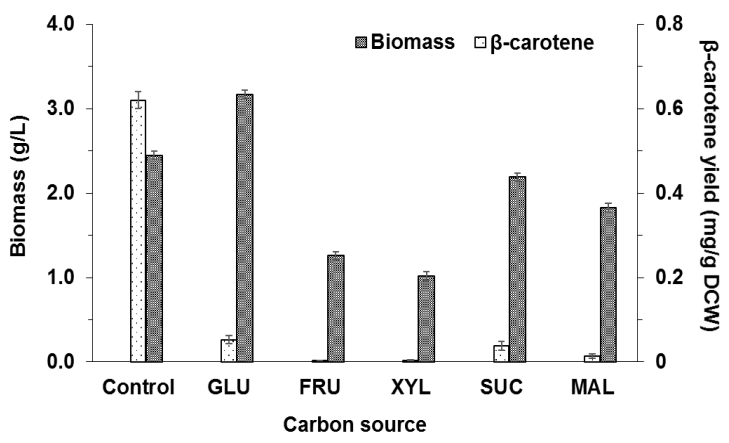

(B)

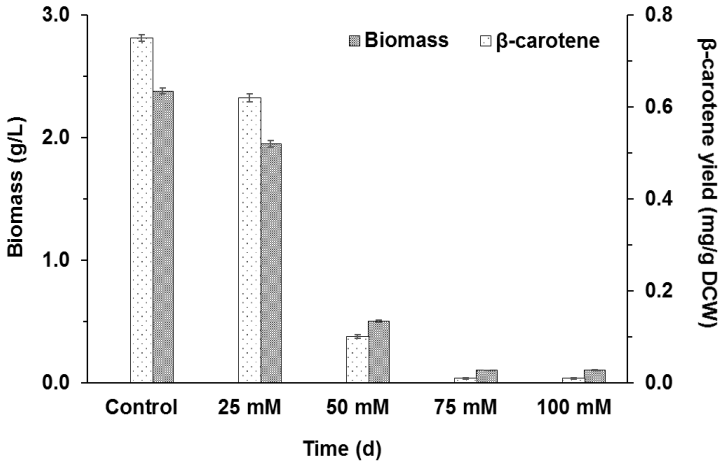

(C)

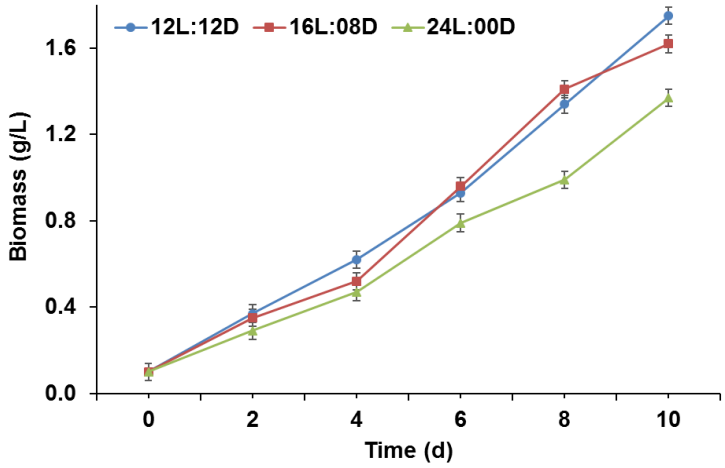

(D)

Figure 2.3. Influence of growth parameters on biomass concentration and β-carotene content of *T. obliquus* SGM19. (A) Nitrogen sources, (B) Carbon sources, (C) Salinity level, (D) Photoperiod

2.3.2.5 Biomass, lipids and β-carotene profiles at optimum conditions

Based on results described in preceding sections (sections 2.3.2.1 to 2.3.2.4), the final growth medium and conditions used for simultaneous lipid and β-carotene production in *T. obliquus* SGM19 were as follows: (1) sodium nitrate as nitrogen source, (2) no carbon source and zero salinity, and (3) 12L:12D photoperiod. On the basis of other preliminary experiments, the light intensity was kept at 5000 lux and culture was

incubated at 30°C. The concentration of sodium nitrate was varied as 0.5, 1.5, 3, and 4.5 g/L, and total growth period was 10 days. Figs. 2.4A, B and C show the individual time profiles of biomass, lipid, and β-carotene at varying sodium nitrate concentrations.

The biomass profiles (Fig. 2.4A) for every nitrate concentration showed similar trends with the highest value of 1.5 g/L for relatively low nitrate concentration of 1.5 g/L. The lipid profile also shows similar trends, and the highest concentration of 0.44 g/L was obtained for 0.5 g/L sodium nitrate. β-carotene content of biomass, on the other hand, was marginally higher (1.15 mg/L) at 1.5 g/L nitrate as compared to 0.5 g/L nitrate (1 mg/L). This experiment shows that higher lipid production is triggered in nitrogen-limited environment whereas β-carotene accumulation within the cell requires relatively higher levels of nitrogen.

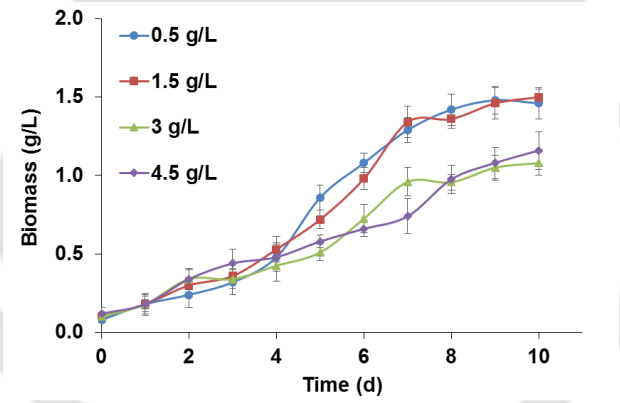

(A)

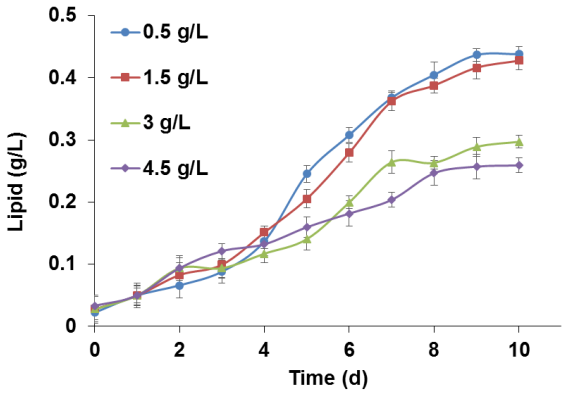

(B)

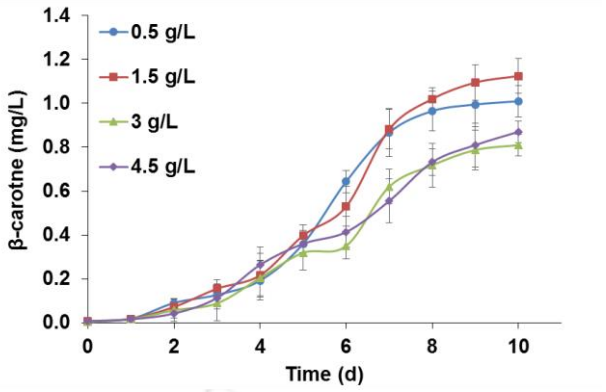

(C)

Figure 2.4. Time profiles of concentrations of biomass and its contents for various initial sodium nitrate concentrations. (A) Biomass, (B) Lipid and (C) β-carotene

2.3.3 TGA and Structural composition analysis

TGA of biomass samples: The thermogravimetric curves of the raw and spent algal biomass with nitrogen and air as carrier gasses are shown in Fig 2.5. The thermogravimetric curves in Fig. 2.5A with nitrogen as carrier gas represents pyrolytic behavior (or characteristics) of biomass. Under inert atmosphere, decomposition of both raw and spent biomasses occurred in three stages. In the initial stage, i.e., temperature range from 40°–150°C, the principal mechanism of mass reduction was removal of moisture and volatile matters. The mass loss for raw biomass was significantly higher than spent biomass. In the next stage (i.e., stage 2 with temperature range 150°–500°C), maximum mass loss occurred. The mechanism of mass loss in this zone is the pyrolysis of three main components of biomass, viz. carbohydrates, lipids, and proteins. With increasing temperature and heat supply, these components undergo depolymerization and cracking, which resulted in major mass loss. In the last stage (stage 3 with temperature range 500°–900°C), the residual biomass (compromising of high molecular weight components) undergoes decomposition resulting in char formation. Quantitatively, the

percentage mass losses in each of the three stages are: stage 1 = 15.8%, stage 2 = 62.7%, stage 3 = 9.65% for raw biomass, and stage 1 = 4.3%, stage 2 = 65.54%, stage 3 = 8% for spent biomass.

Differential thermogravimetric (DTG) curves depicted in Fig. 2.5B for inert atmosphere show two peaks, viz. at 300°C and 450°C. The peak at 300°C is attributed to the decomposition of holocellulose, which essentially is a mixture polysaccharides. As reported by Collazzo et al. (2017), the typical temperature ranges of decomposition of hemicellulose and cellulose are 150°–325°C and 325°–377°C. Lignin, being an amorphous entity, undergoes decomposition in temperature range of 227°–500°C.

The TGA curves depicted in Fig. 2.5C with air as carrier gas show combustion profile of microalgal biomass. In these TGA curves, temperature ranges of first two stages of mass loss closely coincide with the corresponding stages in the TGA profile in inert atmosphere. However, the extent of mass in these stages is significantly higher than the mass loss in inert atmosphere. Another notable feature of TGA curve with air as carrier gas is close overlap of the curves for raw and spent biomass. At approximately 460°C, the TGA curve for spent biomass shows sharp fall, which essentially corresponds to ignition of biomass. Practically, no mass loss is seen for spent biomass for temperature higher than 460°C. This represents complete oxidation of the structural components of biomass with formation of ash. Quantitatively, the percentage mass losses in each of the three stages are: stage 1 = 9.03%, stage 2 = 82.05%, stage 3 = 3.77% for raw biomass, and stage 1 = 8.86%, stage 2 = 86.43% for spent biomass. The TGA curve of raw biomass shows relatively slower mass loss in the temperature range 460°-650°C. This is attributed to resistance to oxidation offered by membrane lipids, which are essentially glycol- and phospholipids. These lipids comprise of up to ~ 40% polyunsaturated fatty acids, e.g.,

eicosapentanoic acid. Beyond 650°C, the TGA curve of raw biomass is horizontal indicating formation of ash after complete oxidation of biomass.

The DTG curves of raw and spent biomass reveal peaks at approx. 280°C. However, the peak corresponding to spent biomass represents weight loss at much higher rate as compared to raw biomass. In the temperature range of 240°-320°C, DTG curve of spent biomass shows two peaks which probably correspond to separate oxidation of cellulose and hemicellulose. At 460°C, the DTG curve of spent biomass shows sharp peak (with mass loss rate up to 25%), which essentially corresponds to ignition of biomass. The DTG curve of raw biomass shows occurrence of a minor peak at ~ 460°C (see inset of Fig. 2.5D), which could be attributed to ignition of residual biomass. Due to resistive behavior of membrane lipids, as noted earlier, the oxidation proceeds at slower rate.

Analysis of structural composition: The powdered raw biomass of *T. obliquus* SGM19 was found to contain holocellulose (67.6 w/w %) comprising cellulose (41.2 w/w %) & hemicellulose (26.4 w/w %), and lignin (14 w/w %). The biomass after extraction of lipids, i.e. spent biomass, comprises of holocellulose (56 w/w %) with cellulose (13.2 w/w %) & hemicellulose (42.7 w/w %), and lignin (25 w/w %).

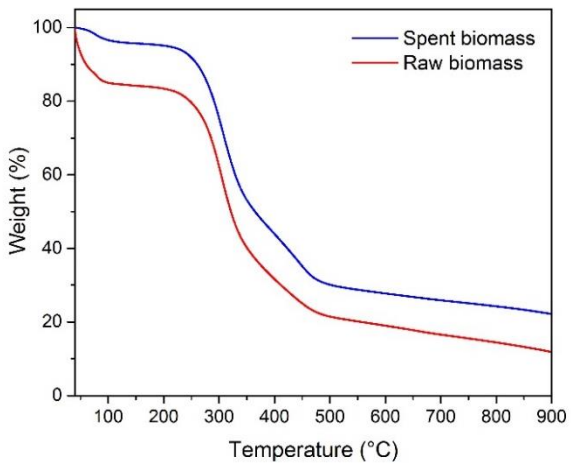

(A)

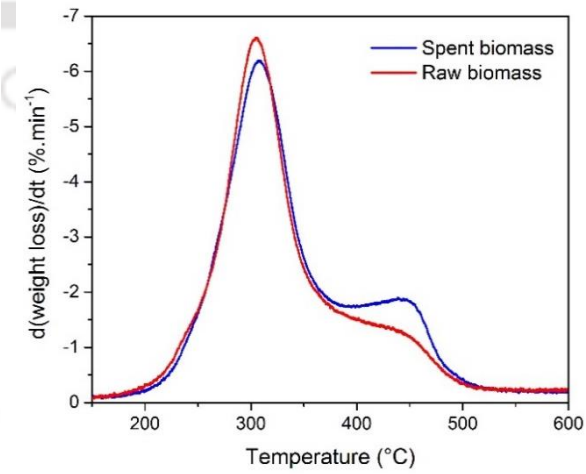

(B)

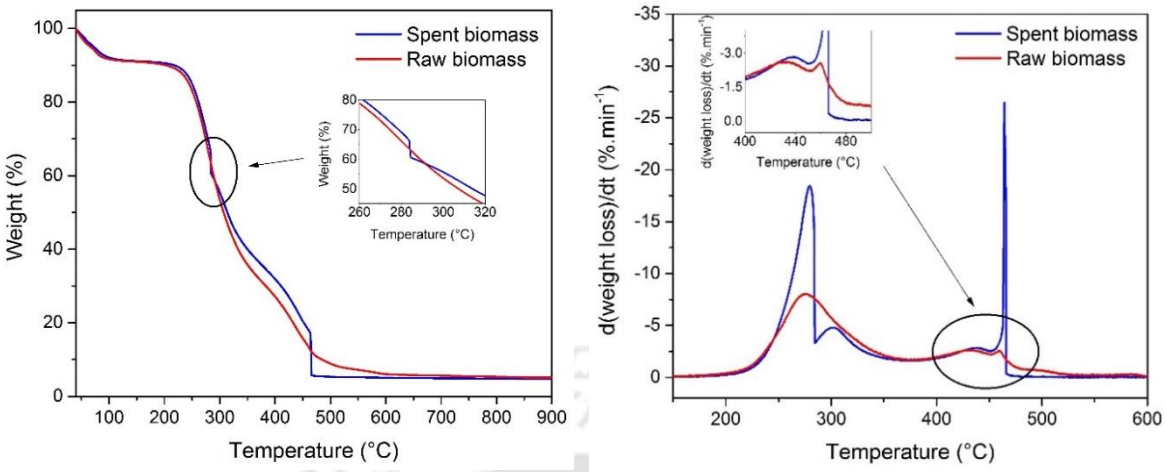

(C) (D)

Figure 2.5. (A) Thermogravimetric analysis (TGA) profiles, and (B) Differential thermogravimetric (DTG) profiles of raw and spent biomass in inert (N_2) atmosphere**;** (C) Thermogravimetric analysis (TGA) profiles, and (D) Differential thermogravimetric (DTG) profiles of raw and spent biomass in air (oxidative) atmosphere

2.3.4 Analysis and characterization of biodiesel

***GC-MS analysis of FAME composition*:** Biodiesel produced during transesterification comprised of esters of several fatty acids in microalgal lipids. The composition of FAME (essentially the fatty acids contained in the esters) was studied using GC-MS. Representative GC-MS spectrum of a FAME sample is shown in Appendix A. The percentage contents of different fatty acids in the FAME (as per relative intensity of different peaks in the GC-MS spectrum) are listed in Table 2.3. The individual weight percentages of fatty acids/esters identified by software NIST-2008 adds up to 79%. However, there are many other peaks corresponding to fatty acids and esters present in small quantities. A much wider fatty acid profile has been reported by other authors (for example, Francisco et al., 2010). The fatty acids having major fractions in total FAME were palmitic acid (C16:0), palmitoleic acid (C16:1), stearic acid (C18:0), oleic acid

(C18:1), and linoleic acid (C18:2). The total content of these fatty acids in the FAME sample was ~ 85%. Biodiesel produced through conventional feedstock of vegetable oils (which is suitable for blending with regular diesel) also has these fatty acids as major components (Kumar and Kant, 2013). Relatively smaller oleic acid content in the microalgal lipids could result in better fuel properties, e. g., combustion heat, viscosity, oxidative stability and cold filter plugging point (Arora et al., 2016). Nonetheless, the properties of the biodiesel produced from *T. obliquus* SGM19 need to be ascertained through standard tests.

Table 2.3. FAME profile of *T. obliquus* SGM19

Fatty acids	Content (% w/w)*
C13:0	0.95
C14:1	2.01
C15:0	1.57
C15:1	1.17
C16:0	16.93
C16:1	1.30
C16:2	1.06
C17:0	6.02
C18:0	3.70
C18:1	4.69
C18:2	11.54
C18:3	16.50
C20:0	9.51
C20:5	0.92
C22:6	0.88
Total SFA	38.68
Total UFA	40.07

***:** calculated on the basis of area of each peak in GC-MS spectra

Characterization of biodiesel and comparison against standards: The principal characteristics (or properties) of biodiesel as per global standard are: cetane number (CN), iodine value (IV), saponification value (SV), cold filter plugging point (CFPP) kinematic viscosity (KV) and higher heating value (HHV). These characteristics essentially signify the suitability of biodiesel for blending with petroleum diesel for smooth and efficient operation of the IC engine. Greater details on definition and significance of these characteristics can be found in previous literature (Chandra et al., 2016; Francisco et al., 2010). Based on FAME profiles determined by GC-MS, the characteristics of biodiesel can be determined using the empirical formulae (eqs. 2.7–2.10) given by Francisco et al. (2010) as follows:

Saponification value (SV) = $\sum \frac{(560 \times N)}{M}$ [2.7]

Iodine value (IV) = $\sum \frac{(254 \times D \times N)}{M}$ [2.8]

Cetane number (CN) = $46.3 + (5458/SV) - (0.225 \times IV)$ [2.9]

Cold filter plugging point (CFPP) = $3.1417 \begin{bmatrix} 0.1 \cdot C16 + 0.5 \cdot C18 + C20 + \\ 1.5 \cdot C22 + 2 \cdot C24 \end{bmatrix} - 16.477$ [2.10]

Notations: N – % of the fatty acid, M – molecular weight of the fatty acid, D – number of double bonds in the fatty acid. Ramírez-Verduzco et al. (2012) have given following correlations (eqs 2.11 and 2.12) for higher heating value and kinematic viscosity for a particular FAME in terms of its molecular weight and structure:

Kinematic viscosity (KV, mm^2/s) = $\ln(\eta_i) = -12.503 + 2.496 \times \ln(M_i) - 0.178 \times D$ [2.11]

Higher heating value (HHV, MJ/kg) = $\delta_i = 46.19 - (1794/M_i) - 0.21 \times D$ [2.12]

where M_i is the molecular mass of the corresponding fatty acid, while D is the number of double bonds in the corresponding fatty acid. The gross or overall KV and HHV of biodiesel comprising of mixture of esters of various fatty acids are calculated on the basis of weighted average of individual properties of FAME (f_i) as: $f = \sum z_i \times f_i$, where, f is the overall property of the biodiesel and z_i is the mass fraction of corresponding FAME. Typical standard values of these properties are listed in Table 2.4.

Table 2.4. Conservative# estimate of biodiesel properties

Property	Standard ASTM D6751/EN 14214	This study
Saponification value (mg KOH/g)	370 (max)	205.09
Iodine value (g I_2/100 g)	120 (max)	108.12
Cetane number	47 (min)	48.59
Cold filter plugging point (°C)	+5 (max)	-15.20
Kinematic viscosity at 40°C (mm^2/s)	1.9 - 6.0	3.79
Higher heating value (MJ/kg)	40	39.37

properties calculated on the basis of components identified in FAME profile (Table 2.3).

As noted by Islam et al. (2013), the higher iodine valve and lower cetane number of biodiesel are contributed by higher content of polyunsaturated fatty acids. The kinematic viscosity is proportional to saturated fatty acid content, while HHV is proportional to the content of higher saturated fatty acids. In the present study, we could identify approx. 79% of the components of lipids, which could be categorized as: total polyunsaturated fatty acids = 30.91 wt%, total saturated fatty acids = 38.68 wt% and total higher saturated fatty acids = 9.51 wt%. This peculiar composition of the structural lipids has imparted desirable properties to the biodiesel. Table 2.4 lists the properties of biodiesel synthesized in this study using the above formulae, vis-à-vis two standards, viz. ASTMD 6751 and EN 14214. It could be inferred from Table 2.4 that all properties of biodiesel synthesized using microalgal lipids under optimum culture conditions are within the desired limits.

***FTIR analysis of functional groups*:** The FTIR spectrum of biodiesel produced from *T. obliquus* SGM19 is shown in Appendix A. The band at 1743 cm^{-1} corresponds to intense (-C=O) stretching in monoalkyl esters (Kumar et al., 2014). The transmittance peaks obtained at 1200 cm^{-1} and 1183 cm^{-1} are attributed to stretching vibration of (CC(=O)-O) bonds of ester (anti-symmetric axial) and (O-C-C) bonds (asymmetric axial) respectively. Also, peak at 1444 cm^{-1} may be present due to the vibrations of CH_3 anti-symmetric deformations.

2.4 Conclusions

Major results of this study can be summarized as follows:

- The freshwater microalga *T. obliquus* SGM19 has shown high potential for simultaneous production of lipids and β-carotene.
- Under optimum conditions, the microalgal concentration attained 2.5 g/L with 28.5 wt% lipids (dry biomass) and 0.67 mg/g (dry biomass) β-carotene with 69% antioxidant activity.
- FAME profile obtained by GC-MS comprised of 71% of C16 and C18 fatty acids, making an ideal feedstock. 31 wt% PUFA content results in lower cetane and higher iodine value.
- The estimated properties of the biodiesel synthesized from lipids meet the ASTM and European standards.

References

Aburai N., Ohkubo S., Miyashita H., Abe K., 2013. Composition of carotenoids and identification of aerial microalgae isolated from the surface of rocks in mountainous districts of Japan. Algal Res. 2, 237–243.

Aghbashlo M., Tabatabaei M., Hosseinpour S., 2018. On the exergoeconomic and exergoenvironmental evaluation and optimization of biodiesel synthesis from waste cooking oil (WCO) using a low power, high frequency ultrasonic reactor. Energy Convers. Manage. 164, 385-398.

Akhtar N., Goya D., Goyal A., 2017. Characterization of microwave-alkali-acid pre-treated rice straw for optimization of ethanol production via simultaneous saccharification and fermentation (SSF).Energy Convers. Manag.141, 133-144.

Arora N., Patel A., Pruthi P.A., Pruthi V., 2016. Recycled de-oiled algal biomass extract as a feedstock for boosting biodiesel production from *Chlorella minutissima*. Appl. Biochem. Biotechnol. 180, 1534-1541.

Arumugam M., Agarwal A., Arya M.C., Ahmed Z., 2013. Influence of nitrogen sources on biomass productivity of microalgae *Scenedesmus bijugatus*. Bioresour. Technol. 131, 246-249.

Chandra T.S., Deepak R.S., Kumar M.M., Mukherji S., Chauha V.S., Sarada, R., Mudliar S.N., 2016. Evaluation of indigenous fresh water microalga *Scenedesmus obtusus* for feed and fuel applications: Effect of carbon dioxide, light and nutrient sources on growth and biochemical characteristics. Bioresour. Technol. 207, 430-439.

Chen Y., Li X., Sun Z., Zhou Z., 2017. Isolation and identification of *Choricystis minor* Fott and mass cultivation for oil production. Algal Res. 25, 142-148.

Collazzo G.C., Broetto C.C., Perondi D., Junges J., Dettmer A., Dornelles Filho A.A., Foletto E.L., Godinho M., 2017. A detailed non-isothermal kinetic study of elephant grass pyrolysis from different models. Appl. Therm. Eng. 110, 1200-1211.

Doria E., Longoni P., Scibilia L., Iazzi N., Cella R., Nielsen E., 2012. Isolation and characterization of a *Scenedesmus acutus* strain to be used for bioremediation of urban wastewater. J. Appl. Phycol. 24, 375–383.

Ferro L., Gentili F.G., Funk C., 2018. Isolation and characterization of microalgal strains for biomass production and wastewater reclamation in Northern Sweden. Algal Res. 32, 44–53.

Francisco E.C., Neves D.B., Jacob-Lopes E., Franco T.T., 2010. Microalgae as feedstock for biodiesel production: Carbon dioxide sequestration, lipid production and biofuel quality. J. Chem. Technol. Biotechnol. 85, 395-403.

Goering H.S., Van Soest P.J., 1970. Forage fiber analyses (apparatus, reagents and some applications). USDA Agricultural handbook no. 379. Washington, DC: Agricultural Research Service, US Depatment of Agriculture.

Islam M.A., Ayok G.A., Brown, R., Stuart D., Magnusson M., Heimann K., 2013. Influence of fatty acid structure on fuel properties of algae derived biodiesel. Procedia Eng. 56, 591-596.

Kumar V., Kant P., 2013. Study of physical and chemical properties of biodiesel from sorghum oil. Res. J. Chem. Sci. 3(9), 64-68.

Kumar V., Muthuraj M., Palabhanvi B., Ghoshal A.K., Das D., 2014. Evaluation and optimization of two stage sequential *in situ* transesterification process for fatty acid methyl ester quantification from microalgae. Renew. Energy 68, 560-569.

Lee K., Eisterhold M.L., Rindi F., Palanisami S., Nam P.K., 2014. Isolation and screening of microalgae from natural habitats in the Midwestern United States of America for biomass and biodiesel sources. J. NatSc. Biol. Med. 5, 333-339.

Lichtenthaler H.K., 1987. Chlorophylls and carotenoids: pigments of photosynthetic biomembranes. Methods Enzymol. 148, 350–382.

Mandal S.; Mallic N., 2009. Microalga *Scenedesmus obliquus* as a potential source for biodiesel production. Appl. Microbiol. Biotechnol. 84, 281–291.

Mata T.M., Martin A.A., Caetano, N.S., 2010. Microalgae for biodiesel production and other applications: a review. Renew. Sust. Energ. Rev. 14, 217–232.

Mishra S., Mohanty K., 2019. Comprehensive characterization of microalgal isolates and lipid-extracted biomass as zero-waste bioenergy feedstock: An integrated bioremediation and biorefinery approach. Bioresour. Technol. 273, 177-184.

Patias L.D., Fernandes A.S., Petry F.C., Mercadante A.Z., Jacob-Lopes E., Zepka L.Q., 2017. Carotenoid profile of three microalgae/cyanobacteria species with peroxyl radical scavenger capacity. Food Res. Int. 100, 260–266.

Patnaik R., Mallick N., 2015. Utilization of *Scenedesmus obliquus* biomass as feedstock for biodiesel and other industrially important co-products: An integrated paradigm for microalgal biorefinery. Algal Res. 12, 328-336.

Ramírez-Verduzco L.F., Rodríguez-Rodríguez J.E., Jaramillo-Jacob A.R., 2012. Predicting cetane number, kinematic viscosity, density and higher heating value of biodiesel from its fatty acid methyl ester composition. Fuel 91, 102-111.

Ren H.Y., Liu B.F., Ma C., Zhao L., Ren N.Q., 2013. A new lipid-rich microalga *Scenedesmus* sp. strain R16 isolated using Nile red staining: effects of carbon and nitrogen sources and initial pH on the biomass and lipid production. Biotechnol. Biofuels 6, 143-152.

Rosen, M.A., 2018. Environmental sustainability tools in the biofuel industry. Biofuel Res. J. 17, 751-752.

Saitou N., Nei M., 1987. The neighbor-joining method: a new method for constructing phylogenetic trees. Mol. Biol. Evol. 4, 406–425.

Scott S.A., Davey M.P., Dennis J.S., Horst I., Howe C.J., Lea-Smith D.J., Smith A.G., 2010. Biodiesel from algae: Challenges and prospects. Curr. Opin. Biotechnol. 21, 277–286.

Selvarajan R., Felföldi T., Tauber T., Sanniyasi E., Sibanda T., Tekere M., 2015. Screening and evaluation of some green algal strains (Chlorophyceae) isolated from freshwater and soda lakes for biofuel production. Energies 8, 7502-7521.

Tale M., Ghosh S., Kapadnis B., Kale S., 2014. Isolation and characterization of microalgae for biodiesel production from Nisargruna biogas plant effluent. Bioresour. Technol. 169, 328-335.

Vasileva I., Marinova G., Gigova L., 2015. Effect of nitrogen source on the growth and biochemical composition of a new Bulgarian isolate of *Scenedesmus* sp. J. BioSci. Biotechnol., 125-129.

Wang H., Fu R., Pei G., 2012. A study on lipid production of the mixotrophic microalgae *Phaeodactylum tricornutum* on various carbon sources. Afr. J. Microbiol. Res. 6, 1041-1047.

Xu S., Elsayed M., Ismail G.A., Li C., Wang S., Abomohra A.E., 2019. Evaluation of bioethanol and biodiesel production from *Scenedesmus obliquus* grown in biodiesel waste glycerol: A sequential integrated route for enhanced energy recovery. Energy Convers. Manag. 197, 111907.

Yen G.C., Chen H.Y., 1995. Antioxidant activity of various tea extracts in relation to their antimutagenicity. J. Agri. Food Chem. 43, 27-32.

Zhang Y.M., Chen H., He C.L., Wang Q., 2013. Nitrogen starvation induced oxidative stress in an oil-producing green alga *Chlorella sorokiniana* C3. PLoS ONE 8(7), e69225.

Zhao G., Yu J., Jiang F., Zhang X., Tan T., 2012. The effect of different trophic modes on lipid accumulation of *Scenedesmus quadricauda*. Bioresour. Technol. 114, 466–471.

CHAPTER 3

ULTRASONIC ENHANCEMENT OF LIPIDS AND β-CAROTENE PRODUCTION BY *T. obliquus* SGM19

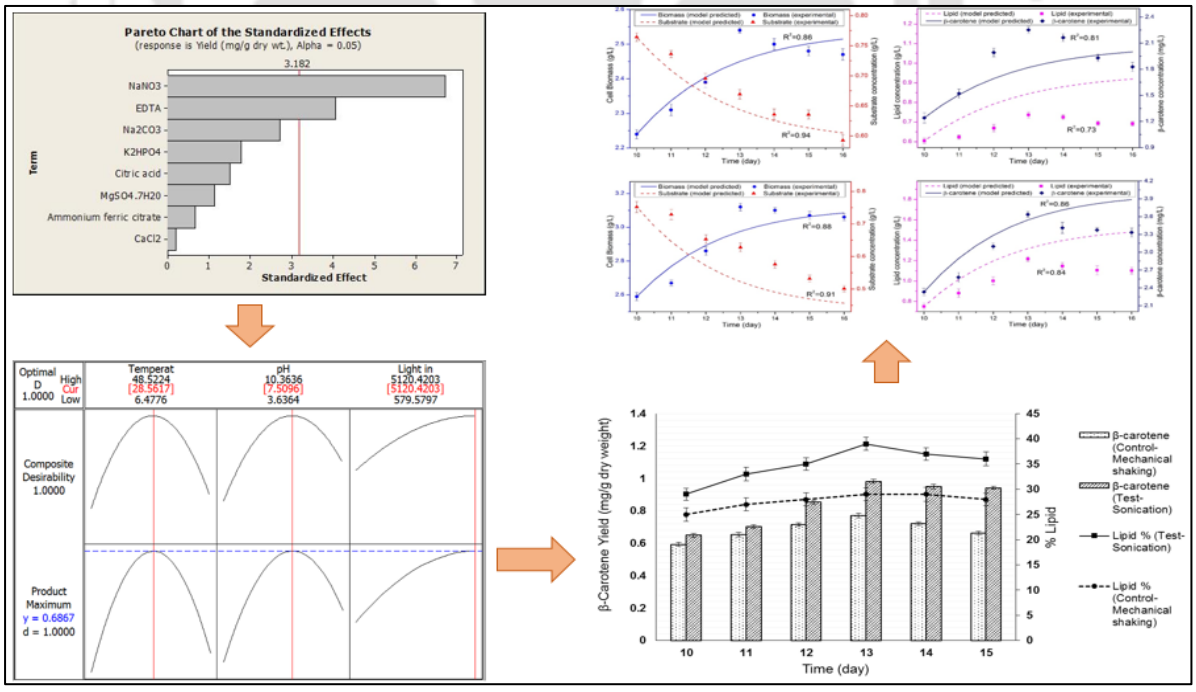

CHAPTER 3

Ultrasonic Enhancement of Lipids and β-carotene Production by *T. obliquus* SGM19

3.1 Introduction

In the previous chapter, we dealt with isolation and characterization of the wild freshwater microalgal strain of *T. obliquus* SGM19. In initial assessments, this strain revealed good potential for simultaneous production of lipids and β-carotene. The preliminary transesterification of the lipids extracted from *T. obliquus* SGM19 also yielded encouraging results. FAME profile was dominated by C16 and C18 fatty acids, making it an ideal feedstock for biodiesel. The properties of this biodiesel estimated from FAME profile were in concurrence with the ASTM and European standards. As noted earlier, enhancement of not only the lipid production but also the other value-added products, along with their extraction and recovery is the key to commercial success of microalgae-based biorefinery (Misra et al., 2014, Chew et al., 2017).

In this chapter, we take ahead the theme with development of new cultivation techniques, which in addition to lipids, can also give high yields of value-added

byproducts like carotenoids. Carotenoids are a group of pigments produced by algae (also called tetraterpenoids). These are used for imparting various characteristic colors like red, orange and bright yellow to leaves, fruits and aquatic animals (Lorenz and Cysewski, 2000). Apart from pigmentation, carotenoids also form important constituent of human nutrients, such as β-carotene, which is a precursor to vitamin A (Spolaore et al., 2006). Microalgae are natural source of carotenoids. These carotenoids are assembled under favorable conditions such as availability of nutrients, optimum radiance and other physical parameters like pH and temperature. An indubitable enhancement of primary carotenoids could be attained by employing conditions of mild stress (either physical or biological) that promote accumulation of carotenoid over chlorophyll without influencing culture growth (Del Campo et al., 2007). Increasing the stress beyond a limit results in decline in chlorophyll production and thus in primary carotenoid production due to a highly maintained stoichiometry of the pigments present within photosynthetic apparatus.

The present study is aimed at enhancing lipid and β-carotene production from wild microalgal strain of *Tetradesmus obliquus* SGM19. As noted earlier, wild strains are more stable in natural (or uncontrolled) environments than genetically engineered strains (Szvjka et al., 2017). The specific objectives of the study are as follows: (1) Statistical optimization of media and physical parameters for the natural microalgal strain, (2) Growth of the microalgal isolate with mechanical shaking for lipid and β-carotene production, (3) Intensification of microalgal growth (biomass and products) with application of sonication at proper duty cycle, (4) Kinetic analysis of time profiles of biomass, substrate (nitrate) and products, i.e., lipid and β-carotene with Luedeking–Piret model, (5) Mechanistic analysis of sonication-induced enhancement of microalgal growth with quantification of NAD(H) concentration within the cells.

3.2 Materials and methods

3.2.1 Microalgae and Culture Conditions

Strains of microalgae *T. obliquus* SGM19 isolated previously were used. The microalgae was maintained on BG-11 medium at a constant temperature of 30°C and pH was 7.0 of the medium. In a 250 mL capacity conical flasks, 100 mL culture medium was exposed to a light of 90 μmol photons·m^{-2}·s^{-1} intensity with a 12/12 h of light/dark cycle. The irradiance was measured under the white fluorescent tube light in an incubator shaker by lux meter.

3.2.2 Analytical Determinations

Dry cell biomass weight (DCW) was estimated by simply taking the cell broth in a centrifuge tube (pre-weighed) at particular time intervals, followed by centrifugation for 10 min at 5000 rpm and 4°C. Cells pellets were collected, washed with distilled water twice, freeze-dried and weighed. For determining the concentration of nitrate in the culture medium, protocol of APHA (1998) was followed and correlated to a standard curve.

Lipids in the biomass were extracted and estimated using chloroform–methanol system (Bligh and Dyer, 1959). The extract was dried and weighed (Mishra et al., 2015). β-carotene was quantified with HPLC using a C18 reverse-phase column with acetone as eluent (Patias et al., 2017). All experiments were conducted in triplicates to ensure reproducibility.

3.2.3 Statistical optimization

The medium components as well as physical parameters for growth of *T. obliquus* SGM19 were optimized using two-step statistical experimental design, viz. Plackett-

Burman design followed by central composite design (CCD). β-carotene content of the biomass (dry basis) was treated as the response variable.

3.2.3.1 Plackett–Burman design for media components

The Plackett-Burman design was used for evaluation of significance of eight variables (viz. $NaNO_3$, $MgSO_4 \cdot 7H_2O$, Na_2CO_3, $CaCl_2$, K_2HPO_4, EDTA (ethylenediamine tetraacetic acid), citric acid and ammonium ferric citrate) in 12 experimental runs. Each of the parameter was tested at two levels coded as (+1) for higher level and (-1) for lower level (details given in Appendix B). MINITAB (Trial Version, Release 15.1, PA, USA) was used for the data analysis.

3.2.3.2 Central composite design

Optimization of the significant growth media components, viz. $NaNO_3$ and EDTA, and physical parameters of growth, viz. temperature and pH of medium and light intensity, was done using central composite design of experiments. The details of two experimental designs are given in Appendix B. The results of the statistical experimental design were analyzed using response surface methodology with a quadratic model. The fitness of this model was assessed using ANOVA (analysis of variance).

3.2.4 Validation experiments

Statistical design of experiments yielded following set of optimum values of growth media components and physical parameters: $NaNO_3$ = 1.5 g/L; EDTA = 0.001 g/L; temperature = 28.5^oC; pH = 7.5 and light intensity = 5120 Lux. The predicted value of response variable (yield of β-carotene) by the quadratic model for these optimum conditions was 0.67 mg/g DCW. The authenticity of the statistical optimization was

assessed by a validation experiment conducted at optimum values of the media components and physical parameters. The validation experiment was conducted for a period of 15 days on the basis of growth cycle (in triplicate to assure the reproducibility). This experiment resulted in β-carotene yield of 0.69 mg/g DCW, which closely matched with the predicted value by the quadratic model.

3.2.5 Ultrasound-assisted growth of *T. obliquus* SGM19

A well-known technique for intensification of biological processes is sonication (Singh et al., 2015; Tizazu et al., 2018). To study effect of sonication on enhancement of growth of *T. obliquus* SGM19 concurrently with lipid content and β-carotene yield, experiments were carried out at optimum conditions predicted by statistical experimental design. Sonication of growth medium containing *T. obliquus* SGM19 was carried out in an ultrasound bath (PCi Analytics, India, 3.5 L). This bath had frequency of 33 kHz with power rating of 100 W. The dimensions of the bath were 30 cm × 15 cm × 10 cm. Actual acoustic power dissipation in the bath and pressure amplitude of the ultrasound waves generated in the medium (1.4 bar) were determined using calorimetric techniques. Sonication was applied to the growth medium at pre–optimized 10% duty cycle (1 min sonication + 9 min mechanical shaking in an incubator-shaker at 120 rpm for every 10 min of process). The sonication experiment requires to maintain the temperature of the bath at 28.5 ± 2°C, i.e., the reaction temperature. Each sonication experiment was conducted during late log phase of the *T. obliquus* SGM19 cells (starting from 10^{th} day, based on the growth curve). From 10^{th} day till the end of experiment (15^{th} day), the growth mixture was exposed to sonication at an interval of 12 h each. Importantly, the growth in each case was allowed for a complete duration of 15 days.

3.2.6 Microassay of NAD(H)

Nicotinamide adenine dinucleotide (NAD^+) is an essential cofactor of metabolism of green microalgae. It participates in metabolic reactions occurring in major organelles of microalgae, viz. chloroplast (or plastid), mitochondria and endoplasmic reticulum. Greater discussion about these metabolic pathways is given in subsequent section.

This method uses a cycling mixture comprising ethanol, phenazine methosulfate, alcohol dehydrogenase and thiazolyl blue for determining NAD(H). When this buffered mixture is supplemented with NAD^+, a cyclic enzymatic reaction is instigated. NADH is produced which reduces thiazolyl blue into a purple-colored compound, formazan, by the mediation of phenazine methosulfate. The concentration of coenzyme and the reduction rate of thiazolyl blue are proportional. The formazan produced has the maximum absorbance in the visible spectrum, hence, it was estimated with the help of spectrophotometer (Nisselbaum and Green, 1969).

***Extraction of metabolites*:** To assist the consistent evaluation of intracellular metabolites that include energetic nucleotides such as NAD(H) and NADP(H), the volume of microalgal culture samples used was sufficient for obtaining atleast 0.1 g of wet weight of microalgae as it is the minimum required cell mass for any intracellular quantifications (Zhao et al., 2016). The microalgal samples were collected and centrifuged for 10 min at 10,000 rpm at 4°C, the supernatant was discarded and cell pellet was washed twice with phosphate-buffered saline (PBS). The pellets were then treated with 0.5 mL of 80% chilled methanol, vortexed well for 2 min and subjected to probe-type ultrasonic treatment (frequency 20 kHz, tip diameter 2 mm, amplitude 30%) for 10 min in ice water for extraction of nucleotides. The mixture was then centrifuged at 10,000 rpm, 4°C for 10 min. The supernatant was collected in a different tube whereas the cell pellet was extracted again with methanol. The supernatant of the two extracts were combined

together and stored in an ice-water bath for analysis of co-enzyme as described by Nisselbaum and Green (1969). More recently, a new technique of ultrasonic (sugaring-out assisted) liquid biphasic flotation for extraction of proteins from biomass has been reported by Sankaran et al. (2018). The synergistic effect in this technique is that bubbles produced via floatation enhance the effect of cavitation. In this technique, surface of the air bubbles enabled adsorption of surface active proteins which float to top phase. This resulted in higher separation efficiency and yield of proteins.

***Measurement of NAD(H)*:** Based on preliminary experiments, the final reaction mixture comprised of 1 mg phenazine methosulfate (PMS)/mL solution (0.8 mL) and 5 mg 3-(4,5-dimethylthiazol-2-yl)-2,5-diphenyl tetrazolium bromide (MTT)/mL solution (0.05 mL). For determining NAD(H), in addition to above components, the mixture also contained 1.0 mg alcohol dehydrogenase (ADH)/mL (0.1 mL) and glycylglycine buffer (1.95 mL, pH 7.4), which included 0.5 M ethanol and 0.1 M nicotinamide. The final pH of the mixture was 7.4.

3.2.7 Viability assessment of microalgae post sonication

The viability of the microalgal cells after treatment with ultrasound was performed by flow cytometry (BD Calibur Flow Cytometer, BD Biosciences, USA). The fluorescence of propidium iodide stained cells was measured to study the viability of algal cells. Propidium iodide is a fluorescent dye which binds with the DNA of the nonviable cell (Ormerod, 1990). When excited at 488 nm, it generates red fluorescence detected by FL3 detector at 585 nm. 50 mL microalgal cell suspension was collected, centrifuged at 4000 rpm for 10 min and pellets were washed twice with PBS, pH 7.0. The cells were then stained with propidium iodide for 1 min in dark before analyzing with flow cytometer.

3.3 Kinetic analysis of experimental profiles

The microalgae was grown on BG-11 medium with different initial nitrate concentrations (0.5, 1.5, 3 and 4.5 g/L) at 28.5°C with pH 7.5. 500 mL Erlenmeyer flasks containing 300 mL culture medium were exposed to a light of 90 μmol photons·m^{-2}·s^{-1} intensity with a light/dark cycle of 12/12 h. The samples were collected and stored at 4°C every day for analysis.

3.3.1 Biomass

The growth of microorganisms was described by following logistic equation (Rao et al., 2009):

$$\frac{dX}{dt} = \mu_m \left(1 - X/X_m\right) X \qquad [3.1]$$

where dX/dt is growth rate, μ_m is the maximum specific growth rate, X is the biomass concentration in the medium, X_m is the maximum biomass concentration. With initial condition, $t = 0$, $X = X_o$, integration of Eq. 3.1 gives:

$$X = \frac{X_0 X_m e^{\mu_m t}}{X_m - X_0 + X_0 e^{\mu_m t}} \qquad [3.2]$$

3.3.2 Products

Luedeking–Piret equation (Luedeking and Piret, 1959) was used to describe formation of both products, viz. lipids and β-carotene. The rate of product formation depends on both the growth rate and the biomass concentration in a linear manner:

$$\frac{dP}{dt} = \alpha \frac{dX}{dt} + \beta X \qquad [3.3]$$

where dP/dt is the rate of product formation, α is the growth-associated product formation coefficient and β is non-growth associated product formation coefficient.

The product formation was categorized into 3 classes based on its relationship with the growth of microalgae by Gaden (2000). Class 1: $\alpha \neq 0$ and $\beta = 0$, which suggest a linear relationship of product formation with the microalgal growth. Class 2: $\alpha \neq 0$ and $\beta \neq 0$, the product formation has a partial relation with the microbial growth. Class 3: $\alpha = 0$ and $\beta \neq 0$, product formation and microalgal growth are unrelated.

3.3.3 Substrate

The consumption of substrate is mainly for the growth of microalgae accumulation of intracellular products and maintaining the microalgal cells. Hence, the kinetics for substrate conversion may be expressed for growth, products and maintenance (Yang et al., 2006).

$$-\frac{dS}{dt} = \frac{1}{Y_{X/S}}\frac{dX}{dt} + mX + \frac{1}{(Y_{P/S})_1}\frac{dP_1}{dt} + \frac{1}{(Y_{P/S})_2}\frac{dP_2}{dt} \quad [3.4]$$

where dS/dt is the rate of substrate consumption, S is substrate concentration, t is time, $Y_{x/s}$ is the growth coefficient, m is the maintenance coefficient, $(Y_{p/s})_1$ is the lipid yield coefficient, $(Y_{p/s})_2$ is the β-carotene yield coefficient, P_1 is the concentration of lipid whereas P_2 is the concentration of β-carotene.

3.3.4 Fitting of experimental profiles to kinetic model

The kinetic model essentially consists of 4 ordinary differential equations (ODEs) for substrate (S), biomass (X), lipid (P_1) and β-carotene (P_2). These equations have 9 parameters, viz. μ_m $Y_{x/s}$, m, α_1, β_1, α_2, β_2, $(Y_{p/s})_1$ and $(Y_{p/s})_2$. The set of ODEs was solved in MATLAB version: R2019a ® (as initial value problem) using Runge-Kutta 4th order method coupled to a Genetic Algorithm module. The numerical profiles of X, S, P_1 and P_2

were compared with the experimental profiles (at the points of sampling) using the objective function:

$$Obj = \left[\left(S^{\exp} - S^{\text{model}} \right)^2 + \left(X^{\exp} - X^{\text{model}} \right)^2 + \left(P_1^{\exp} - P_1^{\text{model}} \right)^2 + \left(P_2^{\exp} - P_2^{\text{model}} \right)^2 \right]^{1/2} \quad [3.5]$$

The objective function is the total root mean square error (RMS) between the experimental values and model predicted values. The genetic algorithm was used to minimize the total error at all sampling points in experimental profile by adjusting the values of kinetic parameters in the model within specified bounds.

3.4 Results and Discussion

3.4.1 Sonication–induced intensification of lipid and β-carotene yield

Table 3.1 depicts the final yields of biomass, lipids and β-carotene resulting after completion of 16-day growth cycle for different initial nitrate concentrations. It could be seen that the highest yields are obtained for initial nitrate concentration of 1.5 g/L, which is in concurrence with the predictions of statistical experimental design. As mentioned in section 3.2.5, the algal broth was exposed to ultrasound (at 10% duty cycle) from 10th day of growth cycle (i.e. late log phase, as seen from biomass growth profile shown in Fig. 3.1A). The trends in yields of lipids and β-carotene for six days of algal growth, viz. 10th to 15th day, are shown in Fig. 3.1B.

In the initial period, viz. 10th and 11th day, the yields in test experiments (employing sonication) are marginally higher than control experiments (employing only mechanical shaking). The yields of both lipid and β-carotene show peak on the 13th day of growth cycle in control and test experiments. Maximum difference between the yields of control and test experiments is also seen on the 13th day of the growth cycle.

Table 3.1. Final yields from microalgal growth

Initial Nitrate concentration (g/L)	Biomass (g/L)	Lipid (g/g DCW)	β-carotene (mg/g DCW)
0.5	2.37±0.03	0.30±0.04	0.79±0.09
1.5	2.54±0.02	0.29±0.03	0.89±0.05
3	1.38±0.05	0.27±0.02	0.68±0.03
4.5	1.34±0.07	0.26±0.03	0.66±0.04
1.5 (Sonicated)	3.12±0.07	0.39±0.03	1.17±0.05
% rise with respect to control experiments	22.8%	34.5%	31.5%

The lipid yields on 13th day are 29% and 40% w/w DCW in control and test experiments, respectively. The β-carotene yields on 13th day are 0.77 mg/g DCW and 0.98 mg/g DCW in control and test experiments, respectively. This essentially shows that augmentation in lipid and β-carotene yield in test experiments is 38% and 27.5%. After 13th day of growth cycle, slight reduction in lipid and β-carotene contents of biomass is seen in both control and test experiments. This could be attributed to the prevalent death phase of microalgal cells after 13th day of growth cycle.

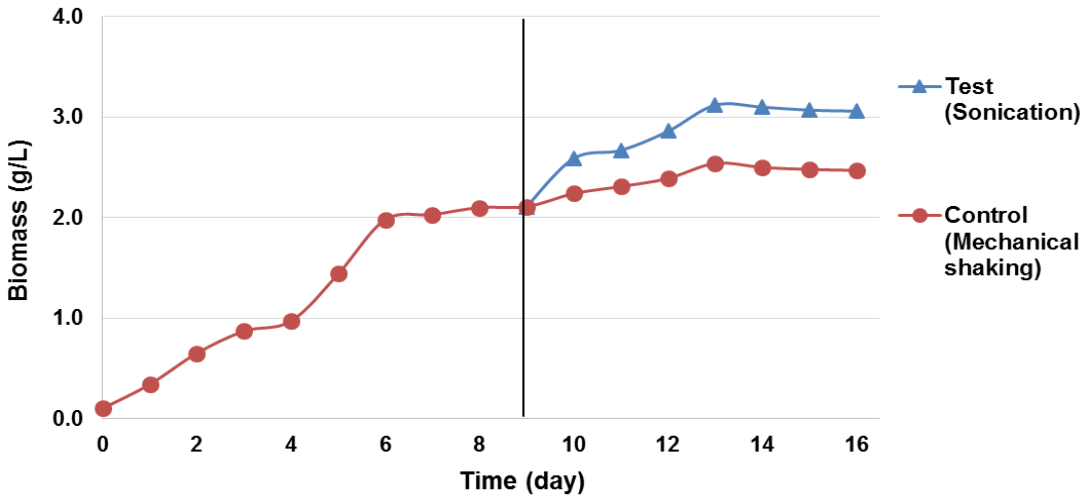

(A)

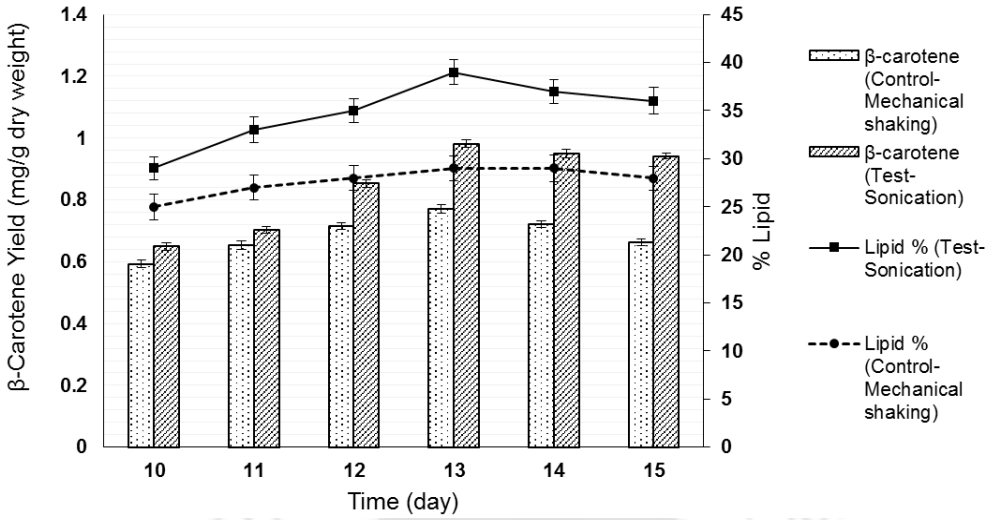

(B)

Figure 3.1 (A) Biomass growth profiles in control and test experiments. (B) Trends in β-carotene yield and % lipid in control and test experiments (sonication was applied from 10th day of growth cycle)

3.4.2 Kinetic analysis of experimental profiles

The experimental and simulated profiles of biomass, substrate, lipids and β-carotene in control and test experiments are shown in Fig. 3.2. The regression coefficients for all simulated profiles are > 0.8 indicating good fitness of the model. It may be noted that profiles shown in Fig. 3.2 are for the period day 10 to day 16, as the sonication was applied after 10th day of the growth cycle.

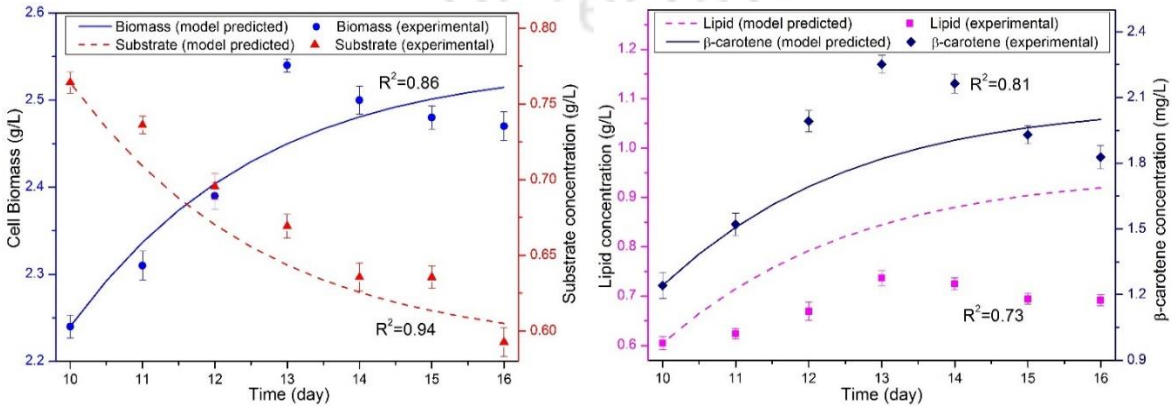

(A) (B)

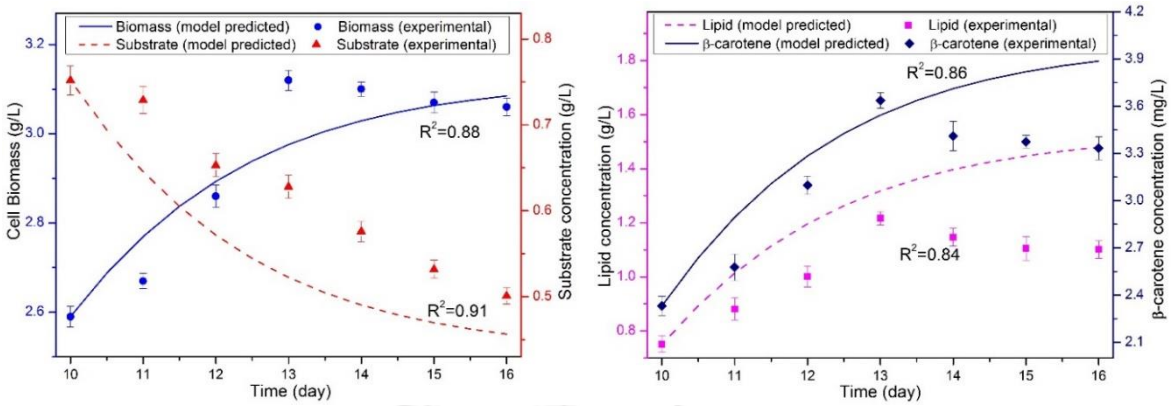

(C) (D)

Figure 3.2. Experimental and model predicted time profiles of biomass, substrate, lipid and β-carotene during growth of *T. obliquus* SGM19 for initial substrate concentration of 1.5 g/L. (A, B) Control (only mechanical shaking); (C, D) Test (mechanical shaking with sonication at 10% duty cycle)

The kinetic model was fitted to the profiles in control and test experiments so as to get physical insight into the influence of sonication on microalgal growth and the concurrent lipid and β-carotene yields. The values of the kinetic parameters obtained after fitting of the experimental profiles to the model are listed in Table 3.2.

Table 3.2. Values of parameters obtained after fitting of kinetic model to experimental profiles

Parameters	Control	Test
	Biomass	
μ_m (d^{-1})	0.43	0.48
	Substrate	
$Y_{x/s}$ (g g^{-1})	9.13	10.10
m (g g^{-1} d^{-1})	2.1×10^{-4}	1.1×10^{-4}
	Lipid	
α_1	1.13	1.46
β_1 (d^{-1})	2.2×10^{-4}	2.8×10^{-4}
$(Y_{p/s})_1$ (g g^{-1})	7.82	8.46
	β -carotene	
α_2	2.74	3.13
β_2 (d^{-1})	2.9×10^{-4}	3.2×10^{-4}
$(Y_{p/s})_2$ (mg g^{-1})	8.86	9.81

Rise in μ_m under test conditions shows that sonication enhances biomass growth. This is also reflected in higher yield coefficient $Y_{x/s}$ in test experiments. For both lipids and β-carotene, the growth-associated product formation coefficients (α_1 and α_2) are several orders of magnitude higher than non-growth (or stationary phase) associated coefficients (β_1 and β_2). This feature is consistent in both control and test experiments. Nonetheless on comparative basis, values of α_1 and α_2 are higher for test experiments, which indicates enhanced metabolism. This feature is also reflected in terms of higher yield coefficients $(Y_{p/s})_1$ and $(Y_{p/s})_2$ for both products in test experiments. Thus, in summary, the values of kinetic parameters in control and test experiments clearly suggest intensification of cell metabolism induced by sonication.

3.4.3 Microassay of NAD(H)

To further ascertain the influence of sonication on metabolism of green microalgae, the total concentration of NAD^+ and NADH in the microalgal cells was determined in both control and test experiments. The protocol followed for NAD^+/NADH estimation is noted earlier in section 3.2.6. This parameter is essentially a marker of the kinetics of metabolism in microalgal cells. Prior to discussion on trends in NAD^+/NADH concentrations in control and test experiments, the metabolic pathways in green microalgae's different organelles are outlined here. Fig. 3.3 depicts the major metabolic pathways in cytoplasm, mitochondria, plastid and endoplasmic reticulum leading to formation of lipids and β-carotene.

As CO_2 enters plastid, it gets converted to glyceraldehyde-3-phosphate (G3P) through Calvin cycle. This G3P is utilized by cells in many pathways. In one pathway, it gets converted to pyruvate facilitating formation of acetyl-CoA by pyruvate dehydrogenase complex. This is one major step for lipid production. Acetyl CoA is then

converted to malonyl-CoA which is used for fatty acid synthesis. This conversion helps in formation of free fatty acids that move to endoplasmic reticulum via cytosol for conversion to triacylglycerols and are stored in the form of lipid bodies. Some G3P is converted to sugars which moves to cytosol and get stored. The cells break these sugars to glucose for generating energy. Thus, glycolysis results in ATP, NAD^+ and pyruvate formation that enters into the mitochondria where it is converted to acetyl CoA. This acetyl coA enters citric acid cycle and forms citrate which elutes out in cytosol to enter endoplasmic reticulum as PUFAs. In endoplasmic reticulum the free fatty acids react with glycerol to form triacylglycerols.

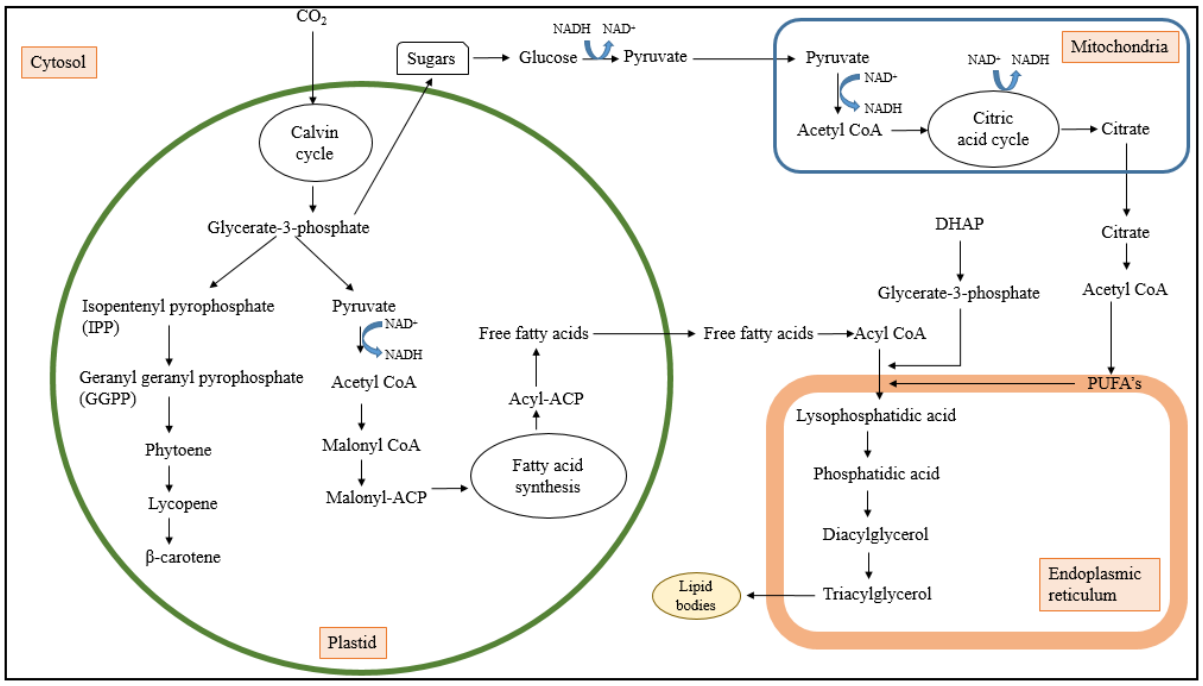

Figure 3.3. Schematic of major metabolic pathways of triacylglycerol (TAG) and β-carotene synthesis in green microalgae in different organelles, viz. cytosol, plastid, mitochondria and endoplasmic reticulum [adopted and redrawn from refs. Chen and Smith, 2012; Mondal, 2017; Radakovits et al., 2010; Sun et al., 2018; Zhu et al., 2016]

Biosynthesis of carotenoids commences with formation of isopentanyl pyrophosphate (IPP), a common precursor for synthesis of all isoprenoids from G3P.

Acetyl CoA synthesizes IPP via mevalonic acid which further reacts with dimethyl allyl pyrophosphate (DMAPP) to form geranyl geranyl pyrophosphate (GGPP). When two molecules of GGPP react they form phytoene which undergoes series of desaturation reactions to form lycopene. Lycopene undergoes cyclization by lycopene-β-cyclases which add two β–rings at the ends to form β-carotene. Transfer of electron between oxidized form NAD^+ and its reduced state, NADH is an essential transformation accompanying enzymatic reactions of all segments of metabolic pathway of microalgae, viz. citric acid cycle, glycolysis and regeneration of ADP to ATP.

In order to get insight into kinetics of intracellular metabolism of green algae in control and test conditions, the total concentrations of NAD(H) (and not for the oxidized and reduced forms separately) has been determined. Fig. 3.4 shows the profiles of NAD(H) concentrations in control and test experiments. Although the profiles of NAD(H) in both control and test experiments do not show any distinct profile, the total NAD(H) concentration in test experiment is consistently higher than control experiments – indicating relatively faster metabolism. The highest difference of 0.7 µg/g DCW between NAD(H) concentrations in control (2.9±0.1 µg/g DCW) and test (3.7±0.2 µg/g DCW) experiments is observed on 11^{th} day of growth cycle. At the end of experiments on 15^{th} day the values where 2.9±0.2 µg/g DCW in control and 3.3±0.1 µg/g DCW in the test samples.

The enhanced metabolism of the microalgal cells can be explained on the basis of following hypotheses, which need further experimental confirmation: (1) enhanced transport of substrate and other nutrient across cell membrane, and (2) enhancement in the activities of the intracellular enzymes – which could possibly result from conformational changes in the secondary structure that leads to unfolding of enzyme proteins [as demonstrated by Agarwal et al., 2016; Dikshit et al., 2018].

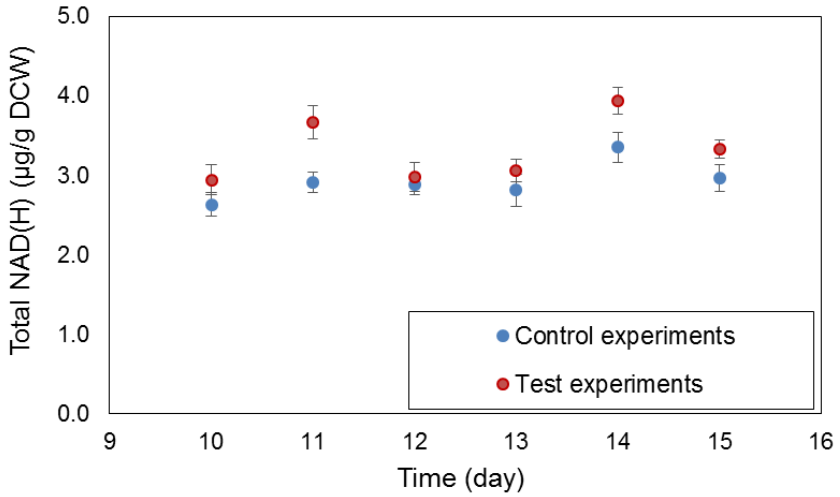

Figure 3.4. Profiles of total NAD(H) concentration in control and test experiments

3.4.4 Viability assessment through Flow cytometry

To determine the viability of microalgal cells exposed to sonication, the control and test samples were examined with flow cytometric analysis. It may be noted that only the dead cells in the samples were stained using propidium iodide. The plots of FL1-H vs FL3-H are shown in Fig. 3.5.

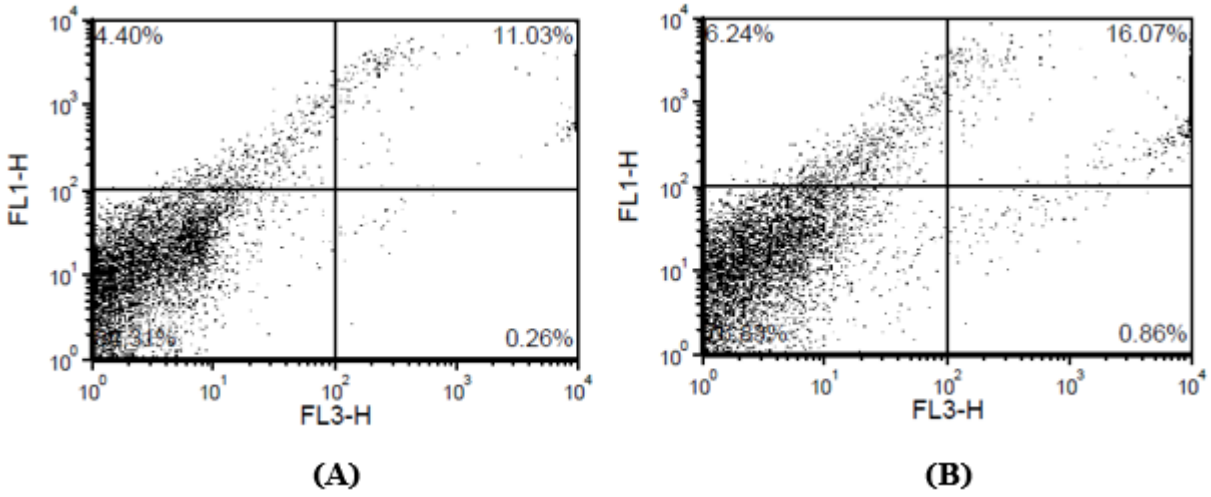

Figure 3.5. Viability assessment of *T. obliquus* SGM19 cells after exposure to ultrasound by Flow cytometry. (A) and (B) show acquisition dot plots of FL1 vs. FL3 for *T. obliquus* SGM19 in control and test samples, respectively

The upper right quadrant shows the percentage of damaged cells and lower right quadrant denote the dead cells. The lower left quadrant shows the unstained cells. It can be seen that the percentages of dead cells are 0.26% and 0.86% in control and test experiments; whereas the percentages of damaged cells are 11.03% and 16.07% in control and test experiments, respectively. These results indicate that the morphology of the microalgal cells remains undisturbed after exposing cells to sonication for short durations (10% duty cycle) and there is no marked adverse effect of sonication on the cells.

3.5 Conclusion

The results presented in this chapter have demonstrated the influence of sonication in enhancing the lipid and β-carotene yields from microalgal species of *T. obliquus* SGM19. Statistical optimization of media components using Placket-Burman method followed by central composite design resulted in identification of two major components, viz. $NaNO_3$ and EDTA. The operational parameters such as pH, temperature and light intensity were also optimized using statistical tool of central composite design. Optimum initial substrate (nitrate) concentration for maximum growth and product yield was 1.5 g/L. For 10% duty cycle sonication applied for last 6 days of growth cycle (corresponding to late log phase), the increments in lipid and β-carotene synthesis were 34.5% and 31.5% respectively. Intracellular NAD(H) concentrations were consistently higher in test experiments – confirming faster metabolism induced by sonication. Kinetic analysis revealed significant rise in maximum specific growth rate with sonication, and also that both lipid and β-carotene were growth associated products.

References

Agarwal M., Dikshit P.K., Bhasarkar J.B., Borah A.J., Moholkar V.S., 2016. Physical

Insight into Ultrasound–Assisted Biodesulfurization using Free and Immobilized Cells of *Rhodococcus rhodochrous* MTCC 3552. Chem.Eng. J. 295, 254–267.

APHA, 1998. Standard Methods for the Examination of Water and Wastewater, 20th ed. American Public Health Association, Washington, DC, USA.

Bligh E.G., Dyer W.J., 1959. A rapid method of total lipid extraction and purification. Can. J. Biochem. Physiol. 37, 911–917.

Chen J.E., Smith A.G., 2012. A look at diacylglycerol acyltransferases (DGATs) in algae. J. Biotechnol. 162, 28–39.

Chew K.W., Yap J.Y., Show P.L., Suan N.H., Juan J.C., Ling T.C., Lee D.J., Chang J.S., 2017. Microalgae biorefinery: high value products perspectives. Bioresour. Technol. 229, 53-62.

Del Campo J., García-González M., Guerrero M., 2007. Outdoor cultivation of microalgae for carotenoid production: current state and perspectives. Appl. Microbiol. Biotechnol. 74 (6), 1163-1174.

Desikachary T.V., 1959. Cyanophyta. Indian Council of Agricultural Research, New Delhi, India.

Dikshit P.K., Kharmawlong G.J., Moholkar V.S., 2018. Investigations in sonication-induced intensification of crude glycerol fermentation to dihydroxyacetone by free and immobilized *Gluconobacter oxydans*. Bioresour. Technol. 256, 302–311.

Gaden E.L., 2000. Fermentation process kinetics. Biotechnol. Bioeng. 67: 629–635.

Lorenz R.T., Cysewski G.R., 2000. Commercial potential for *Haematococcus* microalgae as a natural source of astaxanthin. Tre. Biotechnol. 18, 160-167.

Luedeking R., Piret E.L., 1959. A kinetic study of the lactic acid fermentation: batch process at controlled pH. J. Biochem. Microbiol. Technol. Eng. 1, 363–394.

Mishra S., Singh N., Sarma A.K., 2015. Assessment of a Novel Algal Strain

Chlamydomonas debaryana NIREMACC03 for Mass Cultivation, Biofuels Production and Kinetic Studies. Appl. Biochem. Biotechnol. 176(8), 2253-2266.

Misra R., Guldhe A., Singh P., 2014. Electrochemical harvesting process for microalgae by using nonsacrificial carbon electrode: a sustainable approach for biodiesel production. Chem. Eng. J. 255, 327–33.

Mondal P., 2017. Waste to Energy Conversion, Video Course, National Program on Technology Enhanced Learning, Govt. of India. (http://nptel.ac.in). Accessed June 2019.

Nisselbaum J.S., Green S., 1969. A Simple Ultramicro Method for Determination of Pyridine Nucleotides in Tissues. Anal. Biochem. 27, 212-217.

Ormerod M.G., 1990. Analysis of DNA. General methods. In: Ormerod, M.G. (Ed.), Flow Cytometry. A Practical Approach. Oxford University Press, Oxford, pp. 69–87.

Patias L.D., Fernandes A.S., Petry F.C., Mercadante A.Z., Jacob-Lopes E., Zepka L.Q., 2017. Carotenoid profile of three microalgae/cyanobacteria species with peroxyl radical scavenger capacity. Food Res. Int. 100, 260-266.

Radakovits R., Jinkerson R.E., Darzins A., Posewitz M.C., 2010. Genetic Engineering of Algae for Enhanced Biofuel Production. Eukaryot. Cell 9(4), 486-501.

Rao C.S., Sathish T., Brahamaiah P., Kumar T.P., Prakasham R.S., 2009. Development of a mathematical model for *Bacillus circulans* growth and alkaline protease production kinetics. J. Chem. Technol. Biotechnol. 84, 302–307.

Sankaran R., Manickam S., Yap Y.J., Ling T.C., Chang J.S., Show P.L., 2018. Extraction of proteins from microalgae using integrated method of sugaring-out assisted liquid biphasic flotation (LBF) and ultrasound. Ultrason. Sonochem. 48, 231-239.

Singh S., Agarwal M., Sarma S., Goyal A., Moholkar V.S., 2015. Mechanistic insight

into ultrasound induced enhancement of simultaneous saccharification and fermentation of *Parthenium hysterophorus* for ethanol production. Ultrason. Sonochem. 26, 249-256.

Spolaore P., Joannis-Cassan C., Duran E., Isambert A., 2006. Commercial Applications of Microalgae. J. Biosci. Bioeng. 101(2), 87-96.

Sun X.M., Ren L.J., Zhao Q.Y., Ji X.J., Huang H., 2018. Microalgae for the production of lipid and carotenoids: a review with focus on stress regulation and adaptation. Biotechnol. Biofuels 11:272.

Szyjka S.J., Mandal S., Schoepp N.G., Tyler B.M., Yohn C.B., Poon Y.S., Villareal S., Burkart M.D., Shurin J.B., Mayfield S.P., 2017. Evaluation of phenotype stability and ecological risk of a genetically engineered alga in open pond production. Algal Res. 24, 378-386.

Tizazu B.Z., Roy K., Moholkar V.S., 2018. Mechanistic investigations in ultrasound-assisted xylitol fermentation. Ultrason. Sonochem. 48, 321-328.

Yang J.S., Huang J.X., Ni J.R., 2006. Mathematical modeling of batch fermentation of *Zoogloea* sp. GY3 used for synthesizing polyhydroxyalkanoates. J. Chem. Technol. Biotechnol. 81, 789–793.

Zhao X., Condruz S., Chen J., Jolicoeur M., 2016. A quantitative metabolomics study of high sodium response in *Clostridium acetobutylicum* ATCC 824 acetone-butanol-ethanol (ABE) fermentation. Sci. Rep. 6, 28307.

Zhu L.D., Li Z.H., Hiltunen E., 2016. Strategies for Lipid Production Improvement in Microalgae as a Biodiesel Feedstock. Biomed Res. Int. (http://dx.doi.org/10.1155/2016/8792548).

भारतीय प्रौद्योगिकी संस्थान गुवाहाटी
Indian Institute of Technology Guwahati

CHAPTER 4

In-situ TRANSESTERIFICATION OF *T. obliquus* SGM19 BIOMASS FOR BIODIESEL SYNTHESIS

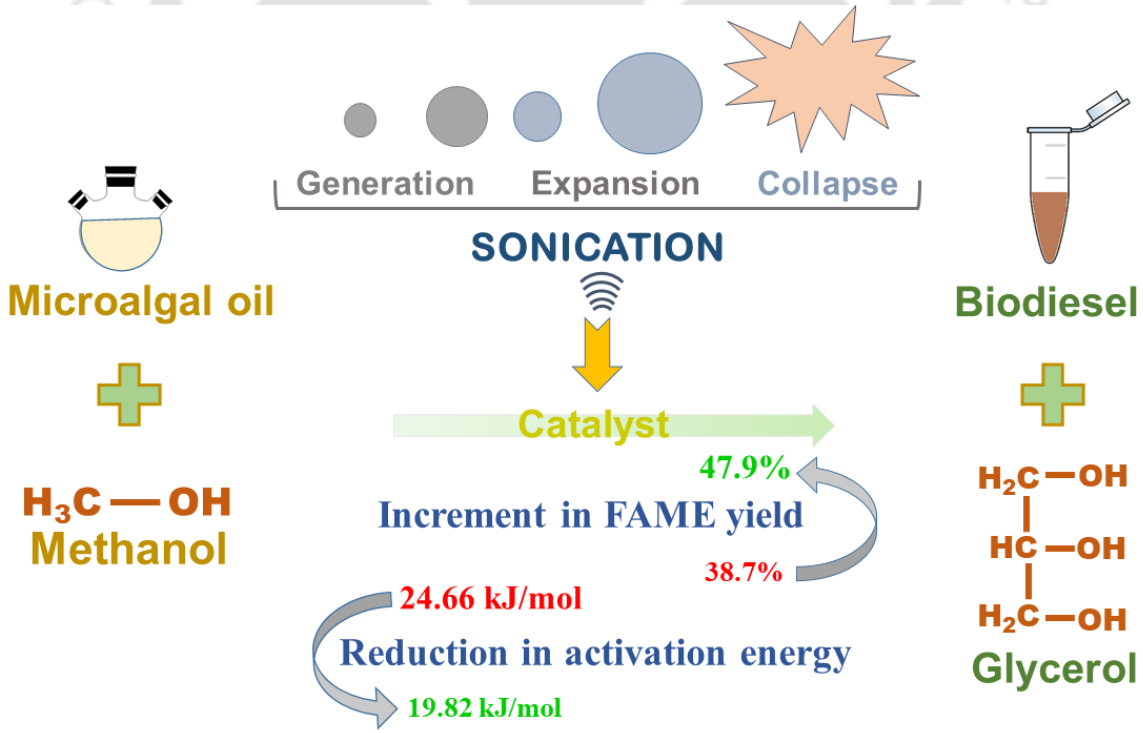

CHAPTER 4

In-situ Transesterification of *T. obliquus* SGM19 Biomass for Biodiesel Synthesis

4.1 Introduction

The global biodiesel production as green alternative fuel has seen significant growth owing to its renewable and eco-friendly nature (Selvarajan et al., 2016). Therefore, various new and cheap feedstocks for commercial biodiesel production have been explored starting with 1st generation (edible oil crops such as canola, corn), 2nd generation (non-edible oil crops such as *Jatropha curcus*, Karanja, rubber seed etc.) and finally 3rd generation (microalgal lipids) (Salam et al., 2016). Biodiesel derived from microalgae has major potential due to its distinct capabilities of higher photosynthetic efficiency and higher specific growth rate as compared to plants (Zepka et al., 2008). Additionally, the microalgal biodiesel production, unlike other oil crops, do not compete with agriculture, feed, food or other industries (Sivagurulingam et al., 2019).

The economy of the microalgal biodiesel production depends mainly on the lipid content of the microalgal strain as it reveals the energy yield from the microalgal biomass

(Davis et al., 2011). Hence, it is utmost important to select the most suitable microalgal strain for given climatic conditions, optimize its growth conditions, lipid extraction and transesterification process to obtain the maximum biodiesel production. However, lipid extraction from the microalgal biomass is key bottleneck in the commercialization of microalgal biodiesel production. Yang et al. (2015) reported the total energy inputs as 13%, 85% and 2% for biomass production, lipid extraction and transesterification process, respectively. The conventional lipid extraction methods require dry microalgal biomass, as the water residues in wet biomass causes mass transfer limitations, thus decreasing the lipid extraction efficiency (Yang et al., 2015). It has been also reported that the total energy input of the drying of microalgal biomass alone accounts up to 85-90% of the energy input for the extraction process (Biz et al., 2019), thus, obstructing the commercialization of the microalgal biodiesel. Moreover, the lipid extraction from biomass is also hindered due to the small size of the microalgae and the roughness of the complex structure of its cell wall (Johnson and Wen, 2009). Additional pretreatment of biomass (chemical or physical) to facilitate lipid extraction may increase the overall cost of process. Microalgal biodiesel can also be produced by *in situ* transesterification. *In situ* transesterification eliminates requirement of lipid extraction, thus reducing the overall steps in process, the process time, and requirement of extraction solvents. Previous authors have addressed the matter of new techniques of biodiesel synthesis from microalgae. Johnson and Wen (2009) have reported fatty acid methyl ester (FAME) synthesis by single-step direct transesterification of *Schizochytrium limacinum*. Griffiths et al. (2010) described a two stage sequential direct transesterification for 3 algal strains (viz. *Chlorella vulgaris*, *Scenedesmus* sp., *Nannochloropsis* sp.) with higher FAME yield. Salam et al. (2016) have reported *in situ* transesterification of biomass of *Nannochloropsis occulata* using different catalysts.

In this chapter, we have presented results of studies in direct or in-situ

transesterification of biomass of *T. Obliquus*. The major components of this study are: (1) selection of initial condition of microalgal biomass (wet or lyophilized) for different protocols of transesterification (viz. conventional technique of lipid extraction followed by transesterification, single-step *in-situ* and 2-step *in-situ*), (2) statistical optimization of the process parameters with central composite design, (3) transesterification reaction in presence of sonication, and (4) kinetic analysis of the process, FAME profiling with GC-MS analysis, and characterization of the resultant biodiesel.

4.2 Materials and Methods

4.2.1. Microalgal biomass preparation

The culture of *Tetradesmus obliquus* SGM19 was incubated in 500 mL Erlenmeyer flask having 200 mL BG11 medium in an incubator shaker at 28.5°C with continuous shaking at 150 rpm and illumination of 5000 lux with a 12:12 h light:dark cycle for 15 days. 0.5 vvm atmospheric air was provided continuously in the flask for uniform mixing with a pump. The dissolved oxygen (DO) content of microalgal culture was monitored by DO meter (Make: Thermo Scientific, Model: Eutech DO 700) which was close to saturation (8±0.5 ppm) for the entire cycle. After attaining the stationary phase, the microalgal cells were centrifuged for 10 min at 10,000 rpm for harvesting. The biomass was washed with saline and stored as wet and lyophilized. The wet biomass comprised of air-dried cells with approximately 80% water content whereas the lyophilized cells had approximately 20% water content (w/w).

4.2.2. Selection of biomass type and transesterification method

For the synthesis of FAME (or biodiesel) from the microalgal biomass, fourteen different combinations of biomass type (or conditions) and transesterification protocol, as

shown in Table 4.1, were attempted to obtain the best combination for the highest FAME yield. The conventional protocol for FAME synthesis from microalgae comprises of lipid extraction using Bligh and Dyer method (1959) followed by transesterification of the extracted lipids, whereas the *in-situ* process involves direct transesterification of the microalgal biomass. In each process, both wet and equivalent lyophilized biomass were used with a different catalyst. In a reflux setup, the transesterification reaction was conducted for 1 hour. In a round bottom flask on a magnetic stirrer, 250 mg of the microalgal lipid/biomass was reacted with the solvent (1:20 molar ratio) and catalyst (1.5 wt%) with following parameters: solvent – methanol, catalysts - acid (H_2SO_4) and/or base (NaOH), temperature - 90°C. After the completion of the cycle, the FAME was collected by using hexane. The sample was washed thoroughly with distilled water for separation of glycerol and removal of catalyst. The best combination for transesterification process was selected based on FAME yield (% w/w).

4.2.3. Statistical optimization of transesterification process parameters

From Table 4.1, it can be concluded that the lyophilized biomass in all the cases, exhibited more FAME yield as compared to the wet biomass. The maximum FAME yield was obtained in base-catalyzed single step *in-situ* transesterification of the lyophilized biomass. Hence, the process parameters for biodiesel production from lyophilized biomass using single-step *in-situ* transesterification were statistically optimized using central composite design with the FAME yield as the response as shown below in Table 4.2. The four major parameters selected were catalyst loading, reaction temperature, duration and ratio of methanol to biomass. Data analysis was done using MINITAB (Trial Version, Release 15.1, PA, USA).

Table 4.1. Different transesterification process performed with different catalyst and biomass of *Tetradesmus obliquus* SGM19

Process	Biomass	Catalyst	FAME yield (% w/w)
Conventional	Lipid from wet biomass	Base (NaOH)	22.3
		Acid (H_2SO_4)	21.4
		Acid + Base	25.8
	Lipid from lyophilized biomass	Base (NaOH)	35.9
		Acid (H_2SO_4)	31.5
		Acid + Base	29.7
Single step *in-situ*	Wet biomass	Base (NaOH)	31.5
		Acid (H_2SO_4)	30.6
	Lyophilized biomass	Base (NaOH)	37.5
		Acid (H_2SO_4)	31.1
Two step *in-situ*	Wet biomass	Acid + Base	26.6
		Base + Acid	27.6
	Lyophilized biomass	Acid + Base	34.2
		Base + Acid	30.7

Table 4.2. Factors and levels used in Central composite design matrix

Factors	Levels	
	Low (-1)	High (+1)
(X_1) – Catalyst loading, wt% biomass	1	2
(X_2) – Methanol to biomass ratio (v/w)	30	60
(X_3) – Temperature (°C)	50	90
(X_4) – Reaction Time (min)	20	60

The Central composite design consisted of 30 experimental sets for 4 factors (parameters). The details of each experimental set are given in Table 4.3. Each transesterification experiment was conducted in batch mode.

Table 4.3. Full factorial central composite design matrix and the response FAME yield

Catalyst loading (% wt biomass)	Methanol to biomass ratio (v/w)	Temperature (°C)	Time (min)	FAME yield (%)	Predicted yield (%)
1.5	75	70	40	35.1	34.58
1.5	45	30	40	30.9	32.29
1.5	15	70	40	27.8	31.24
1.5	45	110	40	26.7	27.23
1.5	45	70	0	5.6	7.03
2.5	45	70	40	35.7	36.71
1.5	45	70	40	33.4	33.41
1.5	45	70	80	15.2	14.69
0.5	45	70	40	26.7	27.11
1.5	45	70	40	37.1	33.41
2	30	90	20	24.4	24.00
2	60	90	20	36.3	35.77
1	60	90	60	28.7	29.05
1	30	50	20	27.9	27.29
1.5	45	70	40	36.3	36.40
2	30	90	60	30.3	29.84
2	30	50	60	40.8	40.72
1.5	45	70	40	35.1	36.40
1	30	50	60	35.8	35.67
2	60	50	20	27.2	27.20
1	60	50	20	25.6	25.40
1	30	90	60	22.3	22.04
1	60	90	20	31.4	31.22
1.5	45	70	40	35.2	36.40
2	30	50	20	31.9	30.89
1	30	90	20	18.5	17.65
2	60	90	60	34.7	35.05
2	60	50	60	30.3	30.49
1	60	50	60	27.1	27.24
1.5	45	70	40	35.3	36.40

4.2.4. Ultrasound-assisted transesterification process

To further enhance the FAME yield, ultrasound-assisted transesterification approach was used. Therefore, the effect of ultra-sonication was studied on the transesterification process by carrying out the experiments at optimum parameters predicted by the statistical

optimization in section 4.2.3. In ultrasound-assisted transesterification, the normal mechanical shaking (control) was replaced with sonication (test). In the control experiments, a magnetic stirrer (Make: Tarson, Model: MC–02) was used to provide mechanical shaking. The test transesterification experiments were conducted using 30 cm × 15 cm × 10 cm ultrasound bath (PCi Analytics, India, 3.5 L), having 100 W power rating and 33 kHz frequency. The pressure amplitude of sonication and actual energy dissipation in bath was determined using calorimetric techniques as 1.4 bar. The transesterification experiments were done in 25 mL round bottom flask attached to coiled condenser for methanol reflux. The temperature was maintained by a circulating water bath. The flask position in the bath was maintained vigilantly as there was significant spatial variation in pressure amplitude of ultrasound in bath (Gogate et al., 2002). To confirm reproducibility of results, experiments were performed in triplicates.

4.2.5. Analysis of kinetic and Arrhenius parameter

The time profiles of FAME was determined by collecting aliquots of reaction mixture at 10 min intervals from 10 to 50 min and analyzing FAME by gas chromatograph–mass spectrometer (GC–MS). The kinetic parameter (rate constant) for the transesterification reactions was determined by fitting the time profiles of FAME conversion to pseudo first order kinetic model. The kinetic expression for pseudo first order reaction is:

$$\ln(1-X) = -kt \qquad [4.1]$$

Notations: X - methyl ester concentration, k - kinetic constant of pseudo first order, t - time.

The rate constant was obtained by plotting a graph between ln(1-X) and t. For calculating Arrhenius parameter (activation energy), rate constant of transesterification

reaction was obtained at 40°, 50° and 60°C. Kinetic expression used to determine the activation energy is as follow:

$$k = A\exp\left(\frac{-E_a}{RT}\right) \quad [4.2]$$

Notations: k - rate constant (time^{-1}), A - pre-exponential coefficient (time^{-1}), E_a - activation energy (kJ mol^{-1}), R - universal gas constant (J mol^{-1} K^{-1}), T - temperature (K)

4.2.6. Analysis of FAME/biodiesel obtained from microalgal biomass

The composition of the resultant FAME was determined by GC–MS with a Clarus 680, Perkin Elmer, USA gas chromatograph using 60 m × 0.25 mm × 0.25 μm Elite-5MS capillary column with 5% diphenyl and 95% dimethylpolysiloxane stationary phase and a mass spectrometer (Clarus 600C, Perkin Elmer, USA). The peak identification involved NIST-2008 data analysis software.

As per the global standards, the principal biodiesel properties like cold filter plugging point (CFPP), cetane number (CN), higher heating value (HHV), iodine value (IV), kinematic viscosity (KV) and saponification value (SV) were determined as described previously.

4.3 Results and Discussion

4.3.1. Optimization of transesterification process parameters

The preliminary optimization of feedstock and process for transesterification showed the highest FAME yield in *in-situ* transesterification with lyophilized biomass and base catalyst. It can be seen that the FAME yield obtained in case of wet biomass is less as compared to lyophilized biomass. This could be attributed to the high water content in the wet biomass which restricts the reaction of the catalyst, thus, reducing the catalytic activity

and reduced FAME yield (Komers et al., 2001). In case of lyophilized biomass, the water content reduces drastically and thus higher FAME yield is obtained. The *in-situ* transesterification resulted in more FAME yield as compared to the conventional method. This could be due to insufficient lipid extraction. As described previously by Lotero et al. (2005), the acid catalyst has much lower transesterification efficiency as compared to base catalyst. Haas et al. (2004) also suggested base-catalyzed *in situ* transesterification rather than acid-catalyzed transesterification because of its low reagent requirement with mild reaction conditions.

CCD was used to optimize the four major transesterification reaction factors, viz. catalyst loading, methanol to biomass ratio, temperature and reaction time. The CCD generated a total of 30 runs. The experiments were performed accordingly, and the full factorial CCD matrix along with the experimental and predicted FAME yield (result) are shown in Table 4.3. The matrix data showed that the experimental FAME yield ranged from 5.6% to 37.1%. The coded values of both the optimization variables as well as the corresponding response variables obtained after execution of 30 runs were fitted into a quadratic model. The coefficients of the quadratic response model (interaction, square and linear) together with the *t*– and *p*– values of the coefficients are given in Table 4.4A. These coefficients of the quadratic response were calculated by regression analysis and were tested based on the significance of their *p*–value.

Table 4.4B given below depicts the ANOVA (analysis of variance) for quadratic model. A regression coefficient (R^2) value of 0.98 specifies that the experimental data and the quadratic model fits perfectly with each other. The result of analysis of variance showed that $p < 0.01$ for the regression model, thus making it significant. The $p > 0.05$ for the lack of fit makes it not significant. This result thus justifies the proper fitting of the quadratic model into the experimental data and that the probability of getting errors is very low. The

regression coefficients values, viz. R^2 = 0.98, predicted R^2 =0.91, adjusted R^2 =0.95, indicates that the model could be used to explain 98% variations in the response variable.

Table 4.4. Results of statistical analysis for transesterification process parameters optimization

A) Coefficient values, *t* and *p* values for each variable

Model term	Coefficient Estimate	Computed *t*-value	*p*-value
Constant	34.8442	57.791	0.000
Catalyst loading (CL)	2.3583	7.235	0.000
Methanol to biomass ratio (MB)	1.0	3.068	0.008
Temperature (T)	−1.1833	−3.63	0.003
Reaction time (RT)	1.9167	5.880	0.000
CL * CL	−0.3646	−1.196	0.252
MB * MB	−0.3021	−0.991	0.339
T * T	−0.9646	−3.163	0.007
RT * RT	−5.5646	−18.249	0.000
CL * MB	−0.45	−1.127	0.279
CL * T	0.6875	1.722	0.107
CL * RT	0.3625	0.908	0.379
MB * T	3.8625	9.675	0.000
MB * RT	−1.6375	−4.102	0.001
T * RT	−1.0	−2.505	0.025

R^2= 0.9771; Predicted R^2= 0.9061; Adjusted R^2= 0.9526

B) ANOVA for quadratic model

Source	Degree of Freedom	Sum of Squares	Mean Square	F-value	p-value Prob>F
Regression	14	1451.88	103.706	40.67	0.000
Linear	4	279.26	69.814	27.38	0.000
Square	4	862.12	215.529	84.52	0.000
Interaction	6	310.51	51.752	20.29	0.000
Residual Error	14	35.70	2.550		
Lack-of-fit	10	27.93	2.793	1.44	0.388
Pure Error	4	7.77	1.943		
Total	29	1561.73			

The optimal values of transesterification process parameters obtained by the statistical analysis that corresponded to maximum FAME yield, are: Catalyst loading –

1.5%, Methanol to biomass ratio – 30 v/w, Temperature – 50°C and Reaction time – 50 min. The lower FAME yield for low catalyst loading can be due to the insufficient amount of catalyst required to complete the reactions whereas the decreased yield at higher catalyst loading can be attributed by increased fatty acid salt formation (Liu et al., 2006). The optimum methanol to biomass ratio was at lower end, i.e., 30 v/w with decrease in FAME yield at higher methanol concentrations. The higher methanol concentration not only dilutes the catalyst concentration but also adds extra cost for recovery and purification of solvent (Patil et al., 2011).

The statistical analysis for optimization of transesterification process parameters for FAME production was validated by conducting the transesterification experiment using the optimum values obtained from the CCD analyses as explained previously. A maximum predicted FAME yield for these optimum parameters was 38.5 % w/w biomass. These values are illustrated in the desirability plot as shown in Fig. 4.1. The experimental FAME yield was 39.2 ± 1.1 %w/w, which is in proximity to the CCD predicted result. This result mainly infers that optimization of transesterification process parameters enhances the FAME yield.

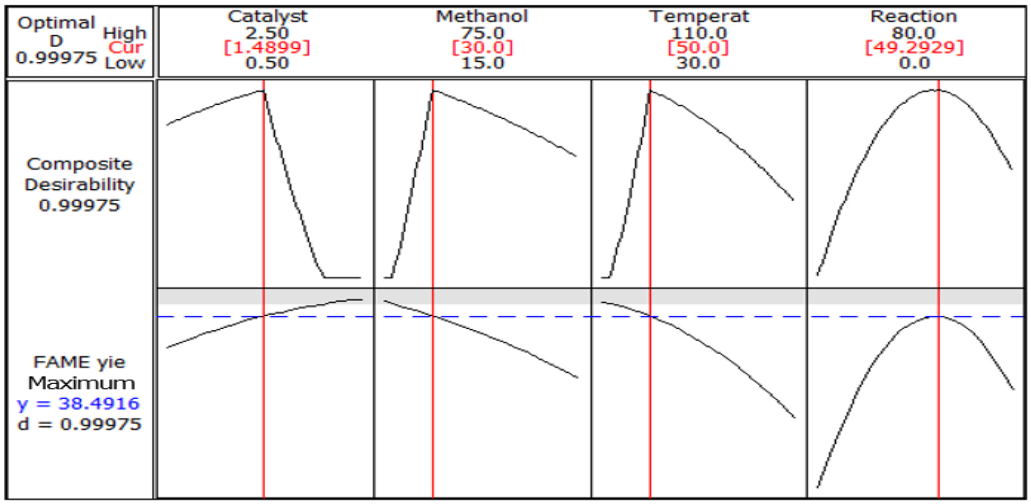

Figure 4.1. Desirability function plot depicting the optimum levels of transesterification process parameters

4.3.2. Ultrasound-assisted transesterification and analysis

As stated earlier in section 4.2.4, in the transesterification experiment, the mechanical shaking was replaced with sonication to study the effect of ultrasound on transesterification process. Accordingly, at the optimum transesterification conditions, i.e. catalyst loading – 1.5%, methanol to biomass ratio – 30 v/w, temperature – 50^{o}C and reaction time – 50 min, the normal mechanical shaking using magnetic stirrer (control) of the reaction was replaced with ultra-sonication (test). The FAME yield obtained in control and test experiments were 38.7% and 47.9%, respectively. Thus, the application of ultrasound enhances the FAME yield by approx. 24%.

To understand the effect of sonication in the biodiesel production process, the kinetic behavior was studied using the pseudo first order kinetic model. The overall rate constant was determined for both test and control experiments by fitting the time profiles to the model. A plot of ln(1-*X*) and *t* used for calculating the rate constants is shown below in Fig. 4.2A. The rate constants obtained were 0.0328 min^{-1} for mechanical shaking whereas 0.0469 min^{-1} for sonicated samples. This increase in the rate constant by application of ultrasound shows that the sonication enhances the rate of reaction, thus, enhancing the FAME yield.

The activation energy of the overall process was also estimated for test and control experiments by using the Arrhenius equation. As previously mentioned, for activation energy analysis, the rate constants of the transesterification reaction for both control and test were calculated at three temperatures, i.e., optimum temperature(50°C) and ± 10°C (40°C and 60°C) keeping the other parameters same in all the cases. The activation energies were calculated by plotting ln k vs 1/T. The Arrhenius plot is shown in Fig. 4.2B. From the Arrhenius plot, the overall activation energy for mechanical shaking was 24.66 kJ/mol wheras 19.82 kJ/mol for the sonicated samples. Hence, sonication reduces the overall

activation energy by 19.6%. The reduction in the activation energy with the application of ultrasound shows the effect of mass transfer on the transesterification reaction.

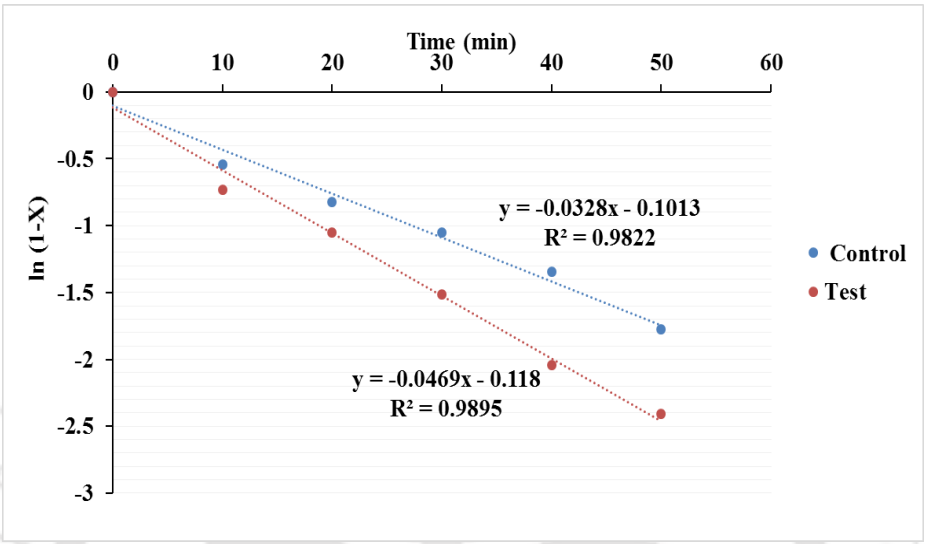

(A)

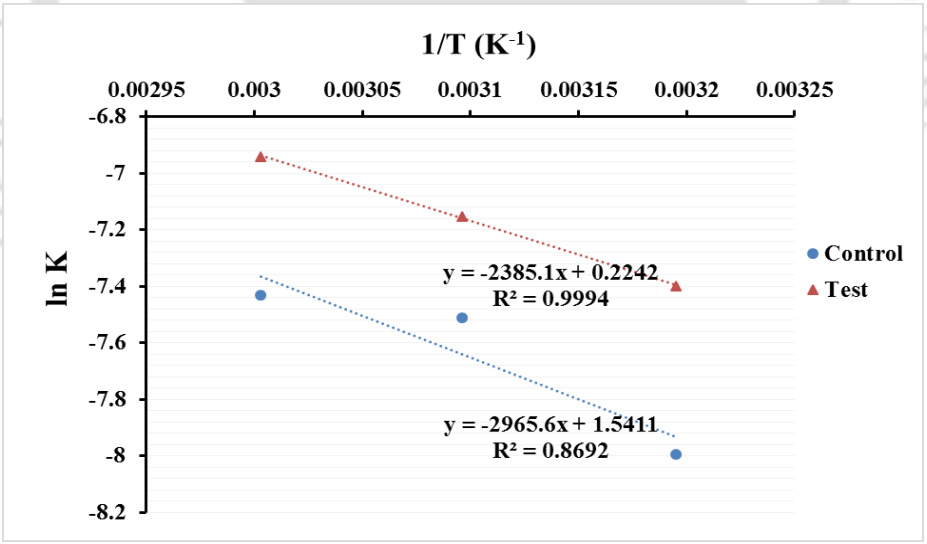

(B)

Figure 4.2. (A) Pseudo first order kinetic plot. (B) Arrhenius plot of overall transesterification process in test and control samples.

Sonication induces micro–mixing which enhances the gas–liquid mass transfer. This helps in enhanced oxygen uptake by the reaction mixture present over liquid surface

(Kumar et al., 2004). Sonication also instigates conformational changes in the secondary structure of enzymes by generating intense micro-turbulence and further boosting the metabolic kinetics (Dikshit and Moholkar, 2016). The above stated phenomena helps in the enhancement of FAME yield.

4.3.3. FAME quantification and evaluation of biodiesel properties

Biodiesel produced by ultrasound-assisted transesterification was analyzed for FAME profiles by GC-MS which showed esters of many fatty acids present in lipids of the microalga *Tetradesmus obliquus* SGM19. Table 4.5 lists the FAME percentage content based on their relative peak intensity in GC-MS spectrum.

Table 4.5. FAME profile obtained from ultrasound-assisted transesterification

Fatty acids	Concentration (% w/w)
C13:0	0.83
C14:1	1.76
C15:0	1.94
C15:1	1.03
C16:0	18.88
C16:1	1.11
C16:2	0.96
C17:0	8.41
C18:0	13.88
C18:1	4.27
C18:2	8.14
C18:3	14.95
C20:0	12.65
C20:5	1.59
C22:6	1.04
Total SFA	56.59
Total UFA	34.85

The total FAME percentage identified is approximately 91% with major fractions of C16 and C18 fatty acids like linoleic, oleic, palmitic, palmitoleic, and stearic. The other 9%

of the fatty acids/esters could not be identified due to comparatively smaller concentration. It is also important to study the fuel properties of the synthesized biodiesel to estimate its commercialization feasibility. Thus, the FAME profile of the synthesized biodiesel was used to estimate the few major fuel properties by using the empirical formula as described previously (Singh et al., 2020) and was compared to the ASTM D6751 standards for biodiesel. These fuel properties are higher heating value, cold filter plugging point, cetane number, iodine value, kinematic viscosity and saponification value and are listed below in Table 4.6. The properties are within the limits of ASTM D6751 standards.

Table 4.6. Estimated biodiesel properties

Property	Standard	This study
Saponification value (mg KOH/g)	370 (max)	236.37
Iodine value (g I_2/100 g)	120 (max)	97.93
Cetane number	47 (min)	47.35
Cold filter plugging point (°C)	+5 (max)	-15.30
Kinematic viscosity at 40°C (mm^2/s)	1.9 - 6.0	4.71
Higher heating value (MJ/kg)	40	45.84

4.4 Conclusions

The present study concludes that the lyophilized biomass using base-catalyzed *in-situ* transesterification process produces highest FAME yield of 37.5% (w/w DCW). The statistical optimization of the transesterification process parameters show the optimum conditions as catalyst loading = 1.5% (w/w biomass), methanol to biomass ratio = 30 (v/w), temperature = 50°C and time = 50 min. Replacement of mechanical shaking with sonication increases FAME yield from 38.7 to 47.9% but reduces the overall activation energy, showing the effect of mass transfer on the transesterification reaction. FAME profile with

ultrasound-assisted transesterification process also satisfies the biodiesel properties as per ASTM D6751 standards. Hence, the biodiesel produced by single step base-catalyzed ultrasound-assisted transesterification can be used as a mixture with petroleum diesel for commercialization without requiring any modifications in the diesel engine.

References

Biz A.P., Cardozo-Filho L., Zanoelo E.F., 2019. Drying dynamics of microalgae (*Chlorella pyrenoidosa*) dispersion droplets. Chem. Eng. Process. 138, 41−48.

Bligh E.G., Dyer W.J., 1959. A rapid method of total lipid extraction and purification. Can. J. Biochem. 8, 911−917.

Davis R, Aden A, Pienkos P.T., 2011. Techno-economic analysis of autotrophic microalgae for fuel production. Appl. Energy. 88, 3524–3531.

Dikshit P.K., Moholkar V.S., 2016. Optimization of 1,3–dihydroxyacetone production from crude glycerol by immobilized *Gluconobacter oxydans* MTCC 904. Bioresour. Technol. 216, 1058–1065.

Gogate P.R., Tatake P.A., Kanthale P.M., Pandit A.B., 2002. Mapping of sonochemical reactors: review, analysis, and experimental verification. AIChE Journal. 48(7), 1542−1560.

Griffiths M.J., Hille-van R.P., Harrison S.T.L., 2010. Selection of direct transesterification as the preferred method for assay of fatty acid content of microalgae. Lipids. 45, 1053−1060.

Haas M.J., Scott K.M., Marmer W.N., Foglia T.A., 2004. *In situ* alkaline transesterification: an effective method for the production of fatty acid esters from vegetable oils. J. Am. Oil Chem. Soc. 81, 83–89.

Johnson M.B., Wen Z.Y., 2009. Production of biodiesel fuel from the microalga *Schizochytrium limacinum* by direct transesterification of algal biomass. Energ.

Fuel. 23, 5179−5183.

Komers K., Machek J., Stloukal R., 2001. Biodiesel from rapeseed oil, methanol and KOH 2. Composition of solution of KOH in methanol as reaction partner of oil. Eur. J. Lipid Sci. Technol. 103(6), 359–362.

Kumar A., Gogate P.R., Pandit A.B., Delmas H., Wilhelm A.M., 2004. Gas–liquid mass transfer studies in sonochemical reactors. Ind. Eng. Chem. Res. 43, 1812–1819.

Liu Y.J., Lotero E., Goodwin J.G., 2006. Effect of water on sulfuric acid catalyzed esterification. J. Mol. Catal. A Chem. 245, 132−140.

Lotero E., Liu Y.J., Lopez D.E., Suwannakarn K., Bruce D.A., Goodwin J.G., 2005. Synthesis of biodiesel via acid catalysis. Ind. Eng. Chem. Res. 44, 5353–5363.

Patil P.D., Gude V.G., Mannarswamy A., Cooke P., Munson-McGee S., Nirmalakhandan N., Lammers P., Deng S., 2011. Optimization of microwave-assisted transesterification of dry algal biomass using response surface methodology. Bioresour. Technol. 102, 1399−1405.

Salam K.A., Velasquez-Orta S.B., Harvey A.P., 2016. Effect surfactant-assisted direct biodiesel production from wet *Nannochloropsis occulata* by *in situ* transesterification/reactive extraction. Biofuel Res. J. 9, 366–371.

Selvarajan R., Felföldi T., Sanniyasi E., Tekere M., 2016. Assessing the potential of some freshwater and saline microalgae as biodiesel feedstock. J. Biobased Mater. Bioenergy. 10, 1–13.

Singh N., Batghare A.H., Choudhury B.J., Goyal A., Moholkar V.S., 2020. Microalgae based biorefinery: assessment of wild fresh water microalgal isolate for simultaneous biodiesel and β-carotene production. Bioresour. Technol. Rep. 11, 100440. https://doi.org/10.1016/j.biteb.2020.100440.

Sivagurulingam A.P.A., Sivanandi P., Pandian S., Arumugamurthi S.S., Sircar A., 2019. Optimization and kinetic studies on biodiesel production from microalgae (Euglena sanguinea) using calcium methoxide as catalyst. Energ. Source. Part. A. 41(12),

1497–1507.

Yang F., Cheng C., Long L., Hu Q., Jia Q., Wu H., Xiang W., 2015. Extracting lipids from several species of wet microalgae using ethanol at room temperature. Energ. Fuel. 29, 2380−2386.

Zepka L.Q., Jacob-Lopes E., Goldbeck R., Queiroz M.I., 2008. Production and biochemical profile of the microalgae *Aphanothece microscopica Nägeli* submitted to different drying conditions. Chem. Eng. Process. 47(8), 1305–1310.

CHAPTER 5

CONCEPTUAL BIOREFINERY: SIMULTANEOUS SYNTHESIS OF MULTIPLE PRODUCTS FROM *T. obliquus* SGM19

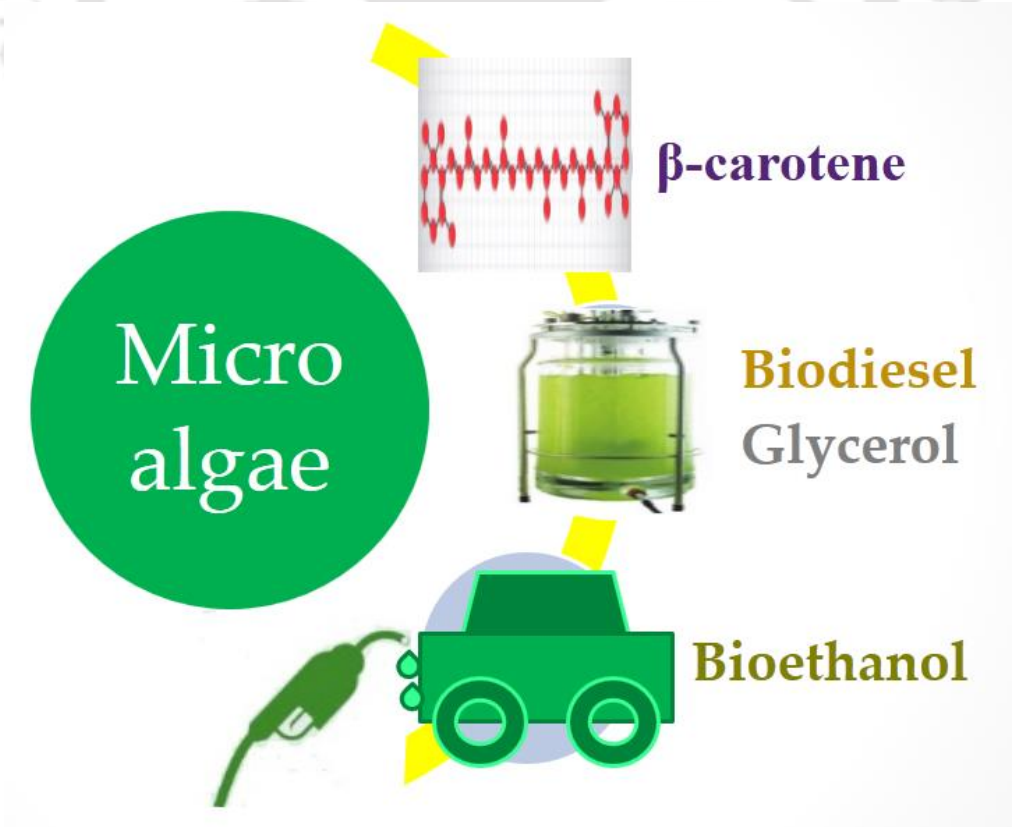

CHAPTER 5

Conceptual Biorefinery: Simultaneous Synthesis of Multiple Products from *T. obliquus* SGM19

5.1 Introduction

The daunting challenge of global warming and climate change risk due to emissions of greenhouse gases from various sources, such as vehicular exhausts, has driven research on liquid biofuels as alternate sources of energy for the greener transport sector (Behera et al., 2019; Panahi et al., 2019; Watts et al., 2019; Ubando et al., 2020). Biorefineries, which produce multiple biofuels and biochemicals from different feedstock through thermochemical and biochemical routes, have offered a simultaneous solution to both energy and environmental issues (Majidian et al., 2018; Panahi et al., 2019; Ubando et al., 2020). Environmental sustainability and financial viability of biorefineries is a major function of the feedstock. Conventional feedstock for biorefineries is lignocellulosic biomass, which is mainly available as agro-residues. In recent years, microalgal biomass is considered as alternate feedstock for biorefineries. Microalgae have higher potential of converting the solar energy to biochemical energy, as compared to terrestrial plants, as

they enclose an identical photosynthetic machinery (Chisti, 2013). Microalgae also have merits of high triacylglycerols content, large productivities per unit area of cultivation, and pliability for non-arable land cultivation. The lipid productivity of microalgae stands far higher than conventional non-edible oil crops. As reported by Vaknin et al. (2018), the total lipid yield from one hectare of microalgae cultivation is approx. 6.5 ton, which is almost 3 to 4× higher than the oil yield from plantation of non-edible oil crop of *Jatropha curcus* (1.5 to 2 tons).

Microalgal structure comprises of two components, viz. lipids and rest biomass, which are potential feedstock for biofuels production. Microalgae forms potential feedstock for different types of gaseous and liquid biofuels such as biodiesel (synthesized from microalgal lipids); biohydrogen and biomethane produced by digestion of algal biomass; and bioalcohols produced via fermentation of the hydrolyzates obtained from algal biomass (Shuba and Kifle, 2018; Vidyashankar et al., 2015). The biochemical composition of the microalgae (percentage contents of lipids and biomass/carbohydrates) can be modified by altering the physical parameters of growth such as light intensity and temperature. Oleaginous microalgae store carbon as lipids. Various strains of the microalgae have the ability to synthesise large quantities of lipids by changing the environmental conditions such as light, temperature and nutrient depletion (Khan et al., 2018). The composition of carbohydrates, proteins and lipids also varies with species. Fatty acids profile found in microalgal biomass belonging to same genus can vary significantly from species to species (Wang et al., 2014). The major fatty acids in microalgal lipids which can boost the quality and properties of biodiesel are saturated fatty acids (e.g. palmitic and stearic acid), and unsaturated fatty acids (e.g. linoleic, linolenic and oleic acid) (Islam et al., 2013; Ma et al., 2014).

In this chapter, we have described our studies on "conceptual biorefinery" based on biomass of *Tetradesmus obliquus* SGM19. The broad objective of this study is to design a *process package* (i.e. group or set of processes) for simultaneous valorization of the whole microalgal biomass with sequential synthesis of products. In essence, the present study has assessed the potential of *Tetradesmus obliquus* SGM19 biomass for synthesis of multiple products, viz. β-carotene, biodiesel, glycerol and bioethanol. Firstly, the wet microalgal biomass was subjected to acetone treatment for extraction of β-carotene. The left biomass was then lyophilized and used for transesterification. Both *in-situ* and 2-step transesterification procedures were used for comparison. After transesterification, biodiesel and glycerol were separated. The spent biomass after extraction of lipids or transesterification was hydrolyzed (acid as well as enzymatic), and the hydrolysate was fermented to produce bioethanol. Lastly, the properties of biodiesel synthesized from *T. obliquus* SGM19 were estimated from FAME composition and checked vis-à-vis the ASTM D6751 standards.

5.2 Materials and Methods

5.2.1 Microalgae and culture maintenance

The microalgal strains of *T. obliquus* SGM19 were maintained on BG-11 medium (pH 7.5) at a constant 28.5°C temperature in an incubator shaker. 100 mL of culture medium in a 250 mL conical flask was exposed to a 5000 lux light intensity with a 12L:12D cycle for 15 days. Lux meter was used to monitor the irradiance provided with white fluorescent tube lights. The experiments were conducted in triplicate independent cultures to confirm their reproducibility.

5.2.2 Extraction and estimation of β-carotene

A noted volume of microalgal sample was centrifuged for 10 min at 5000 rpm, and the collected biomass was put in acetone. The mixture was kept overnight at 4°C for complete extraction and was subsequently centrifuged for 5 min at 5000 rpm for separation of the extracted pigments. β-carotene analysis was done spectrophotometrically by plotting a standard curve at an absorbance of 450 nm.

5.2.3 Extraction of lipid

For lipid extraction, the modified Bligh and Dyer method was employed. The harvested cells were dried, grinded and powdered. All samples were extracted with sonication using 1 mL of chloroform/methanol in a ratio of 2:1 (v/v) followed by centrifugation. The pellets were subjected to re-extraction thrice with same chloroform/methanol mixture whereas the supernatants were collected together, filtered and evaporated to dryness until constant weight. Lipid yield was calculated based on the final and initial weight of sampling tubes.

5.2.4 Transesterification of lipids/microalgal biomass

Transesterification of the extracted lipids were performed by following a 2-step acid-base reaction reported by Mishra and Mohanty (2019). For *in-situ* transesterification, equal quantity of whole microalgal biomass was used. Briefly, 0.25 g extracted lipid/biomass was added to a 25 mL round bottom flask which is continuously immersed in a temperature controlled oil bath in a reflux setup. Methanol at 1:30 (molar ratio) was then added. The reaction was catalysed by NaOH (1.5 wt%) at 50°C for 50 min. The major parameters of the catalytic reactions like methanol to biomass ratio, reaction temperature, catalyst loading and reaction time were optimized in previous chapter. After

each reaction, fatty acid methyl esters (FAMEs) were obtained by using hexane. Glycerol and catalyst were recollected after washing with distilled water.

5.2.5 FAME analysis and Estimation of Glycerol

At optimized conditions, the resultant FAMEs were further analyzed for the profiles using gas chromatography–mass spectrometry (GC–MS). The GC-MS comprised of a gas chromatograph (Clarus 680, Perkin Elmer, USA) with capillary column (Elite-5MS, 60 m × 0.25 mm × 0.25 μm, stationary phase - 5:95 diphenyl:dimethylpolysiloxane) and a mass spectrometer (Clarus 600C, Perkin Elmer, USA). The peaks were identified using data analysis software NIST-2008. The by-product of the transesterification of lipids extracted from *T. obliquus* was glycerol, which was separated from biodiesel and purified by the protocol described of Xiao et al. (2013). The analysis for the presence of functional groups in the biodiesel obtained by transesterification of lipids was done using a Shimadzu Fourier transform infrared (FTIR) spectrophotometer (Model - IR-Affinity-1) from 500 to 4000 cm^{-1}.

5.2.6 Biodiesel properties

Principle properties of biodiesel were calculated based on fatty acid methyl esters (FAMEs) composition obtained by GC-MS. Previous literatures present few equations which are used to calculate the biodiesel properties values based on the FAME profiles and concentrations (Singh et al., 2020). These equations were implemented to calculate biodiesel properties as they produce data in close proximity with the standards defined by ASTM D6751. The equations were majorly used to calculate the saponification value (SV), cetane number (CN) and iodine value (IV) whereas the long-chain saturated factor

(LCSF) has direct correlation with Cold Filter Plugging Point (CFPP), which are related to saturation and FAME chain length.

5.2.7 Bioethanol production

Phenol-sulphuric acid mediated method was employed for carbohydrate estimation as illustrated by DuBois et al. (1956). The left biomass was first acid hydrolysed (concentrated sulphuric acid) to breakdown complex polysaccharides of microalgal biomass to simple sugars. The simple sugars were then fermented with *Saccharomyces cerevisiae* for bioethanol production. Bioethanol produced in fermented broth was collected with Tributyl phosphate (TBP) and was determined by protocol described by Seo et al. (2009).

5.3 Results and Discussion

5.3.1 Transesterification of extracted lipid/whole biomass

The lipid extracted from *T. obliquus* SGM19 biomass was 28 ± 1.2%. The lipid extracted from *T. obliquus* SGM19 biomass was then subjected to a 2-step acid-base catalyzed transesterification reaction to obtain biodiesel. In case of *in-situ* transesterification, the whole algal biomass was subjected to reaction. The feasibility of the biodiesel produced was estimated by studying the fatty acid composition contained in the esters with GC-MS. The spectrum of GC-MS provides the different peaks relative intensity. The major fatty acids in biodiesel from *T. obliquus* SGM19 were palmitic, oleic, linoleic and linolenic acids. C16 and C18 fatty acids formed major fractions in FAME, vis-à-vis the characteristics of an ideal biodiesel feedstock (Cheah et al., 2018).

Given below in Table 5.1 is the summarized comparative analysis of all the attributes from *T. obliquus* SGM19 biomass following both conventional and *in-situ*

transesterification procedures. It can be clearly seen that the amount of biodiesel produced through *in-situ* transesterification is more as compared to that of conventional. This could be attributed to the prevention of loss of lipids in *in-situ* process.

Table 5.1. A comparative analysis of different yields in conventional and *in-situ* transesterified bio-refinery

	Yields	
	Conventional	*in-situ*
Biomass (g/L)	3.13 ± 0.23	3.09 ± 0.27
β-carotene (mg/L)	3.65 ± 0.3	3.52 ± 0.26
Biodiesel (g/L)	0.78 ± 0.12	0.89 ± 0.15
Glycerol (g/L)	0.06 ± 0.04	0.08 ± 0.05
Bioethanol (g/L)	0.28 ± 0.11	0.38 ± 0.1
Lipid (g/L)	1.13 ± 0.19	-
Carbohydrate (g/L)	0.59 ± 0.15	0.8 ± 0.21

5.3.2 Biodiesel characterization

The concentrations of FAMEs obtained for the synthesized biodiesel were used in equations previously described to obtain the biodiesel attributes. Table 5.2 illustrates the biodiesel properties of the synthesized biodiesel by *in-situ* transesterification along with the ASTM standards. It could be clearly seen that the properties of the synthesized biodiesel are within the limits of the ASTM standards making it suitable for blending with petro-diesel for commercialization.

Table 5.2. Biodiesel attributes

Biodiesel Properties	Standard ASTM D6751	Present study
Saponification value (mg KOH/g)	370 (max)	202.15
Iodine value (g I_2/100 g)	120 (max)	111.78
Cetane number	47 (min)	48.15
Cold filter plugging point (^oC)	+5 (max)	-15.05
Kinematic viscosity at 40°C (mm^2/s)	1.9 - 6.0	3.88
Higher heating value (MJ/kg)	40	39.44

Fourier transform infrared (FTIR) spectroscopy: The FTIR spectra of biodiesel presented in Fig. 5.1 showed ester peaks at 1743 cm^{-1} mainly for the mono alkyl esters, which form the biodiesel. The peaks observed at 1200, 1377 and 1460 cm^{-1} represent the vibrations of O-C-C, CC(=O)-O and CH_3 bonds (Patil et al., 2011).

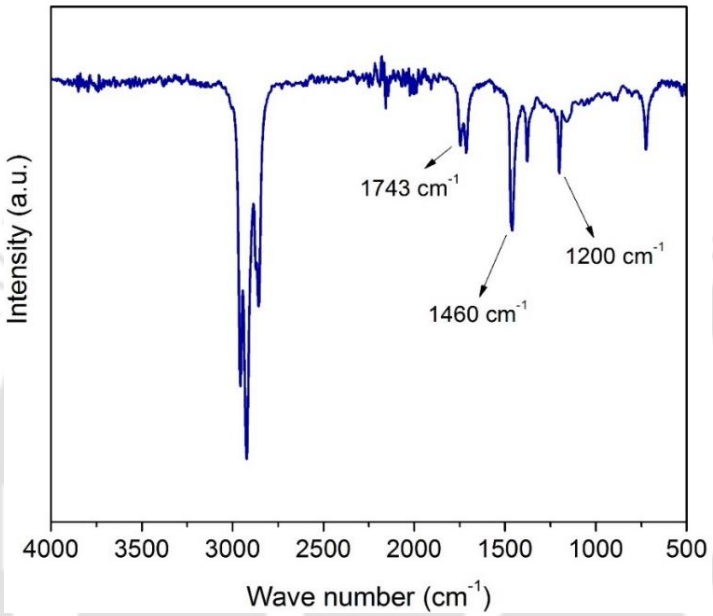

Figure 5.1. FTIR spectrum of microalgal biodiesel

5.3.3 Accumulation of various by-products

5.3.3.1 β-carotene production

The extraction of β-carotene was the first step in this biorefinery approach. The wet microalgal biomass was subjected to acetone treatment as described previously for extracting β-carotene. The spent biomass was then lyophilized for further processing. The amount of β-carotene obtained was similar for both the protocols (*in-situ* and conventional transesterification) as observed from Figs. 5.2 and 5.3, since there was no difference in the protocols followed till β-carotene extraction.

5.3.3.2 Glycerol production

Glycerol is also produced during transesterification reaction of lipids by glycolipid metabolism as a value-added product with biodiesel. The purification process for obtaining biodiesel and removing the impurities also helps in collecting the glycerol produced as a separate layer. The glycerol yield for *in-situ* transesterification was ~ 8 wt% with respect to the biodiesel yield, which was in accordance with previous literature (Crooks, 2007). Comparatively, a lower quantity of glycerol (6 wt%) could be recovered during 2-step transesterification of the biodiesel sample. The glycerol was in crude form (with contamination of alcohol and alkali) and was further purified. The recovered purified yield of the crude glycerol is further reduced due to the several impurities during the transesterification reaction of microalgal oil. Saponification is used to purify the obtained crude glycerol which releases the combined glycerol from the glycerides and hence, improves the glycerol quantity (Crooks, 2007).

5.3.3.3 Bioethanol production

After the transesterification step, the spent biomass was subjected to carbohydrate extraction. Carbohydrates present in the cell walls and chloroplast such as cellulose and starch, respectively, are not readily fermentable for ethanol production by microorganisms (Balat and Balat, 2009). Therefore, it is necessary to hydrolyze the complex polysaccharides. In this study, the polysaccharides were pretreated with 2 N sulphuric acid and were subjected to fermentation with *Saccharomyces cerevisae*. This was in accordance with the findings of Markou et al. (2013) were it was suggested that pretreatment of microalgal cells should be done at sulphuric acid concentration lower than 5 N. The maximum bioethanol yield of 12 g was obtained from 100 g DCW with the *in-situ* transesterification and 9 g with conventional protocol. This enhanced bioethanol yield

with *in-situ* transesterification is because of the enhanced availability of the carbohydrates form the microalgal biomass as shown in Table 5.1 (0.59 g/L and 0.8 g/L for conventional and *in-situ* protocols, respectively).

5.3.4 Microalgal biorefinery

Microalgae are the most promising renewable biodiesel substitute for its biochemical composition and environment-friendly characteristics. To further enhance the economics of the biodiesel production from microalgae, it is important to focus on generating higher revenue from microalgal biomass. This enables us to aim on biorefinery approach which helps in utilization of spent biomass for production of other biofuels as well. In the present study, biodiesel is produced along with β-carotene, glycerol and bioethanol. The detailed approach for the biorefinery with *in-situ* transesterification is depicted in Fig. 5.2. From approx. 100 g DCW of microalgae, 0.11 g of β-carotene is extracted. The left over biomass when subjected to *in-situ* transesterification yielded about 29 g of biodiesel with 2.6 g glycerol. The spent biomass was further used for fermentation which produced 12 g of bioethanol.

In case of conventional 2-step transesterification depicted in Fig. 5.3, 100 g DCW biomass yields approx. 0.12 g β-carotene after acetone treatment. The spent biomass is then lyophilized and the lyophilized biomass was first subjected to lipid extraction. The lipid collected was catalytically converted to biodiesel and glycerol whereas the biomass was acid hydrolyzed and fermented for bioethanol production. From 100 g of *T. obliquus* SGM19 biomass, 25 g of biodiesel and 2 g of glycerol was obtained along with 9 g of bioethanol.

It can be clearly inferred from the data that the quantity of products with *in-situ* transesterification were higher than that of the conventional protocol. The main reason for

the enhanced product formation with *in-situ* protocol was due to higher lipid and biomass concentrations for synthesis of biodiesel and bioethanol, respectively. The lipid extraction step depends on the efficiency of the process. Hence, there is loss of some lipids during the process of extraction which is omitted in *in-situ* protocol. Thus, the quantity of lipid undergoing the transesterification is more, which results in higher biodiesel and glycerol yields. After the removal of maximum lipid, the spent biomass undergoes carbohydrate extraction which is facilitated as there is no solid cell wall for hindrance. Hence, more carbohydrate is extracted yielding higher bioethanol concentration. Apart from this, the biomass left after extraction of carbohydrate, still contains some protein and other minor nutritional pigments, thus, making it a possible feed for animals.

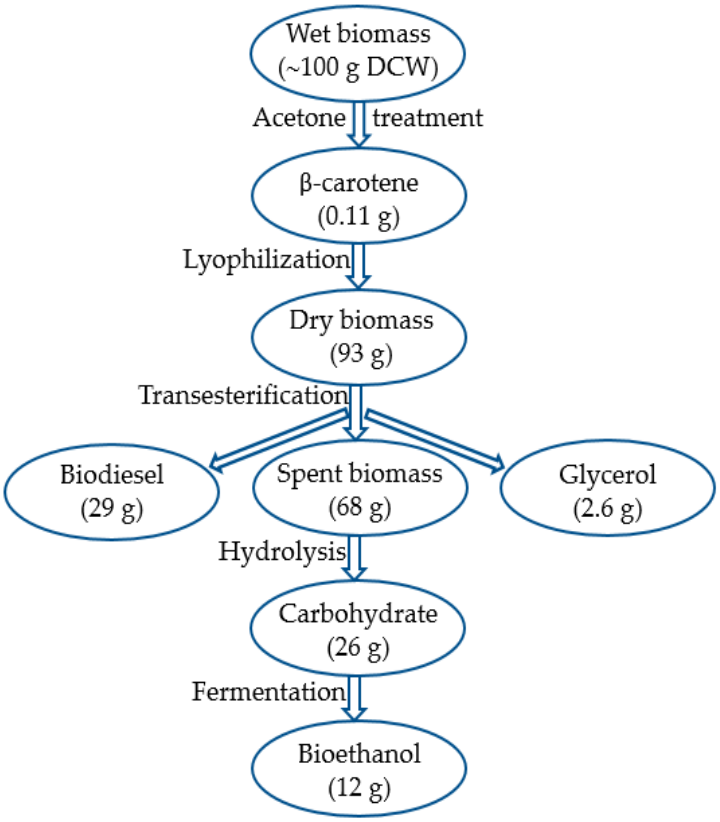

Figure 5.2. Schematic representation of biorefinery with *in-situ* transesterification

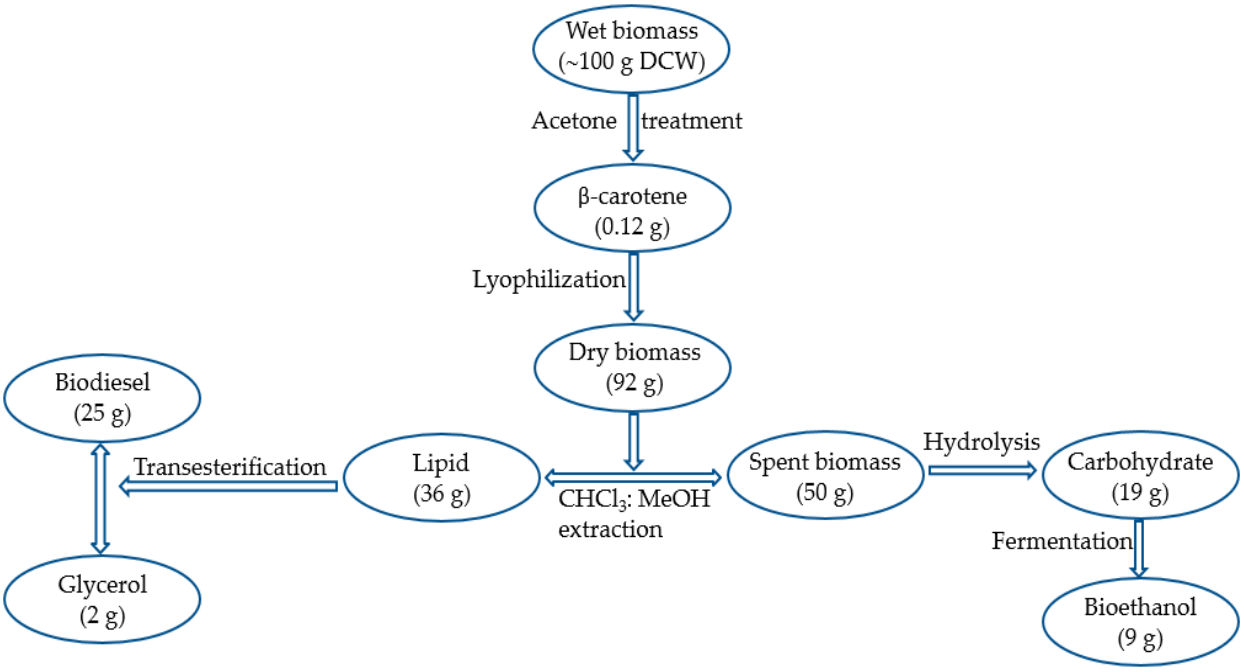

Figure 5.3. Schematic representation of biorefinery with conventional transesterification

5.4 Conclusions

This study has described a conceptual microalgal biorefinery – with biodiesel as main product, and β-carotene, glycerol and bioethanol as secondary products. Among the set of sequential processes, the protocol of *in-situ* transesterification for biodiesel (as compared to the conventional 2-step protocol of lipid extraction followed by transesterification) yielded not only higher quantity of biodiesel but also additional products of bioethanol and glycerol in relatively larger quantities. Omission of the step of lipid extraction in *in-situ* transesterification reduces the number of treatments microalgal biomass is subjected to, thus reducing consumption of chemicals, energy, time. The typical yields from 100 g *T. obliquus* biomass were: (1) conventional 2-step transesterification: 0.12 g β-carotene, 25 g biodiesel, 2 g glycerol and 9 g bioethanol; (2) *in-situ* transesterification: 0.11 g β-carotene, 29 g biodiesel, 2.6 g glycerol and 12 g bioethanol. In summary, the results of this chapter have demonstrated – at least

conceptually on laboratory scale - the feasibility of a biorefinery based on *T. obliquus* SGM19 with *in-situ* transesterification as potential primary process.

References

Balat M., Balat H., 2009. Recent trends in global production and utilization of bio-ethanol fuel. Appl. Energy 86, 2273–2282.

Behera B., Acharya A., Gargey I.A., Aly N., Balasubramanian P., 2019. Bioprocess engineering principles of microalgal cultivation for sustainable biofuel production Bioresour. Technol. Rep. 5, 297–316.

Cheah W.Y., Show P.L., Juan J.C., Chang J.S., Ling T.C., 2018. Enhancing biomass and lipid productions of microalgae in palm oil mill effluent using carbon and nutrient supplementation. Energy Convers. Manag. 164, 188–197.

Chisti Y., 2013. Constraints to commercialization of algal fuels. J. Biotechnol. 167(3), 201–214.

Crooks A., 2007. Evolving technology may generate profit from biodiesel glycerin glut. Rural Coop. 74, 30–32.

DuBois M., Gilles K., Hamilton J., Rebers P., Smith F., 1956. Colorimetric method for determination of sugars and related substances. Anal. Chem. 28(3), 350–356.

Islam M.A., Ayoko G.A., Brown R., Stuart D., Magnusson M., Heimann K., 2013. Influence of fatty acid structure on fuel properties of algae derived biodiesel. Procedia Eng. 56, 591–596.

Khan M.I., Shin J.H., Kim J.D., 2018. The promising future of microalgae: current status, challenges, and optimization of a sustainable and renewable industry for biofuels, feed, and other products. Microb. Cell Fact. 17, 36–57.

Ma Y., Wang Z., Yu C., Yin Y., Zhou G., 2014. Evaluation of the potential of 9 *Nannochloropsis* strains for biodiesel production. Bioresour. Technol. 167, 503-

509.

Majidian P., Tabatabaei M., Zeinolabedini M., Naghshbandi M.P., Chisti Y., 2018. Metabolic engineering of microorganisms for biofuel production. Renew. Sust. Energ. Rev. 82, 3863–3885.

Markou G., Angelidaki I., Nerantzis E., Georgakakis D., 2013. Bioethanol production by carbohydrate-enriched biomass of *Arthrospira* (Spirulina) *platensis*. Energies 6, 3937–3950.

Mishra S., Mohanty K., 2019. Comprehensive characterization of microalgal isolates and lipid-extracted biomass as zero-waste bioenergy feedstock: An integrated bioremediation and biorefinery approach. Bioresour. Technol. 273, 177–184.

Panahi H.K.S., Tabatabaei M., Aghbashlo M., Dehhaghi M., Rehan M., Nizami A.S., 2019. Recent updates on the production and upgrading of bio-crude oil from microalgae. Bioresour. Technol. Rep. 7, 100216.

Patil P.D., Gude V.G., Mannarswamy A., Deng S., Cooke P., Munson-McGee S., Rhodes I., Lammers P., Nirmalakhandan N., 2011. Optimization of direct conversion of wet algae to biodiesel under supercritical methanol conditions. Bioresour. Technol. 102, 118–122.

Seo H.B., Kim H.J., Jung H.K., 2009. Measurement of ethanol concentration using solvent extraction and dichromate oxidation and its application in bioethanol production process. J. Ind. Microbiol. Biotechnol. 36, 285–292.

Shuba E.S., Kifle D., 2018. Microalgae to biofuels: 'Promising' alternative and renewable energy, review. Renew. Sustain. Energy Rev. 81, 743–755.

Singh N., Batghare A.H., Choudhury B.J., Goyal A., Moholkar V.S., 2020. Microalgae based biorefinery: assessment of wild fresh water microalgal isolate for simultaneous biodiesel and β-carotene production. Bioresour. Technol. Rep. 11, 100440. https://doi.org/10.1016/j.biteb.2020.100440

Ubando A.T., Felix C.B., Chen W.H., 2020. Biorefineries in circular bioeconomy: A

comprehensive review. Bioresour. Technol. 299, 122585. https://doi.org/10.1016/j.biortech.2019.122585

Vaknin Y., Yermiyahu U., Bar-tal A., Samocha Y., 2018. Global maximization of Jatropha oil production under semi-arid conditions by balancing vegetative growth with reproductive capacity. GCB Bioenergy 10, 382–392.

Vidyashankar S., VenuGopal K.S., Swarnalatha G.V., Kavitha M.D., Chauhan V.S., Ravi R., Bansal A.K., Singh R., Pande A., Ravishankar G.A., Sarada R., 2015. Characterization of fatty acids and hydrocarbons of chlorophycean microalgae towards their use as biofuel source. Biomass Bioenerg. 77, 75–91.

Wang Y., Guo W., Lo Y., Chang J., Ren N., 2014. Characterization and kinetics of bio-butanol production with *Clostridium acetobutylicum* ATCC824 using mixed sugar medium simulating microalgae-based carbohydrates. Biochem. Eng. J. 91, 220–230.

Watts N., Amann M., Arnell N., Ayeb-Karlsson S., Belesova K., Boykoff M., Byass P., Cai W., Campbell-Lendrum D., Capstick S. and Chambers J., 2019. The 2019 report of The Lancet Countdown on health and climate change: ensuring that the health of a child born today is not defined by a changing climate. The Lancet, 394(10211), 1836–1878.

Xiao Y., Xiao G., Varma A., 2013. A Universal Procedure for Crude Glycerol Purification from Different Feedstocks in Biodiesel Production: Experimental and Simulation Study**.** Ind. Eng. Chem. Res. 52(39), 14291–14296.

भारतीय प्रौद्योगिकी संस्थान गुवाहाटी
Indian Institute of Technology Guwahati

CHAPTER 6

OVERVIEW AND SUGGESTIONS FOR FUTURE RESEARCH

CHAPTER 6

Overview and Suggestions for Future Research

6.1 Overview

Microalgae serve as a potential source of various renewable biofuels (Zhu et al., 2017). Some of these biofuels are biodiesel derived from microalgal oil/lipid, methane generated from the algal biomass by anaerobic digestion and biohydrogen produced photo-biologically. The microalgae are considered as a potential fuel source. They are considered gravely due to the increased petroleum prices and threating effects of global warming caused by depletion and burning of the fossil fuels. Moreover, microalgal biofuel routes are being investigated with interest in recent years for the various noticeable advantages that microalgae offer over conventional routes. The major advantage lies with the cheap feedstock for biofuels production, such as lipids biodiesel and carbohydrates for alcoholic biofuels (Faried et al., 2017). Despite encouraging results on laboratory scale studies, commercial scale production of biofuels through microalgal route hasn't been possible due to several constraints in large scale cultivation due to which the economy of production is

adversely affected. Production of high amount of cheap and lipid-rich biomass could not be achieved as advance technologies are still being developed. Hence, the microalgal route of lipid production has low economic potential.

Production of other byproduct that can fetch higher revenue (or value-added byproducts) is being sought as a solution to boost economy of microalgal route. Therefore, this thesis research was aimed at developing new cultivation techniques that produces other value-added byproducts with high yields such as carotenoids and other biofuels from microalgae. This biorefinery approach could provide solution to overcome the bottlenecks in commercialization of microalgal biodiesel. Recovery and sale of valuable products from other cell constituents of microalgae can be a source of an additional revenue and could boost the economy of the biorefinery (Chew et al., 2017). The constituents of a microalgae cell can be quantitatively divided into major and minor components. The major components include proteins, lipids and carbohydrates, while the minor components include vitamins, pigments and fatty acids (Parniakov et al., 2015). The minor components, however, could be a source of high revenue due to their high cost (and demand) in international market. Many pigments in microalgae such as chlorophylls, carotenoids etc. have gained importance in the food, cosmetics and pharmaceutical industries (Chew et al., 2017). In this chapter, we present an overview of the major results of different studies conducted in this research, which have been presented in preceding chapters. These results, when viewed at a glance and analyzed concurrently, would reveal and highlight the contributions made by this thesis to the area of microalgal biorefinery, and optimization and intensification of different processes in it.

Summaries of the thesis chapters

- In Chapter 2, we dealt with isolation and biochemical characterization of a fresh water microalgal strain for lipid and β-carotene production. Initial screening followed by 18S rRNA sequence analysis of the isolated microalga helped in identification of the genus *Scenedesmus*, and the microalgal species was named as *Tetradesmus obliquus* SGM19. Among various organic and inorganic nitrogen sources, sodium nitrate showed the maximum biomass yield of 2.3 g/L, while carbon source moderately increased the biomass yield, however, with adverse impact on β-carotene production. The growth of microalgae was hindered in saline environment, and photoperiod of 12L:12D showed maximum growth. At these conditions, the highest biomass concentration was 2.5 g/L, with β-carotene yield of 0.67 mg/g dry biomass and lipid content of 28.5 wt%. The antioxidant activity of extracted β-carotene was 69%. Structural composition of *T. obliquus* SGM19 possessed total holocellulose (cellulose + hemicellulose) content of 67.6%, and thus, this biomass had potential to serve as feedstock for fermentation. The extracted lipid was subjected to transesterification for biodiesel synthesis. GC-MS analysis of FAME (fatty acid methyl ester) profile revealed ~71% C16 and C18 fatty acids, which was an excellent composition. The major fatty acids present in the lipids were palmitic, heptadecanoic, linoleic, linolenic and arachidic acids.

- Chapter 3 has depicted the 2-step enhancement of lipids and β-carotene production by microalgae *Tetradesmus obliquus* SGM19. The first step was optimizing the culture conditions, while the second step was application of sonication at optimum parameters. Statistical experimental design was used for maximizing the product yields by optimization of growth cycle of *Tetradesmus obliquus* SGM19. The

optimum set of growth media components and process parameters (pH, light and temperature) was: $NaNO_3$ = 1.5 g/L, EDTA = 0.001 g/L, temperature = 28.5^oC, pH = 7.5, light intensity = 5120 lux. At the optimum culture conditions, the β-carotene yield was 0.67 mg/g DCW (dry cell weight). Now, to enhance the production of lipid and β-carotene, the microalgae was subjected to ultrasound with varying duty cycle (10%, 20%). At 20% duty cycle, the microalgal cells did not show much effect. Hence, application of 33 kHz and 1.4 bar ultrasound at 10% duty cycle was provided. The sonication revealed to enhance the lipid and β-carotene yields by 34.5% and 31.5%, respectively. The kinetic model was fitted to the profiles in control (without sonication) and test (with sonication) experiments so as to get the physical insight into the influence of sonication on microalgal growth and the concurrent lipid and β-carotene yields. The kinetic analysis of the substrate and product profiles in control and test experiments revealed that both the lipid and β-carotene are growth-associated products. The values of kinetic parameters in control and test experiments clearly suggest intensification of cell metabolism induced by sonication. Consistently higher intracellular NAD(H) concentrations were observed for test experiments with sonication indicating faster metabolism. The cell viability in presence of sonication was more than 80%.

- Chapter 4 demonstrated ultrasound–assisted biodiesel production from biomass of *Tetradesmus obliquus* SGM19 in a batch process. Maximization of biodiesel yield was achieved in a 2-step process, viz. optimization of condition of the feedstock followed by optimization of the process parameters. Two protocols were employed for utilization of microalgal biomass: (1) the conventional process of lipid extraction followed by transesterification, and (2) use of whole biomass (in wet and

lyophilized form) for *in-situ* transesterification. In both protocols, lipids/biomass were subjected to transesterification with an acid (H_2SO_4) or a base (NaOH) or a 2-step acid-base (H_2SO_4-NaOH) catalyst. Among all process combinations, *in-situ* base-catalyzed transesterification with lyophilized biomass was the best protocol with the FAME yield of 37.5% (w/w DCW). The transesterification parameters were further optimized using RSM for boosting the biodiesel yield. Maximum FAME yield of $39.2 \pm 1.1\%$ was achieved at the optimum conditions: catalyst loading = 1.5% (w/w biomass), methanol to biomass ratio = 30 (v/w), reaction temperature = 50°C and reaction time = 50 min. Finally, replacement of mechanical shaking of reaction mixture with sonication (at optimum conditions) further enhanced the biodiesel yield to 47.9%. The kinetic analysis of process revealed reduction in activation energy of transesterification from 24.6 to 19.8 kJ/mol. Marked enhancement in biodiesel yield with concurrent reduction in activation energy is attributed to the physical effect of intense micromixing induced by sonication, which eliminates mass transfer barriers in the heterogeneous reaction system with rise in the interfacial area.

- A conceptual biorefinery based on microalgal biomass *T. obliquus* SGM19 as the feedstock has been presented in Chapter 5 – in which the biomass was subjected to various treatments after lipid extraction. The biorefinery approach was designed for the isolated microalgal biomass *T. obliquus* SGM19 as the feedstock, which was subjected to various treatments for extracting desired products. In the biorefinery design, the microalgal biomass was sequentially used to produce β-carotene, biodiesel, glycerol and bioethanol. The spent biomass at last also had protein content, thus making it probable feed for animal consumption. Among the two

approaches (viz. both in-situ and conventional transesterification protocols) attempted in this conceptual biorefinery, the in-situ protocol had higher yields of the end products (biodiesel, glycerol and bioethanol) as compared to the conventional protocol. It can be inferred from the results that the removal of lipid extraction process in *in-situ* transesterification benefits the quality (components) of microalgal biomass as it reduces the number of treatments microalgal biomass is subjected to, thus eliminating extra consumption of chemicals, energy, time and finally reducing the total cost of production. The detailed bio-refinery process produced approximately 0.12 g β-carotene, 25 g biodiesel, 2 g glycerol and 9 g bioethanol from 100 g *T. obliquus* biomass using conventional 2-step transesterification whereas, 0.11 g β-carotene, 29 g of biodiesel, 2.6 g glycerol and 12 g bioethanol from 100 g *T. obliquus* biomass with *in-situ* transesterification. The spent biomass content was 50 g and 68 g after conventional and *in-situ* transesterification processes, respectively, showing that some biomass is also lost in lipid extraction process.

Several general conclusions can be drawn from the above results when viewed at a glance. (1) Wild microalgae species have excellent potential of being a feedstock for not just biodiesel production but also other products such as nutraceuticals and bioalcohol. (2) In order to maximize the yield of products from microalgal biomass, it is utmost essential to optimize the growth conditions – in terms of both media composition and process parameters. (3) Application of external stimuli in the form of sonication can give marked enhancement in the growth kinetics, the final biomass concentration attained and yield of various products from the biomass.

These results are highly encouraging as they present rather simpler yet effective solution to improve performance and output of the microalgal processes based on wild strains that are readily available in nature, and are also stable and resistant to variations in environmental conditions. This thesis has also demonstrated new protocols of direct *in situ* transesterification for biodiesel synthesis. Last but not the least, the conceptual biorefinery has also been attempted with as many as 4 simultaneous products. The spent biomass can also earn some revenue as fish food.

6.2 Future challenges and prospects of microalgal biorefineries

As evident from results of this study, the wild microalga are excellent candidates for a biorefinery producing biofuels and other value-added products. Although the results of present study are encouraging, significant translational research is necessary before realizing commercial scale refineries that are sustainable and economically viable. A useful tool for evaluation of sustainability of biorefineries is life cycle assessment (LCA), and exergo-economic/exergo-environmental analysis. Life cycle analysis takes into account the life cycle inventory and life cycle impact of the process. LCA is a measure to map the impact of the process by quantification of energy and material consumption and waste and emissions to the environment. Another issue is the exergo-economic and exergo-environmental analysis of the process (Aghbashlo et al., 2018). Conventionally, energy analysis based on first law of thermodynamics is used to assess the efficient of the process. Rosen (2018) has pointed out that energy analysis is incapable of providing insight into sustainability of biofuel production as it does not account for irreversible nature of the process. Therefore, exergy-based analysis needs to be done that accounts for thermodynamic irreversibility, and resource depletion, and thus provides appraisal of degree of sustainability. Rigorous LCA and exergy studies on the results reported in this

study (and also on previous literature) is absolutely essential for a microalgal biorefinery producing biofuels and nutraceuticals.

All the experiments in the present thesis were conducted in batch in Erlenmeyer flask. Large scale production, with different cultivation methods such as raceway ponds or photo-bioreactors can be employed. This will not only help in understanding the effect of scale-up on the microalgae but will also help to study the effect of open and closed systems on microalgal growth and the microalgal composition. For further enhancing the end products of transesterification, various new catalyst could be synthesized and used.

References

Aghbashlo M., Tabatabaei M., Hosseinpour S., 2018. On the exergoeconomic and exergoenvironmental evaluation and optimization of biodiesel synthesis from waste cooking oil (WCO) using a low power, high frequency ultrasonic reactor. Energy Convers. Manage. 164, 385-398.

Chew K.W., Yap J.Y., Show P.L., Suan N.H., Juan J.C., Ling T.C., Lee D.J., Chang J.S., 2017. Microalgae biorefinery: high value products perspectives. Bioresour. Technol. 229, 53-62.

Faried M., Samer M., Abdelsalam E., Yousef R.S., Attia Y.A., Ali A.S., 2017. Biodiesel production from microalgae: processes, technologies and recent advancements. Renew. Sustain. Energy Rev. 79, 893–913.

Parniakov O., Barba F.J., Grimi N., Marchal L., Jubeau S., Lebovka N., Vorobiev E., 2015. Pulsed electric field assisted extraction of nutritionally valuable compounds from microalgae *Nannochloropsis* spp. using the binary mixture of organic solvents and water. Innov. Food Sci. Emerg. Technol. 27, 79–85.

Rosen, M.A., 2018. Environmental sustainability tools in the biofuel industry. Biofuel Res. J. 17, 751-752.

RESEARCH OUTPUTS

Research papers out of thesis

1. **N Singh**, A Goyal, VS Moholkar. Microalgal bio-refinery approach for utilization of *Tetradesmus obliquus* biomass for biodiesel production. Materials Today: Proceedings, 2020, 32(4), 760-763.
2. **N Singh**, AH Batghare, BJ Choudhury, A Goyal, VS Moholkar. Microalgae based biorefinery: assessment of wild fresh water microalgal isolate for simultaneous biodiesel and β-carotene production. Bioresource Technology Reports, 2020, 100440.
3. **N Singh**, K Roy, A Goyal, VS Moholkar. Investigations in ultrasonic enhancement of β-carotene production by isolated microalgal strain *Tetradesmus obliquus* SGM19. Ultrasonics sonochemistry, 2019, 58, 104697.
4. **N Singh**, A Goyal, VS Moholkar. Biodiesel synthesis by *in-situ* transesterification of microalgal biomass of *Tetradesmus obliquus* SGM19 and its intensification with ultrasound. (Under Review)

Other publication

- AH Batghare, **N Singh**, VS Moholkar. Investigations in ultrasound–induced enhancement of astaxanthin production by wild strain *Phaffia rhodozyma* MTCC 7536. Bioresource technology, 2018, 254, 166-173.

Manuscript under preparation

1. **N Singh**, A Goyal, VS Moholkar. *Tetradesmus obliquus* SGM19 biomass as feedstock for production of biodiesel and other value-added co-products: a microalgal biorefinery approach.

Conferences Presentations

- Oral presentation at American Chemical Society Fall 2020 Virtual Meeting and Expo (17-20 August, 2020).
- Oral presentation at International Conference on "Innovative Technologies for Clean and Sustainable Development (ITCSD) 2020", Hosted by National Institute of Technical Teachers Training and Research (NITTTR), Chandigarh (19–21 February, 2020).
- Poster presentation at International Conference on 'Biotechnological Research and Innovation for Sustainable Development', the XV BRSI Convention, India, Hosted by CSIR-Indian Institute of Chemical Technology (CSIR-IICT), Hyderabad (22-25 November, 2018).
- Poster presentation at International Conference on "Emerging Trends in Biotechnology for Waste Conversion (ETBWC) 2017", the XIV Annual Convention of The Biotech Research Society (BRSI), India, Hosted by CSIR-NEERI, Nagpur (8-10 October, 2017).

Appendix A

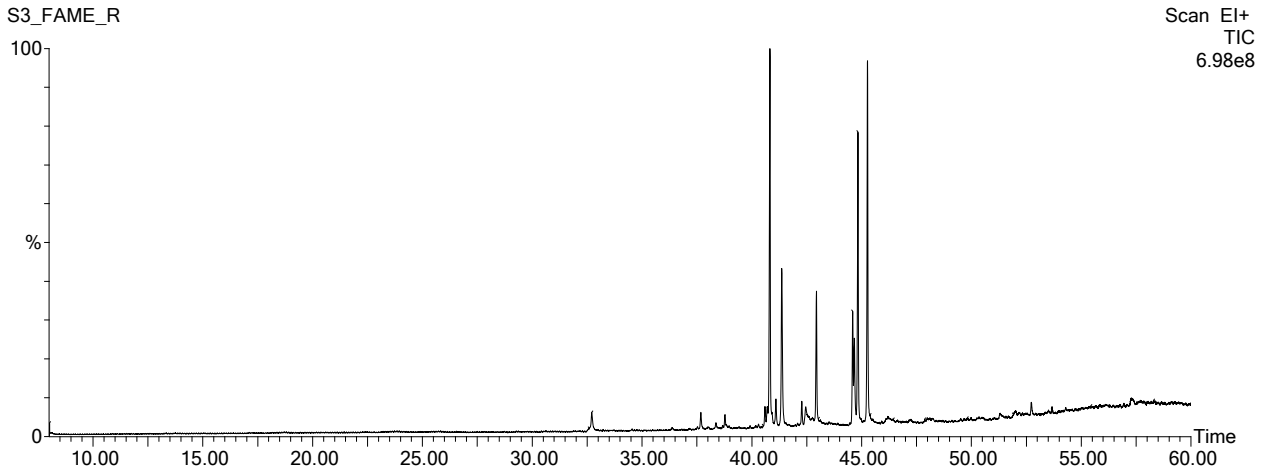

Figure S1. GC-MS spectrum of fatty acid methyl esters

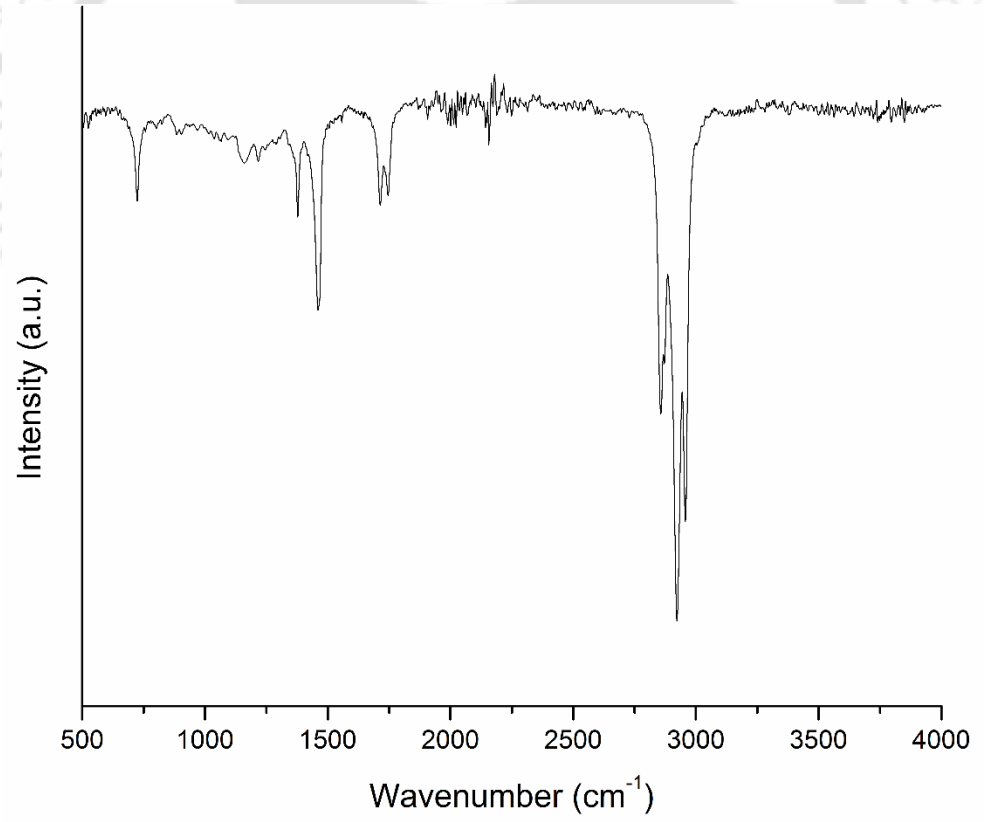

(B)

Figure S2. FTIR spectrum of biodiesel synthesized from lipids extracted from *T. obliquus* SGM19

Appendix B

Table A.1: Factors and levels used in Plackett–Burman design matrix

Factors (g/L)	Levels	
	Low (–1)	High (+1)
(X_1) – K_2HPO_4	0.004	0.04
(X_2) – $MgSO_4.7H_2O$	0.0075	0.075
(X_3) – $CaCl_2$	0.0036	0.036
(X_4) – Citric acid	0.001	0.006
(X_5) – EDTA	0.0001	0.001
(X_6) – Ammonium ferric citrate	0.001	0.006
(X_7) – Na_2CO_3	0.002	0.02
(X_8) – $NaNO_3$	0.15	1.5

Table A.2: Plackett–Burman design matrix with coded units for eight variables along with the β-carotene yield (mg/g DCW)

Run order	X_1	X_2	X_3	X_4	X_5	X_6	X_7	X_8	β-carotene (mg/g DCW)	
									Experimental	Predicted
1	−1	−1	−1	−1	−1	−1	−1	−1	0.295	0.299
2	−1	−1	+1	+1	+1	−1	+1	+1	0.415	0.416
3	+1	−1	+1	−1	−1	−1	+1	+1	0.410	0.409
4	−1	−1	−1	+1	+1	+1	−1	+1	0.396	0.395
5	−1	+1	−1	−1	−1	+1	+1	+1	0.397	0.407
6	−1	+1	+1	+1	−1	+1	+1	−1	0.340	0.330
7	+1	+1	−1	+1	−1	−1	−1	+1	0.390	0.377
8	+1	−1	−1	−1	+1	+1	+1	−1	0.400	0.387
9	−1	+1	+1	−1	+1	−1	−1	−1	0.355	0.351
10	+1	−1	+1	+1	−1	+1	−1	−1	0.300	0.310
11	+1	+1	−1	+1	+1	−1	+1	−1	0.365	0.378
12	+1	+1	+1	−1	+1	+1	−1	+1	0.435	0.439

Table A.3: Statistical analysis of Plackett–Burman experimental design for media optimization

(A) Coefficient values, *t*– and *p*– values for each variable

Model term	Coefficient Estimate	Computed *t*-value	*p*-value
Intercept	0.374833	77.85	0.000*
X1	0.008500	1.77	0.176
X2	0.005500	1.14	0.336
X3	0.001000	0.21	0.849
X4	−0.007167	−1.49	0.233
X5	0.019500	4.05	0.027*
X6	0.003167	0.66	0.558
X7	0.013000	2.70	0.074
X8	0.032333	6.71	0.007*

*- Significant *p* values, $p \leq 0.05$; $R^2 = 0.962$; Predicted $R^2 = 0.391$; Adjusted $R^2 = 0.861$

(B) Analysis of variance (ANOVA)

Source	DF	SS	MS	F-value	*p*-value Prob>F
Model	8	0.0211150	0.0026394	9.49	0.045
X1	1	0.0008670	0.0008670	3.12	0.176
X2	1	0.0003630	0.0003630	1.30	0.336
X3	1	0.0000120	0.0000120	0.04	0.849
X4	1	0.0006163	0.0006163	2.22	0.233
X5	1	0.0045630	0.0045630	16.40	0.027
X6	1	0.0001203	0.0001203	0.43	0.558
X7	1	0.0020280	0.0020280	7.29	0.074
X8	1	0.0125453	0.0125453	45.09	0.007
Residual Error	3	0.0008347	0.0002782		
Total	11	0.0219497			

DF– Degree of freedom; SS– Sum of squares; MS– Mean square

Table A.4: Full factorial central composite design (CCD) matrix of medium components in coded and actual (in parentheses) values

Run order	$NaNO_3$ (X_1, g/L)	EDTA (X_2, g/L)	β-carotene (mg/g DCW)	
			Experimental	Predicted
1	0 (0.825)	0 (0.00055)	0.311	0.310
2	0 (0.825)	0 (0.00055)	0.324	0.310
3	0 (0.825)	0 (0.00055)	0.310	0.310
4	0 (0.825)	0 (0.00055)	0.299	0.310
5	0 (0.825)	+α (0.0012)	0.415	0.421
6	–1 (0.15)	+1 (0.001)	0.401	0.394
7	0 (0.825)	0 (0.00055)	0.305	0.310
8	–1 (0.15)	−1 (0.0001)	0.330	0.329
9	+1 (1.5)	+1 (0.001)	0.416	0.412
10	0 (0.825)	–α (0.00009)	0.360	0.358
11	+α (1.78)	0 (0.00055)	0.400	0.399
12	−α (0.129)	0 (0.00055)	0.340	0.345
13	+1 (1.5)	–1 (0.0001)	0.385	0.388

Table A.5: Results of statistical (CCD) analysis for media components optimization

(A) Coefficient values, *t* and *p* values for each variable

Model term	Coefficient Estimate	Computed *t*-value	*p*-value
Intercept	0.30980	84.219	0.000
NaNO3	0.01923	6.613	0.000
EDTA	0.02235	7.685	0.001
NaNO3 × NaNO3	0.03110	9.972	0.000
EDTA × EDTA	0.03985	12.778	0.000
NaNO3 × EDTA	−0.01025	−2.492	0.041

R^2= 0.98; Predicted R^2= 0.938; Adjusted R^2= 0.9657

(B) ANOVA of quadratic model

Source	DF	SS	MS	F-value	*p*-value Prob>F
Regression	5	0.023170	0.004634	68.49	0.000
Linear	2	0.006954	0.003477	51.39	0.000
Square	2	0.015795	0.007898	116.73	0.000
Interaction	1	0.000420	0.000420	6.21	0.041
Residual Error	7	0.000474	0.000068		
Lack-of-fit	3	0.000131	0.000044	0.51	0.697
Pure Error	4	0.000343	0.000086		
Total	12	0.023643			

DF– Degree of freedom; SS– Sum of squares; MS– Mean square

Table A.6: Factors and levels used in Central composite design matrix

Factors	Levels	
	Low (-1)	High (+1)
(X_1) - Temperature, ^oC	15	40
(X_2) - pH	5	9
(X_3) - Light intensity, Lux	1500	4200

Table A.7: Full factorial central composite design matrix of 3 physical parameters in coded and actual (in parentheses) values and the response of β-carotene yield

Run order	Temperature (°C) (X_1)	pH (X_2)	Light intensity (Lux) (X_3)	β-carotene (mg/g DCW)	
				Experimental	Predicted
1	−1 (15)	+1 (9)	–1 (1500)	0.260	0.271
2	+1 (40)	+1 (9)	–1 (1500)	0.325	0.327
3	0 (27.5)	0 (7)	0 (2850)	0.620	0.624
4	–1 (15)	–1 (5)	–1 (1500)	0.217	0.197
5	–1 (15)	+1 (9)	+1 (4200)	0.485	0.477
6	+1 (40)	−1 (5)	+1 (4200)	0.475	0.471
7	0 (27.5)	0 (7)	0 (2850)	0.610	0.624
8	0 (27.5)	−α (3.6)	0 (2850)	0.301	0.306
9	+α (48.5)	0 (7)	0 (2850)	0.351	0.331
10	–1 (15)	–1 (5)	+1 (4200)	0.313	0.318
11	+1 (40)	−1 (5)	–1 (1500)	0.390	0.405
12	−α (6.5)	0 (7)	0 (2850)	0.145	0.155
13	+1 (40)	+1 (9)	+1 (4200)	0.451	0.477
14	0 (27.5)	0 (7)	0 (2850)	0.624	0.624
15	0 (27.5)	0 (7)	+α (5120.4)	0.686	0.678
16	0 (27.5)	0 (7)	0 (2850)	0.617	0.624
17	0 (27.5)	+α (10.3)	0 (2850)	0.389	0.374
18	0 (27.5)	0 (7)	0 (2850)	0.630	0.624
19	0 (27.5)	0 (7)	−α (579.6)	0.453	0.451
20	0 (27.5)	0 (7)	0 (2850)	0.638	0.624

Table A.8: Results of statistical (CCD) analysis for process parameters optimization

A) Coefficient values, *t*− and *p*− values for each variable

Model term	Coefficient Estimate	Computed *t*-value	*p*-value
Intercept	0.62345	90.090	0.000
Temperature	0.05217	11.362	0.000
pH	0.02006	4.370	0.001
Light intensity	0.06765	14.733	0.000
Temperature × Temperature	−0.13448	−30.087	0.000
pH × pH	−0.10018	−22.414	0.000
Light intensity × Light intensity	−0.02081	−4.656	0.001
Temperature × pH	−0.03800	−6.334	0.000
Temperature × Light intensity	−0.01375	−2.292	0.045
pH × Light intensity	0.02125	3.542	0.005

R^2= 0.9942; Predicted R^2= 0.9589; Adjusted R^2= 0.9890

B) ANOVA for quadratic model

Source	DF	SS	MS	F-value	*p*-value Prob>F
Regression	9	0.492197	0.054689	189.95	0.000
Linear	3	0.105101	0.035054	121.75	0.000
Square	3	0.370359	0.123453	428.80	0.000
Interaction	3	0.016677	0.005559	19.31	0.000
Residual Error	10	0.002879	0.000288		
Lack-of-fit	5	0.002390	0.000478	4.89	0.053
Pure Error	5	0.000489	0.000098		
Total	19	0.495076			

DF-degree of freedom; SS-sum of squares; MS-mean square

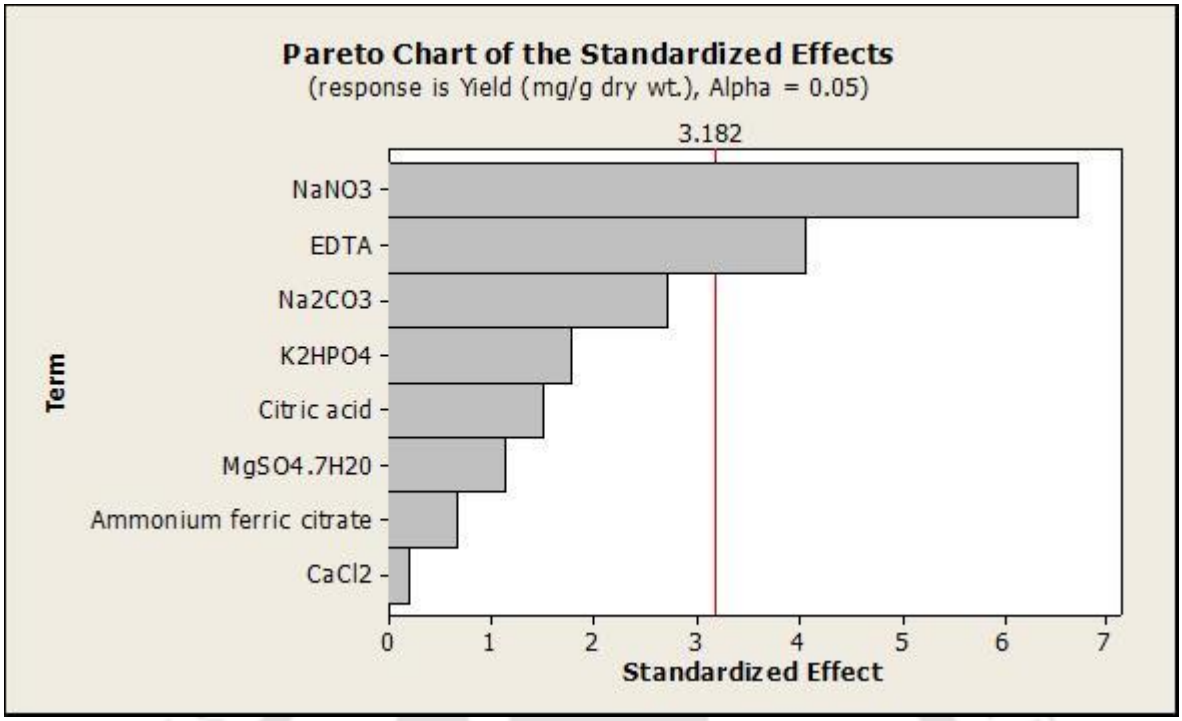

Figure A.1: Pareto plot for Plackett-Burman analysis

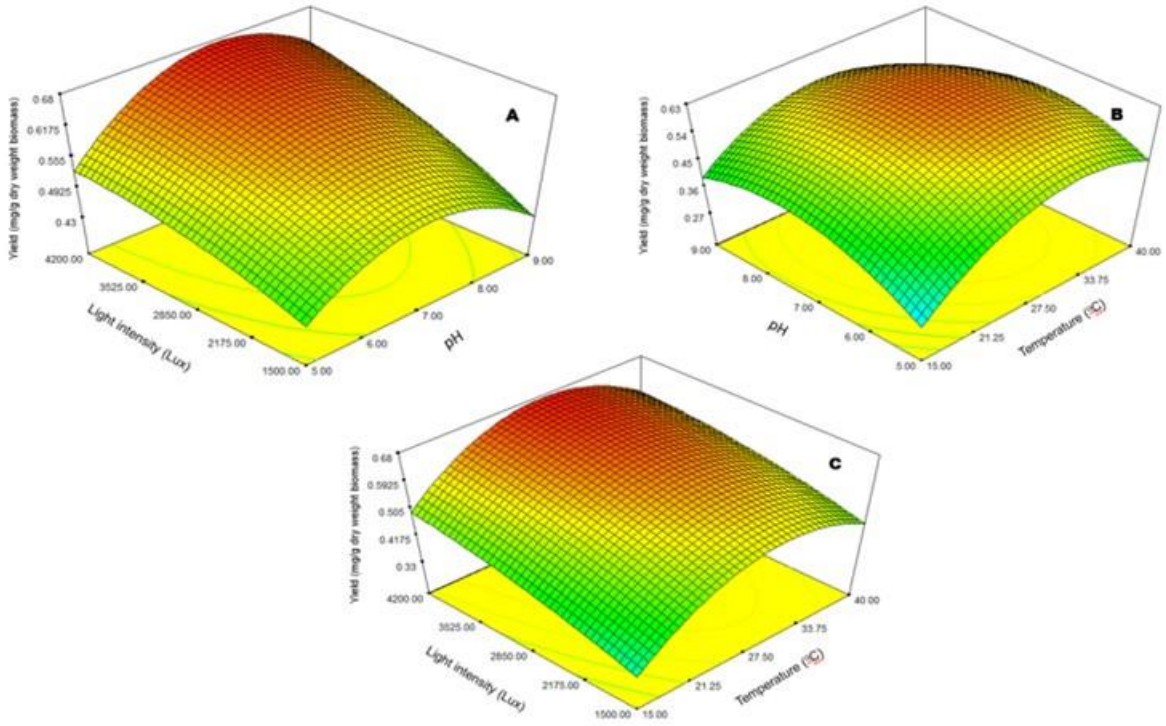

Figure A.2: Surface plot effect of different parameters on the β-carotene concentration (A) Light intensity and pH (B) pH and Temperature (C) Light intensity and Temperature

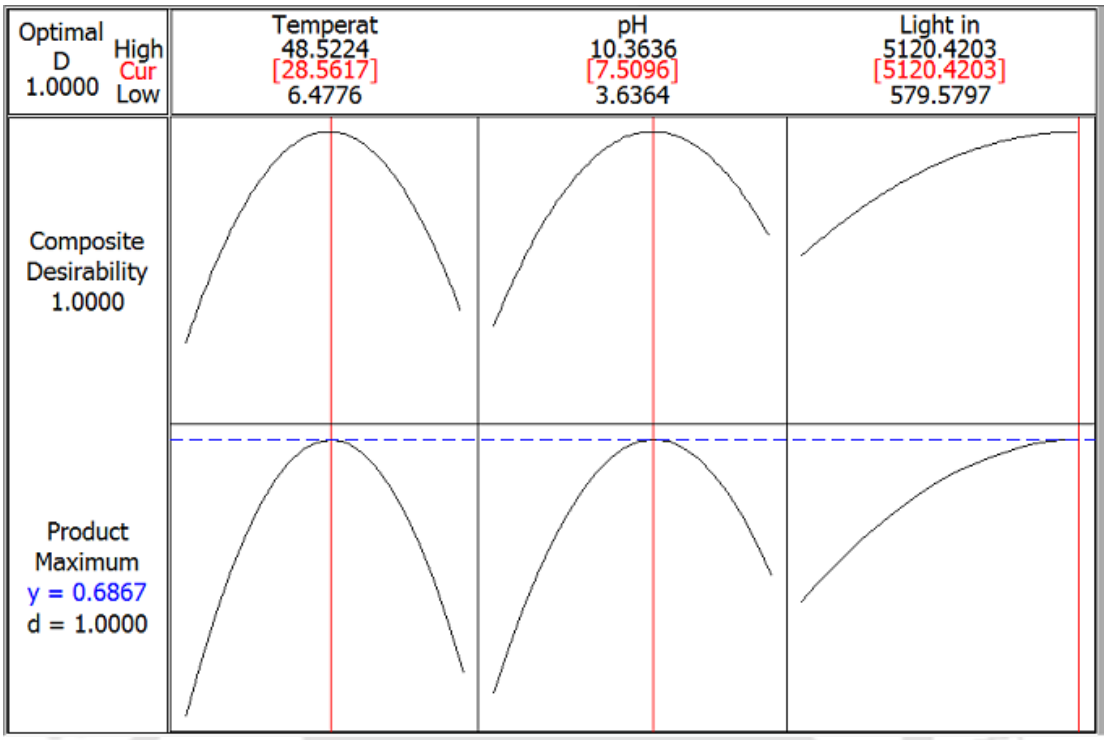

Figure A.3: Desirability function plot showing the optimum levels of physical parameters

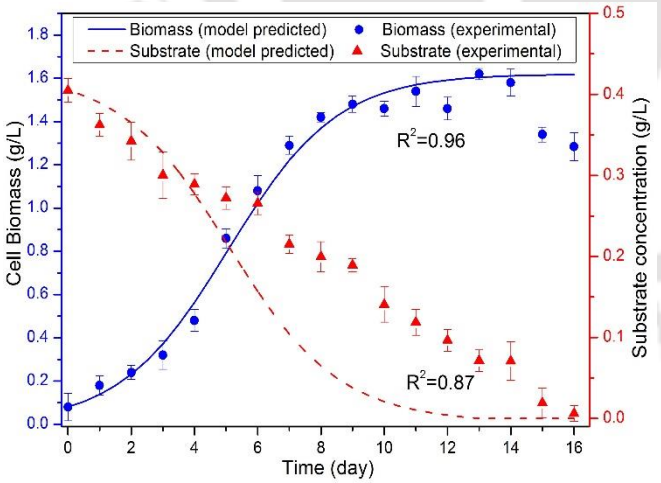

(A)

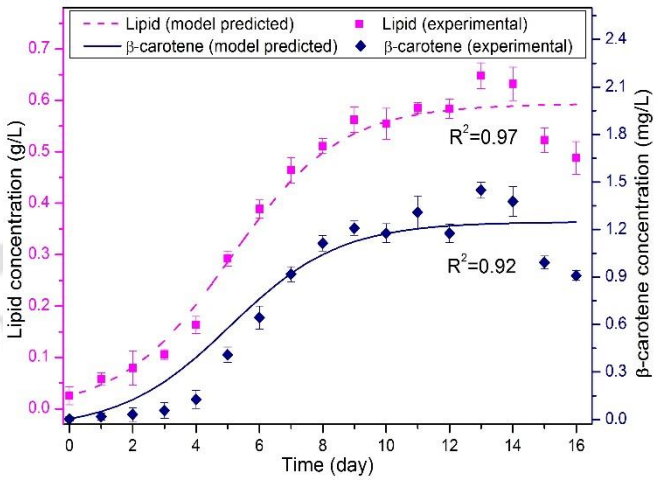

(B)

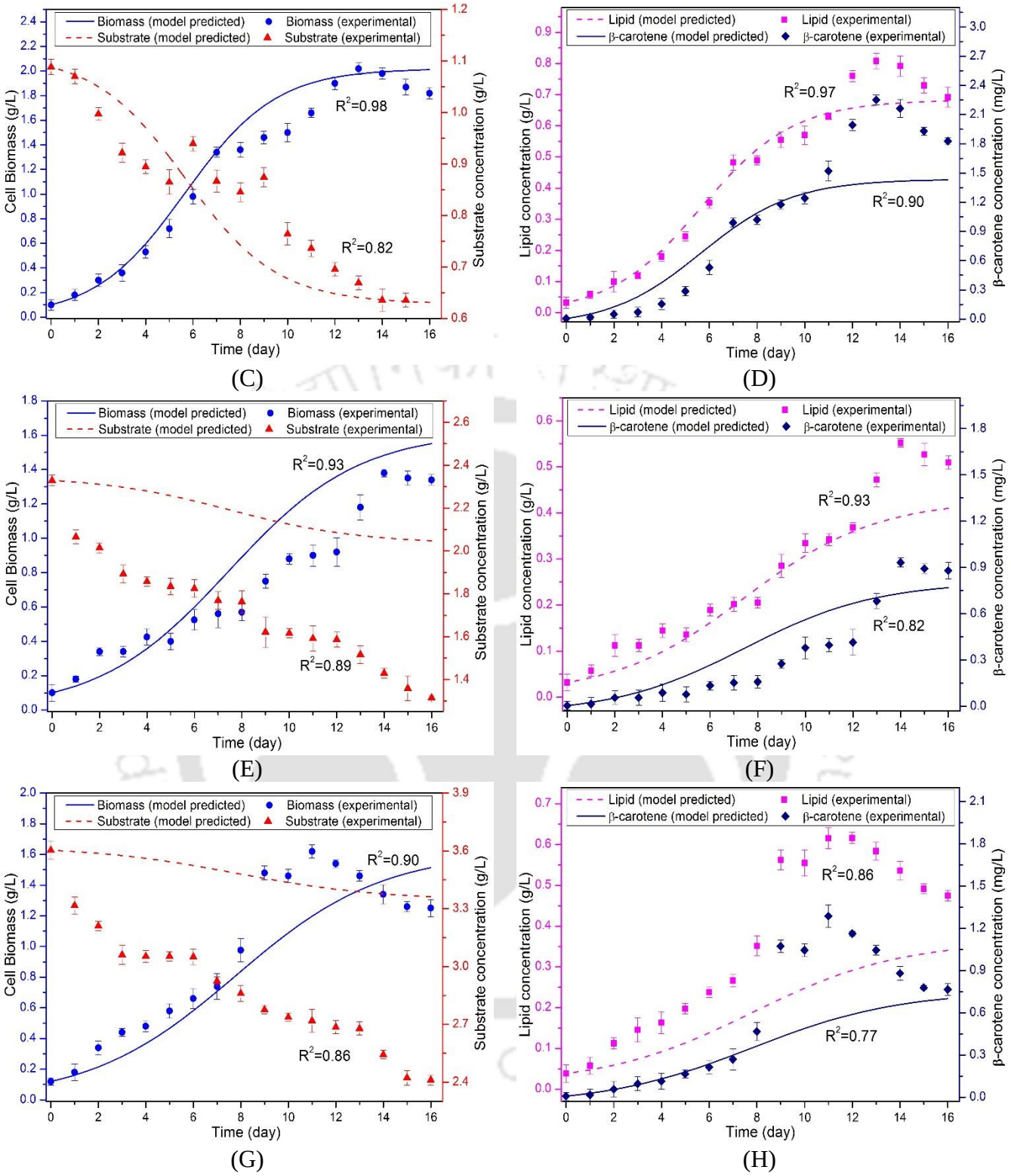

Figure A.4: Experimental and simulated time profiles of biomass, substrate, lipid and β-carotene during growth of *T. obliquus* SGM19 for different initial substrate concentration. (A, B) Initial substrate concentration = 0.5 g/L; (C, D) Initial substrate concentration = 1.5 g/L; (E, F) Initial substrate concentration = 3 g/L; (G, H) Initial substrate concentration = 4.5 g/L.